



ANTARCTIC CLIMATE
& ECOSYSTEMS CRC

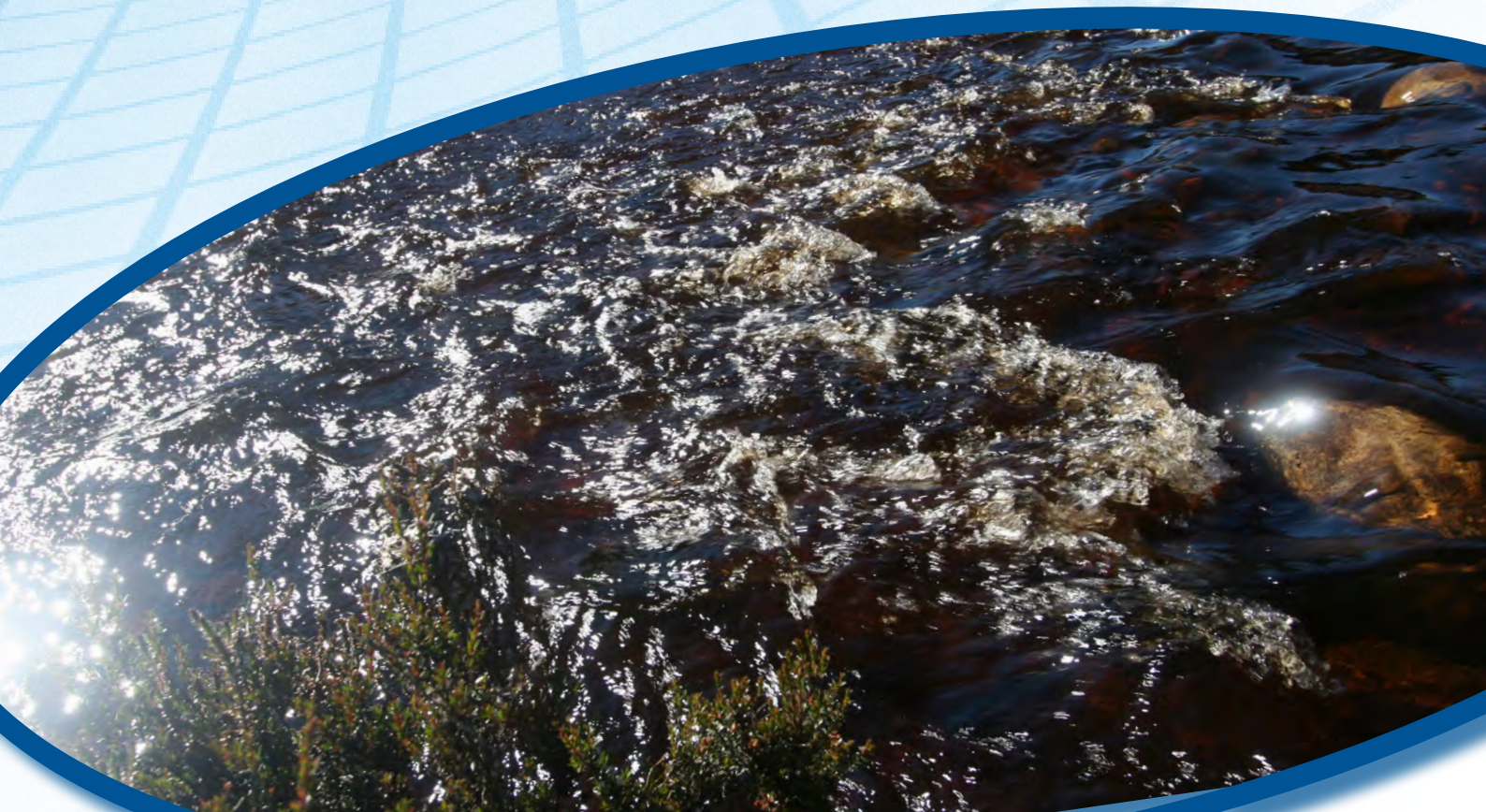
climate futures for tasmania

TECHNICAL REPORT

Water and Catchments

Bennett JC, Ling FLN, Graham B, Grose MR, Corney SP, White CJ, Holz GK,
Post DA, Gaynor SM & Bindoff NL

December 2010



Climate Futures for Tasmania Water and Catchments Technical Report

ISBN 978-1-921197-06-8

© Copyright The Antarctic Climate & Ecosystems Cooperative Research Centre 2010.

This work is copyright. It may be reproduced in whole or in part for study or training purposes subject to the inclusion of an acknowledgement of the source, but not for commercial sale or use. Reproduction for purposes other than those listed above requires the written permission of the Antarctic Climate & Ecosystems Cooperative Research Centre.

Requests and enquiries concerning reproduction rights should be addressed to:

The Manager
Communications
Antarctic Climate & Ecosystems Cooperative Research Centre

Private Bag 80
Hobart Tasmania 7001
Tel: +61 3 6226 7888, Fax: +61 3 6226 2440
Email: climatefutures@acecrc.org.au

Disclaimer

The material in this report is based on computer modelling projections for climate change scenarios and, as such, there are inherent uncertainties in the data. While every effort has been made to ensure the material in this report is accurate, Antarctic Climate & Ecosystems Cooperative Research Centre (ACE) provides no warranty, guarantee or representation that material is accurate, complete, up to date, non-infringing or fit for a particular purpose. The use of the material is entirely at the risk of a user. The user must independently verify the suitability of the material for its own use.

To the maximum extent permitted by law, ACE, its participating organisations and their officers, employees, contractors and agents exclude liability for any loss, damage, costs or expenses whether direct, indirect, consequential including loss of profits, opportunity and third party claims that may be caused through the use of, reliance upon, or interpretation of the material in this report.

Science Reviewers

Dr Francis Chiew (CSIRO), Dr Danielle Verdon-Kidd (University of Newcastle), Dr Neil Viney (CSIRO) and Dr Fiona Dyer (University of Canberra)

The reviewers listed in this report have offered all comments and recommendations in good faith and in an unbiased and professional manner. At no time was the reviewer asked to verify or endorse the project conclusions and recommendations nor was the reviewer privy to the final draft of the report before its release.

The reviewers' role was solely advisory and should not be construed as an endorsement of the project findings by the reviewer or his /her employing organisation. Neither the reviewer nor his/her employing organisation provides any representation or warranty as to the accuracy or suitability of any project findings. Responsibility for all work done in connection with the project remains with the project team.

Photo Credits: Front cover Suzie Gaynor, Hydro Tasmania (pp 5, 88), Sue Roberts (p 69), all remaining photos by Suzie Gaynor.

Graphic Design: Suzie Gaynor

Graphic Layout: Epiphany Public Relations

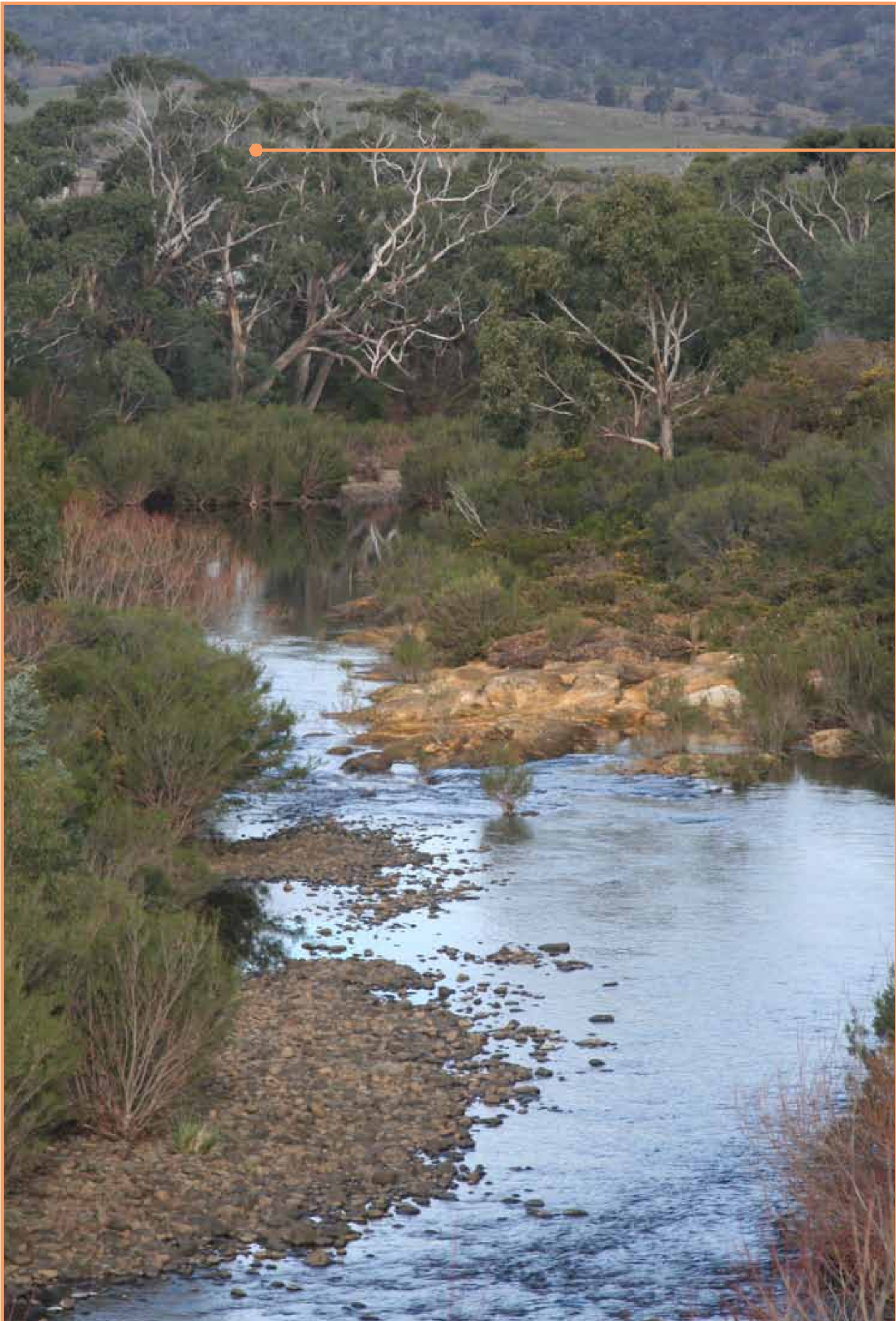
Citation

Bennett JC, Ling FLN, Graham B, Grose MR, Corney SP, White CJ, Holz GK, Post DA, Gaynor SM and Bindoff NL 2010, *Climate Futures for Tasmania: water and catchments technical report*, Antarctic Climate & Ecosystems Cooperative Research Centre, Hobart, Tasmania.

Climate Futures for Tasmania:
water and catchments

Bennett JC, Ling FLN, Graham B,
Grose MR, Corney SC, White CJ, Holz GK, Post DA, Gaynor SM and Bindoff NL

December 2010



Foreword

The Climate Futures for Tasmania research project is Tasmania's most important source of climate change information at a local scale. It is an essential part of the Tasmanian Government's climate change strategy and is invaluable in informing evidence-based decision making in all sectors of government, industry, business and communities in Tasmania.

This collaborative research project, led by Professor Nathan Bindoff, has demonstrated innovative leadership by involving and engaging external stakeholders on all levels. The project is unique in the research environment in that they have invited input and direction from interested end-users from the beginning of the project. The opportunity for our organisation to be involved from the start has meant that the results and outcomes from the science are directly usable in our business systems, applied models and decision-making processes.

The potential impact of climate change on community, business and industry is nowhere more apparent than in hydropower. At Hydro Tasmania we're pleased to continue an association with cutting-edge climate research that commenced in 2005 with the initial trial application of dynamical downscaling to the complex Tasmanian context. The results of the Climate Futures for Tasmania project will inform both our strategic investment decisions and operational plans as we adapt our business to be sustainable in a changing climate.

We have worked closely with the lead author James Bennett (seconded to the project from Entura, Hydro Tasmania's consulting business) and his colleagues. The report has passed the rigours of an external scientific review process and I appreciate the efforts of the respected scientists who gave their time and expertise to review the research outcomes. Thank you to Dr Francis Chiew (CSIRO), Dr Danielle Verdon-Kidd (University of Newcastle), Dr Neil Viney (CSIRO) and Dr Fiona Dyer (University of Canberra).

In acknowledging the research contributors, it is also important to highlight the valuable input of the Component Leaders, Bryce Graham (Department of Primary Industries, Parks, Water and Environment) and Dr Fiona Ling (Entura). Fiona and Bryce provided invaluable vision and guidance in directing the scientific activities in the Water and Catchment component to ensure the science outcomes met the needs of the end-user organisations.

The project has become one of the high profile climate change projects under the auspices of the Antarctic Climate & Ecosystems Cooperative Research Centre (ACE CRC).



Roy Adair

Chief Executive Officer, Hydro Tasmania

Executive Summary

Climate Futures for Tasmania has produced sophisticated hydrological projections for Tasmania to 2100.

Climate Futures for Tasmania has combined state-of-the-art regional climate modelling and hydrological models to project future catchment yields for Tasmania. The project has produced runoff projections from an ensemble of six dynamically downscaled global climate models and five runoff models to 2100. River flows were projected for more than 1900 subcatchments in 78 river catchments that cover more than 70% of the state by area. Only changes caused by increases in greenhouse gases were considered and changes in land use or water use were not investigated. The future operations of Tasmania's hydro-electric system and 14 major irrigation storages were also simulated to 2100.

Runoff across Tasmania is projected to increase slightly by 2100.

The statewide annual runoff shows significant decadal variations throughout the 21st century. On average, statewide annual runoff is likely to increase by 559 GL (1.1%) by 2100. Individual climate models project increases in statewide annual runoff of up to 7085 GL (14.6%) or decreases up to 2110 GL (4.2%) by 2100.

In a changing climate, patterns of runoff will differ from the current climate.

Changes to runoff by 2100 vary between different regions. These patterns of change are more important than the relatively small statewide changes. Annual runoff is likely to decrease significantly in Tasmania's central highlands, with 30% less runoff in some areas. On average, annual runoff in eastern areas of the state are generally projected to increase, particularly in the lowlands. Runoff in the lower Derwent Valley is likely to increase, with increases of more than 50% in some areas. Annual runoff is likely to increase in the lower South Esk River and lower Macquarie River catchments, increasing by more than 15% in most areas.

In a changing climate, seasonal runoff is likely to differ markedly from the current climate.

Marked seasonal changes to runoff are likely to occur over the coming century. Annual runoff on the west coast is not projected to change greatly by 2100, however west coast runoff is likely to increase in winter and decrease markedly in summer and autumn. Increases in runoff in the lower South Esk River and the lower Macquarie River are projected to be greatest in winter, increasing by more than 15% in most areas.

In a changing climate, some river flows will decrease and some will increase by 2100.

Of the 78 rivers modelled, on average 32 are projected to have changes to mean annual flows of more than $\pm 10\%$ by 2100. Changes of this size may have implications for water management and infrastructure development. On average, 28 of the 78 rivers modelled are projected to have decreased flows by 2100, while 50 rivers are projected to have increased flows. However, in one climate projection as many as 55 of 78 rivers have decreased flows, while in another climate projection 77 of 78 rivers will have increased flows.

Large irrigation storages fed from runoff from the central highlands are likely to have reduced inflows by 2100.

The likely reduction in runoff to the central highlands will mean reduced inflows to irrigation storages. For example, the mean inflows to Lake Crescent/Sorell and Meander Dam are projected to fall by 20% and 13% respectively. The driest model projections indicated that inflows to Lake Crescent could fall by up to 48%, while inflows to Meander Dam could fall by up to 21% by 2100. Declines in inflows to these storages could affect the reliability of supply to downstream water users who rely on releases from these storages.

Large irrigation storages supplying the Macquarie River and Coal River catchments are projected to experience increased inflows by 2100.

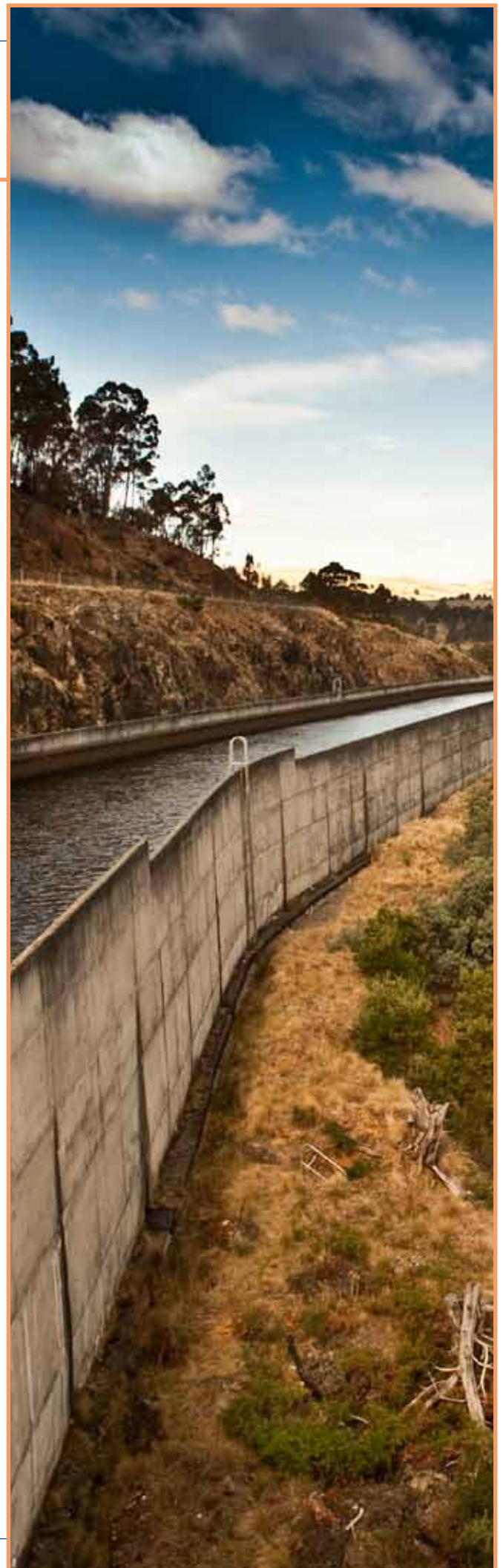
The irrigation storages Lake Leake and Tooms Lake in the Macquarie River catchment are both projected to have increased inflows. Mean inflows to Lake Leake and Tooms Lake are projected to increase by 23% and 25% respectively. Mean inflows to Craigbourne Dam in the Coal River catchment are projected to rise by 24%, although one climate model projected an increase of 83%.

Climate change is likely to reduce inflows to catchments used for hydro-electricity generation throughout the 21st century, and this could reduce the power-generation capacity of the Hydro Tasmania hydro-electric system.

Reduced inflows to catchments supplying hydro-electric power stations could lead to a gradual and continuous reduction in overall power generation capacity throughout the 21st century. Power generation capacity could also be reduced by seasonal and spatial changes to runoff. Declines to inflows in the central plateau catchments are likely to have a marked impact on power generation, because these catchments feed a large-capacity, highly efficient power station. More strongly seasonally delineated inflows in the western catchments are likely to result in lost power generation in run-of-river hydro-electric schemes.

Some catchments experience both increased and decreased runoff in different parts of the catchment.

The fine-resolution modelling allows projections of changes within catchments. Catchments that are fed by the central highlands and flow east generally experience decreased runoff in the upper part of the catchment. These decreases are partially offset by increased runoff in the lower parts. For example, the Derwent catchment is projected to experience an average decline in flows of 5.2% by 2100. Here the increased runoff in the lower Derwent catchment is outweighed by the larger decrease in runoff in the upper parts of the catchment. Conversely, the decrease in runoff in the upper part of the Clyde River catchment is offset by the larger increase in runoff in the lower Clyde catchment, and the Clyde River catchment is projected to experience an average increase in flows of 17%.



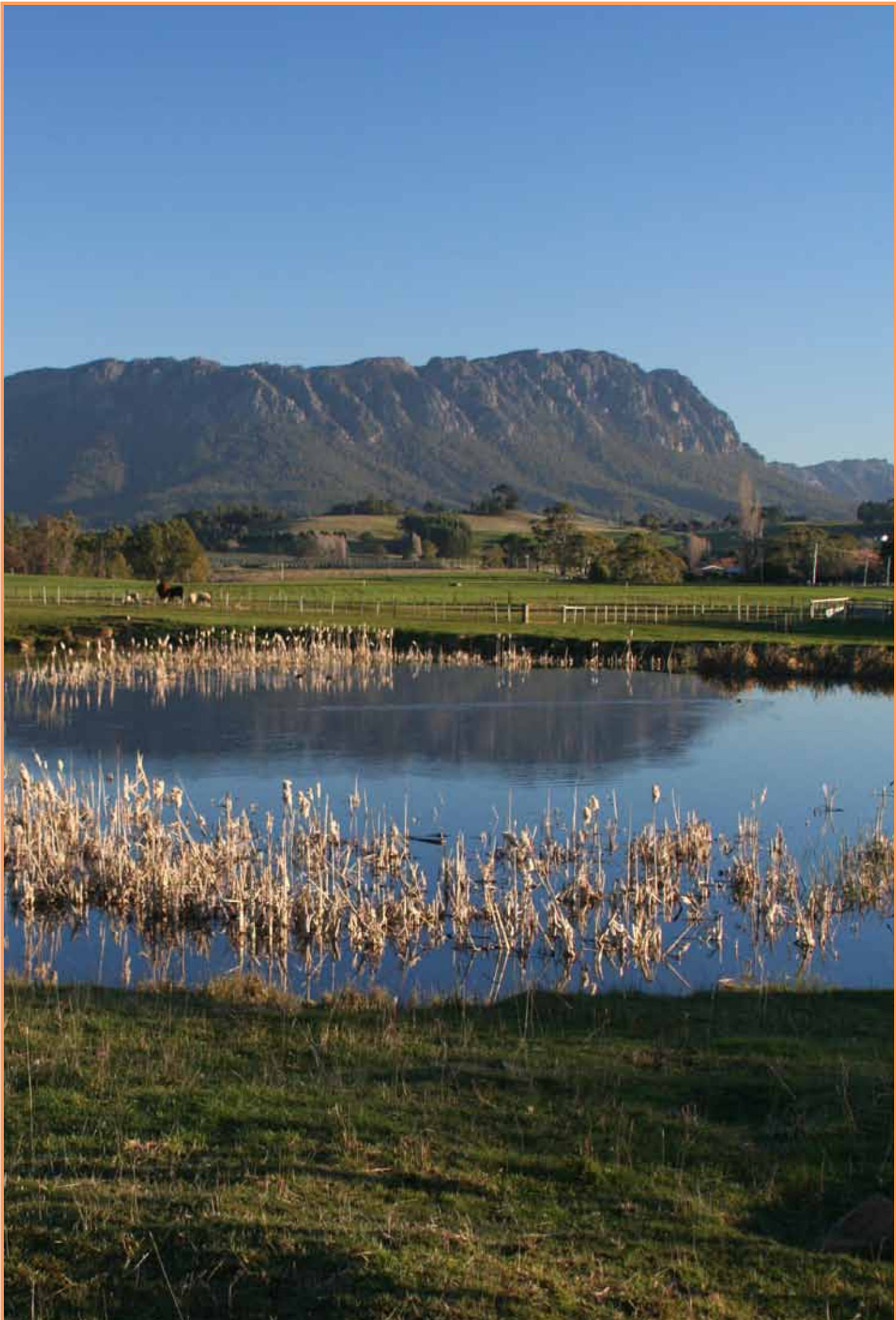
FREQUENTLY USED ABBREVIATIONS

| | |
|---|--------|
| Areal potential evapotranspiration | APET |
| IPCC Fourth Assessment Report | AR4 |
| Australian Water Availability Project | AWAP |
| Bureau of Meteorology | BoM |
| Bureau of Meteorology High Quality Interpolated Dataset | BoM-HQ |
| Conformal Cubic Atmospheric Model | CCAM |
| Creek | Ck |
| Commonwealth Scientific and Industrial Research Organisation | CSIRO |
| Coefficient of Variation | CV |
| Tasmanian Department of Primary Industries, Parks, Water and Environment | DPIPWE |
| Global Climate Model | GCM |
| Highway | Hwy |
| Intergovernmental Panel on Climate Change | IPCC |
| National Electricity Market | NEM |
| Nash-Sutcliffe Efficiency | NSE |
| River | R |
| Queensland Department of Environment and Resource Management gridded interpolated climate observations | SILO |
| Special Report on Emissions Scenarios | SRES |
| Sea Surface Temperature | SST |
| Tasmania Sustainable Yields Project | TasSY |
| Track | Tk |
| Tasmanian Electricity Market Simulation Model | Temsim |
| Tasmanian Partnership for Advanced Computing | TPAC |
| Water Information Management System | WIMS |

Table of Contents

| | |
|---|-----------|
| Foreword | 3 |
| Executive Summary | 4 |
| 1 Introduction | 10 |
| 1.1 <i>Choice of reference and future time periods</i> | 11 |
| 1.2 <i>Runoff and river modelling outputs</i> | 13 |
| 1.3 <i>Terms used in this report</i> | 15 |
| 1.3.1 <i>The central estimate</i> | 15 |
| 1.4 <i>Interpreting projections presented in this report</i> | 16 |
| 1.5 <i>Regions referred to in this report.....</i> | 16 |
| 2 Projecting future river flows | 18 |
| 2.1 <i>Modelling approach</i> | 18 |
| 2.2 <i>Overview of the hydrological modelling program.....</i> | 19 |
| 2.3 <i>Climate projections.....</i> | 20 |
| 2.3.1 <i>Selection of GCMs.....</i> | 20 |
| 2.3.2 <i>Selection of emissions scenario</i> | 20 |
| 2.3.3 <i>Dynamical downscaling.....</i> | 20 |
| 2.3.4 <i>Ability of climate simulations to match recently observed statewide rainfall trends.....</i> | 21 |
| 2.3.5 <i>Downscaled-GCM variables used as inputs to hydrological models.....</i> | 21 |
| 2.3.6 <i>Bias-adjustment</i> | 22 |
| 2.3.7 <i>Regridding climate projections.....</i> | 27 |
| 2.4 <i>Hydrological modelling</i> | 28 |
| 2.4.1 <i>Runoff models</i> | 28 |
| 2.4.2 <i>Temsim.....</i> | 30 |
| 2.4.3 <i>River models</i> | 32 |
| 3 Performance of runoff models | 34 |
| 3.1 <i>Performance of runoff models with downscaled-GCM inputs compared to SILO inputs</i> | 34 |
| 3.2 <i>Performance of Simhyd runoff model with downscaled-GCM inputs.....</i> | 36 |

| | |
|---|-----------|
| 4 Changes to rainfall and areal potential evapotranspiration | 40 |
| 4.1 Historical rainfall..... | 40 |
| 4.2 Projected changes to rainfall..... | 40 |
| 4.3 Areal potential evapotranspiration (APET)..... | 43 |
| 5 Changes to runoff | 44 |
| 5.1 Runoff during the reference period (1961-1990)..... | 44 |
| 5.2 Variation in runoff projections | 48 |
| 5.3 Future runoff..... | 48 |
| 6 Changes to river flows | 56 |
| 6.1 Changes to irrigation storage inflows and reliabilities..... | 61 |
| 6.2 Changes to inflows to the hydro-electric system..... | 64 |
| 7 Future Work..... | 66 |
| References | 68 |
| Appendices | 72 |
| Appendix A Bias-adjustment tests..... | 72 |
| Appendix B Adapting Temsim to operate with downscaled-GCM simulations..... | 76 |
| Appendix C River catchments modelled | 77 |
| Appendix D Change in runoff in millimetres | 80 |
| Appendix E Change in annual river flows by catchment..... | 81 |
| Appendix F Changes to storage inflows | 84 |
| Appendix G Changes to reliability of water supplied by irrigation storages..... | 85 |
| Appendix H Reference period flows and changes to river flows for all downscaled-GCMs by end-of-century | 86 |
| Appendix I Modelling outputs to be made available to researchers..... | 88 |



1 Introduction

The *Climate Futures for Tasmania Water and Catchments Technical Report* is one of a series of technical reports written for the Climate Futures for Tasmania project. The purpose of this project is to supply climate projections and information that will meet the information requirements of Tasmanian state and local governments, local and state businesses, industry and agriculture. These projections will allow policy makers and communities to better understand the risks and opportunities posed by a changing climate.

Climate projections from this project are founded on global climate model (GCM) simulations that have been dynamically downscaled to a high spatial resolution (0.1-degree) over Tasmania to 2100. The dynamical downscaling was performed using CSIRO's Conformal Cubic Atmospheric Model (CCAM) (McGregor & Dix 2008). Dynamical downscaling takes account of the interaction between meteorological systems and Tasmania's rugged topography and geographic factors, including land surface and vegetation type.

The aim of the water and catchments component is to project and analyse changes to surface water yields in Tasmania to 2100. Only changes caused by anthropogenic climate change are considered. Possible future changes to land and water use could also have substantial impacts on Tasmanian catchments, but these are not considered in this report. Groundwater is not considered in this report, while changes to flooding are reported elsewhere (Brown 2011). The purpose of this report is to describe the methods and results of the hydrological modelling performed for this project. Other technical reports describe the climate modelling program and the performance of the downscaled climate simulations against historical observations (Corney et al 2010), future changes to general climate (Grose et al 2010), future changes to climate extremes (White et al 2010), future changes to agriculture (Holz et al 2010), future changes to extreme tides and sea levels (McInnes et al in prep), and future changes to severe winds (Cechet et al in prep).

This project builds on methods developed by a pilot study carried out by the Tasmanian Partnership for Advanced Computing (TPAC) and CSIRO (McIntosh et al 2005). The pilot study was commissioned by Hydro Tasmania to gain a better understanding of the impact of future climate on future power generation. A major recommendation of the pilot study was to downscale multiple GCMs to give a range of plausible climate change projections, a recommendation which

we adopted. We have also significantly increased the involvement of a number of end-users, including the two major water managers in Tasmania, Hydro Tasmania and the Department of Primary Industries, Parks, Water and Environment (DPIPWE). This project complements climate analysis and projections done at the continental scale for the *Intergovernmental Panel on Climate Change (IPCC) Fourth Assessment Report (AR4)* (Christensen et al 2007), at the national scale in the *Climate Change in Australia* report and data tool (CSIRO & Bureau of Meteorology 2007), as well as work done in the south-east Australia region as part of the *South Eastern Australia Climate Initiative (SEACI)*. The work also complements projections of water availability in Tasmania by the *Tasmania Sustainable Yields Project (TasSY)* (CSIRO 2009).

A diverse body of evidence shows that the earth's atmosphere and oceans have warmed since the mid-20th century. The evidence includes rises in temperature records (eg Thompson et al (2008)), rising ocean temperatures (eg Domingues et al (2008)), paleoclimate reconstructions (eg Mann et al (2008)), retreat of glaciers and ice caps (eg Hock et al (2009)), reduced polar ice-sheets (eg Allison et al (2009a)) and rising sea levels (eg Rahmstorf et al (2007)). The IPCC AR4 – probably the most exhaustive review of scientific literature ever conducted – concluded that warming of the climate system was “unequivocal” (IPCC 2007). During this period, emissions of carbon dioxide into the atmosphere elevated atmospheric concentration to the highest level in at least 800,000 years (Lüthi et al 2008). The warming effect of carbon dioxide and other greenhouse gases is consistent with our understanding of atmospheric physics and observations. IPCC AR4 concluded that “most of the observed increase in global average temperatures since the mid-20th century is *very likely* due to the observed increase in anthropogenic greenhouse gas concentrations” (IPCC 2007, their italics).

Increases in atmospheric greenhouse gases change the radiative heat balance of the earth, influencing the entire climate system. A change in global mean temperature is just one effect. Anthropogenic climate change will also cause changes to rainfall, wind, evaporation, radiation and other climate variables. Changes to rainfall and evaporation will manifest in changed river flows. Global climate modelling indicates that the effects of a changing climate will not be evenly distributed around the globe. For example, most GCMs project that rainfall will decline steeply for south-western Australia, while Tasmania sits at a boundary between possible future increases in rainfall and possible future decreases (Christensen et al 2007; Meehl et al 2007, Figure 1.1a and Figure 1.2).

Box 1

About the project

Climate Futures for Tasmania is the Tasmanian Government's most important source of climate change data at a local scale. It is a key part of Tasmania's climate change strategy as stated in the *Tasmanian Framework for Action on Climate Change* and is supported by the *Commonwealth Environment Research Facilities* as a significant project.

The project used a group of global climate models to simulate the Tasmanian climate. The project is unique in Australia: it was designed from conception to understand and integrate the impacts of climate change on Tasmania's weather, water catchments, agriculture and climate extremes, including aspects of sea level, floods and wind damage. In addition, through complementary research projects supported by the project, new assessments were made of the impacts of climate change on coastal erosion, biosecurity and energy production, and tools developed to deliver climate change information to infrastructure asset managers and local government.

As a consequence of this wide scope, Climate Futures for Tasmania is an interdisciplinary and multi-institutional collaboration of twelve core participating partners (both state and national organisations). The project was driven by the information requirements of end users and local communities.

Climate Futures for Tasmania complements climate analysis and projections done at the continental scale for the *Fourth Assessment Report* from the *Intergovernmental Panel on Climate Change*, at the national scale in the *Climate Change in Australia* report and data tool, as well as work done in the south-east Australia region for the *South Eastern Australia Climate Initiative*. The work also complements projections done specifically on water availability and irrigation in Tasmania by the *Tasmania Sustainable Yields Project*.

GCM projections from IPCC AR4 showed that during the 21st century evaporation over Tasmania will increase (Figure 1.1d) and rainfall will decrease (Figure 1.1a), resulting in decreases in soil moisture (Figure 1.1b) and runoff (Figure 1.1c). The 200 km to 300 km grid cell resolution of GCMs means that Tasmania is covered by one or two GCM grid cells. Consequently, the changes projected by GCMs are essentially uniform for the whole state. This uniformity is inconsistent with Tasmanian meteorological and hydrological observations: observed changes to Tasmanian river flows, rainfall and evaporation have not been uniform across the state (eg see Figure 1.3) or across seasons (Bureau of Meteorology 2010).

Tasmanian rivers show a diverse range of hydrological characteristics, from high-discharge mountain streams in the west to ephemeral streams in the east. These differences reflect Tasmania's rainfall distribution. Tasmania's mountainous topography and climate drivers of rainfall lead to a highly uneven rainfall distribution (Grose et al 2010) that is not represented by GCMs (Corney et al 2010). For this reason, the two major earlier Tasmania-specific climate change studies used downscaled GCM projections. The TasSY project used a form of statistical downscaling for 15 GCMs (Post et al (2009) and see Box 2, page 14), while the precursor to this project by McIntosh et al (2005) used an earlier version of CCAM to dynamically downscale the CSIRO-Mk3 GCM. These studies both projected a decrease in rainfall in the east of the state – including the central plateau - by 2030 (Post et al 2009) and 2040 (McIntosh et al 2005). Post et al (2009) projected little change in rainfall in the state's south-west and a decrease in rainfall in the state's north-east, while McIntosh et al (2005) projected increases in rainfall along the length of the west coast. Climate Futures for Tasmania extends the work of McIntosh et al (2005) by downscaling projections to 2100 for an ensemble of six GCMs and using these six projections directly in hydrological models previously used by TasSY (Viney et al 2009b).

1.1 Choice of reference and future time periods

Tasmania has experienced a near statewide decline in rainfall since the mid-1970s (Figure 1.3). The decline has been particularly marked since the mid-1990s, and has led to a decrease in runoff. Viney et al (2009b) reported a statewide decrease in runoff of 7% from modelled historical flows for the period 1997-2007 compared to the long-term average (1924-2007). It is unclear what proportion of the recent runoff decline can be attributed to anthropogenic climate

change. As our project is attempting to assess the impacts of anthropogenic climate change on runoff, it was desirable to minimise any climate change signal present in the reference period. Global average ocean and surface temperatures were lower in the earliest 30-year period available from the simulations (Bindoff et al 2007; Trenberth et al 2007), so 1961-1990 is used as the reference period for comparisons with observations. The reference period of 1961-1990 is frequently used by the climate community and in the IPCC third and fourth assessment reports. Three other periods were used to describe future changes: the near future (2010-2039), medium-term future (2040-2069) and end-of-century (2070-2099). Two additional periods are referred to in this report. One is the period used to train the bias-adjustment (1961-

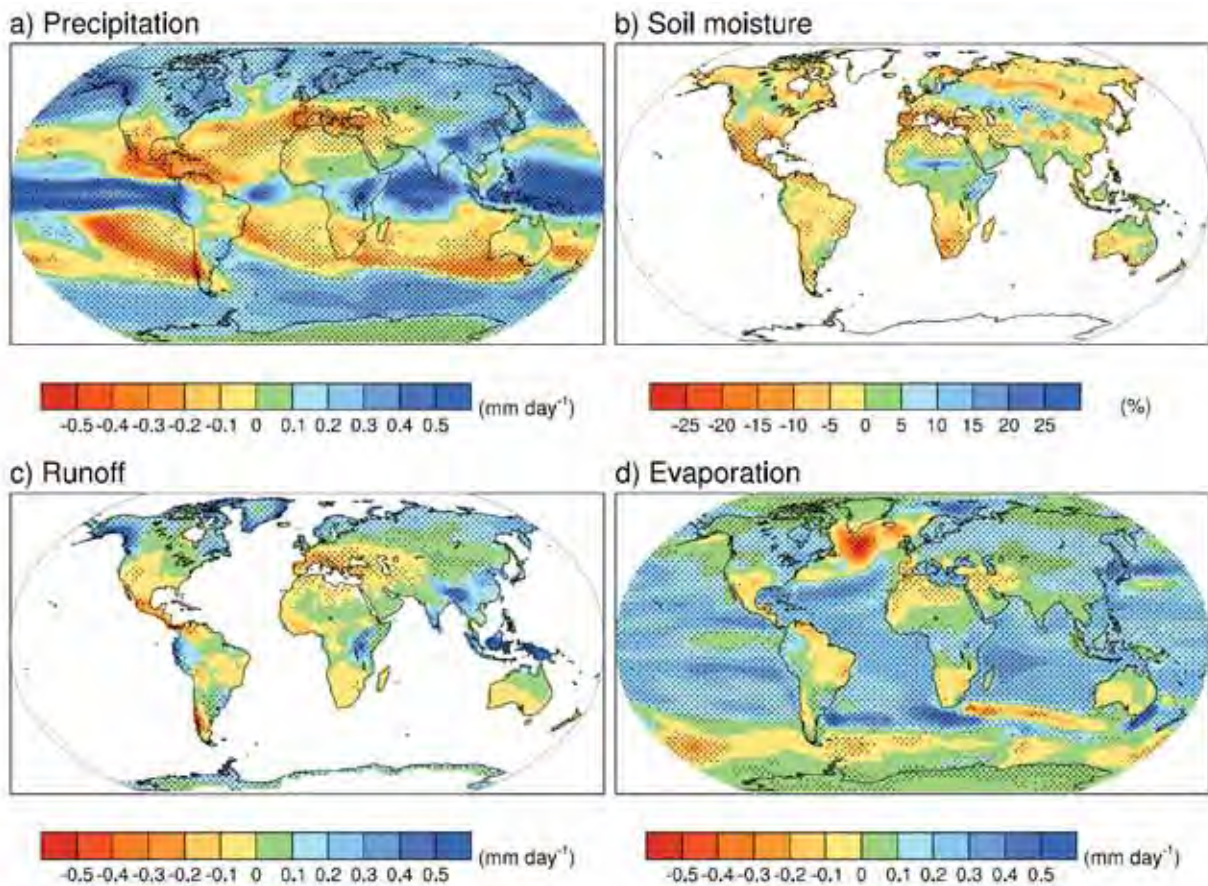


Figure 1.1 Changes in hydrological variables from 23 IPCC AR4 GCMs (Meehl et al 2007). Meehl et al's (2007) description is as follows: "Multi-model mean changes in (a) precipitation (mm.day-1), (b) soil moisture content (%), (c) runoff (mm.day-1) and (d) evaporation (mm.day-1). To indicate consistency in the sign of change, regions are stippled where at least 80% of models agree on the sign of the mean change. Changes are annual means for the SRES A1B [emissions] scenario for the period 2080 to 2099 relative to 1980 to 1999. Soil moisture and runoff changes are shown at land points with valid data from at least 10 models."

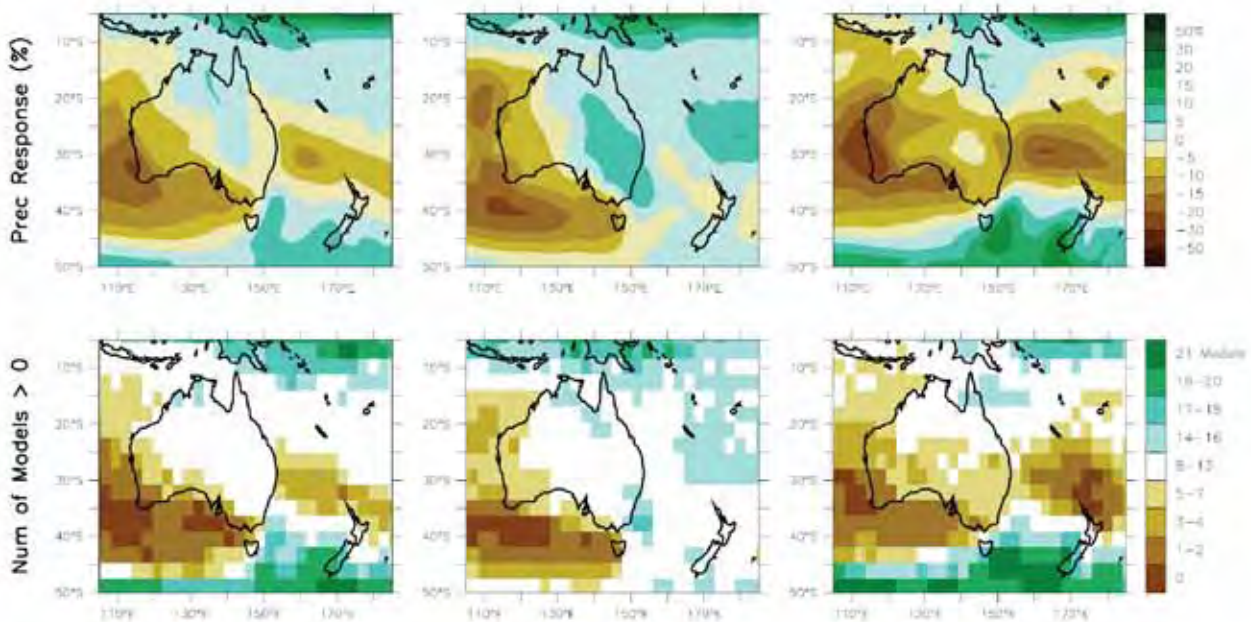


Figure 1.2 Changes in rainfall over Australia and New Zealand from 21 IPCC AR4 GCMs (adapted from Christensen et al (2007)). Description adapted from Christensen et al (2007) is as follows: Precipitation changes over Australia and New Zealand from the Program for Climate Model Diagnosis and Intercomparison A1B simulations. Top row: Annual mean, DJF (summer) and JJA (winter) precipitation change between 1980 to 1999 and 2080 to 2099, averaged over 21 models. Bottom row: number of models out of 21 that project increases in precipitation.

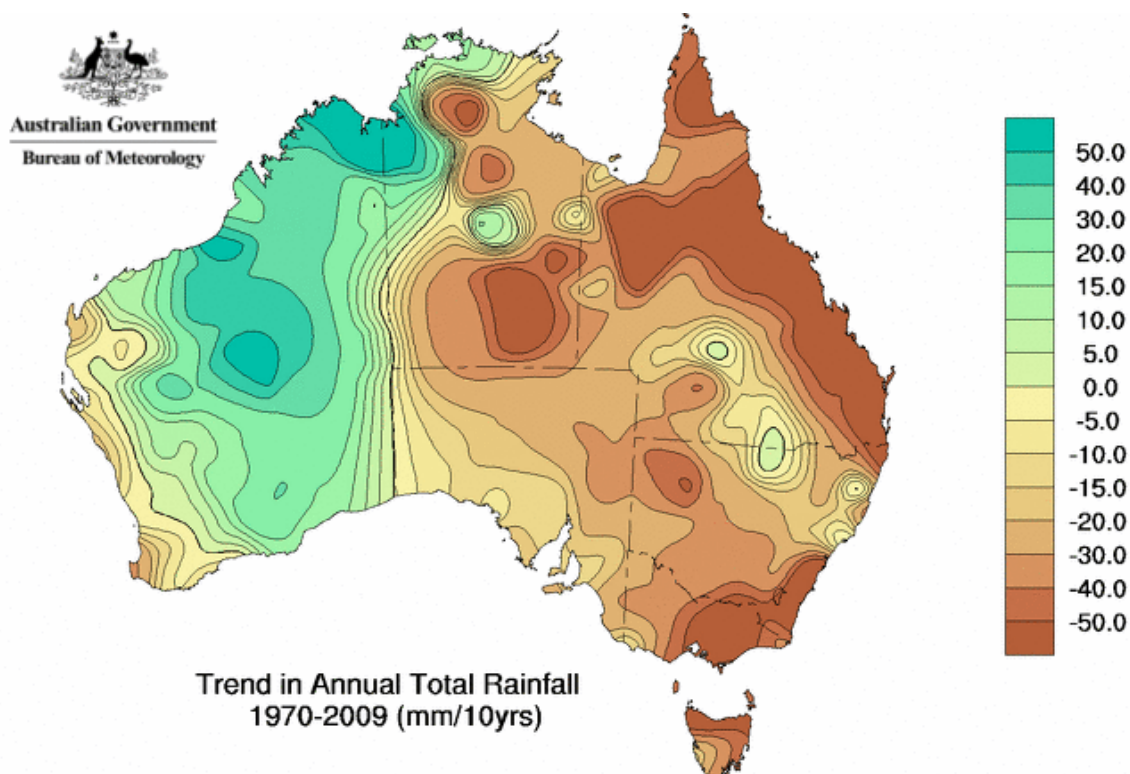


Figure 1.3 Recent trends in Australian Rainfall based on the network of Bureau of Meteorology high-quality observation stations (Bureau of Meteorology 2010).

2007), and the second is the period that Viney (2009b) used to calibrate the hydrological models used in this project (1975-2007). The periods used in this report are shown in Table 1.2.

1.2 Runoff and river modelling outputs

The hydrological models used in this project produced projections of runoff and river flows from an ensemble of dynamically downscaled GCMs. Runoff was simulated at a 0.05-degree grid for the entire state. River flows were projected for more than 1900 subcatchments in 78 rivers that cover more than 70% of Tasmania by area. Inflows, spill, storage levels, losses from evaporation and other metrics were estimated for 14 major irrigation storages. Quantities and reliability of water extractions were calculated for every agricultural region in Tasmania. This report presents only a small proportion of the possible analyses across these catchments. The projections of runoff and river flows constitute a major legacy of the project. The gridded runoff time series outputs produced for this project are freely available from TPAC at www.tpac.org.au.

The final section of this report (Section 7) suggests several possible lines of enquiry and research that could be undertaken with the modelling outputs generated by our project.

Table 1.1 Reference and future periods used in this report.

| Period description | Duration |
|-------------------------------------|-----------|
| Reference period | 1961-1990 |
| Near future | 2010-2039 |
| Medium-term future | 2040-2069 |
| End-of-century | 2070-2099 |
| Training period for bias-adjustment | 1961-2007 |
| Runoff model calibration period | 1975-2007 |

Box 2

The Tasmania Sustainable Yields Project

The CSIRO Tasmania Sustainable Yields Project (TasSY) took a comprehensive assessment of water currently available in Tasmania and assessed water likely to be available to 2030. The project was completed in 2009. TasSY assessed surface water and groundwater, the likely effects of a changing climate on water yields, and the effects of future development of forestry and major irrigation schemes on water yields. In addition, TasSY assessed the impacts of changing water yields on river ecology. TasSY climate scenarios were developed using regression relationships between rainfall and global temperature change combined with spatial patterns taken from Corney et al's (2010) dynamically downscaled projections for the GFDL-CM2.0 downscaled-GCM (Post et al 2009). Historical rainfall and evapotranspiration data were perturbed to reflect the projected changes, and then fed through the hydrological models (Post et al 2009; Viney et al 2009b).

The TasSY surface water models were adapted specifically to assess climate impacts: an ensemble of five runoff models was calibrated, and the models were designed to isolate climate effects on runoff from effects of human regulation of Tasmanian rivers.

TasSY reported on runoff for all of Tasmania, and on river flow in five hydrological regions (Figure 1.4). The TasSY median future scenario projected a statewide reduction in runoff of 2% by 2030 (Viney et al 2009b). Almost no regions showed increases in runoff by 2030, while the largest percentage decreases in runoff were projected to occur on the eastern edge of the central highlands. (Figure 1.5).

Our project builds on TasSY by using dynamically downscaled climate projections as direct inputs to the TasSY hydrological models and extending these projections of runoff and river flows to 2100. Similarities and differences in the projections produced by TasSY and our project are discussed in Box 7 on page 52.

For more information visit
www.csiro.au/partnerships/TasSY.html

Tasmania Sustainable Yields Project



Figure 1.4 Regions for which river flows were reported by the Tasmania Sustainable Yields Project (TasSY). River flows in the west coast region (white) were not reported on. TasSY reported on runoff for all of Tasmania.

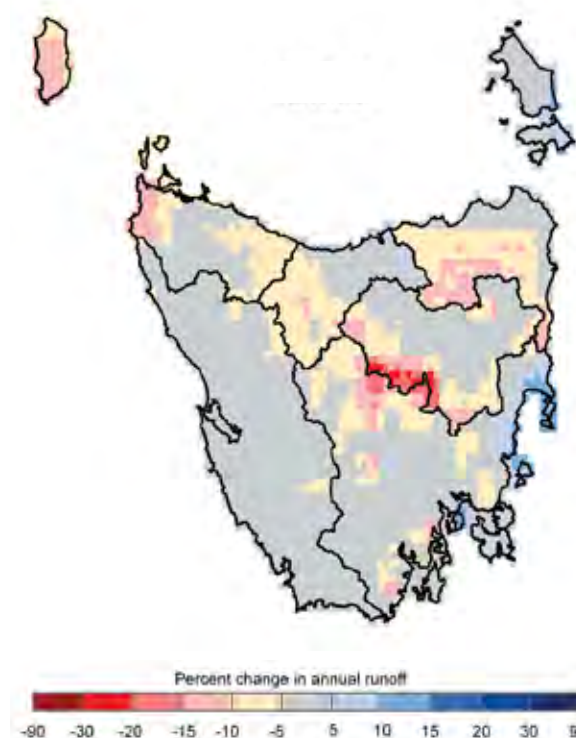


Figure 1.5 Percent change in runoff for 2030 from the Tasmania Sustainable Yields Project for the median warming scenario adapted from Viney et al (2009b).

1.3 Terms used in this report

The projections of water and catchments described in this report have been calculated with five tiers of models: GCMs, the CCAM used to downscale the GCMs, runoff models, the Temsim model that simulates the operation of the Tasmanian hydro-electric system, and river models that simulate flows in 78 rivers. The names of models used for our study are listed in Table 1.2. These models are combined in a variety of ways and the possibilities for ambiguous references to ‘models’ are many.

To avoid ambiguity, we devised a consistent nomenclature. When GCM simulations at their native resolution are discussed, they are simply called *GCMs*. When discussing simulations for a given GCM that have been downscaled to the Tasmanian region, we refer to it as a *downscaled-GCM*. The term *hydrological models* is used to describe the runoff and river models collectively. *Runoff models* describes the models used to calculate daily runoff in millimetres. *River models* describes the models used to aggregate runoff into catchments and account for water extractions, storages and diversions to produce river flow in megalitres per day. The modelling outputs of this study are 140-year time series of daily runoff and river flows for the period 1961-2100. The term *simulation* is used to describe an entire 140-year time series. Any part of the time series occurring in the future (2010-2100) is referred to with the term *projection*.

1.3.1 The central estimate

We have used means from the six downscaled-GCMs to summarise future changes to a given metric. Care is needed when interpreting these mean values. For example, to calculate maximum runoff for 2070-2099 for a particular grid cell, we take the maximum for each downscaled-GCM for that period. To summarise changes to maximum runoff at that grid cell for 2070-2099, the six maxima are averaged to produce a six-downscaled-GCM-mean maximum. Whenever a measure (such as runoff) was averaged across the six downscaled-GCMs in this way, we termed this the *central estimate*.

Averaging projections from an ensemble of climate models is a useful way of summarising changes. It is commonly used in climate studies (for example, throughout IPCC (2007)). Other studies prefer the use of median projections to summarise changes (eg CSIRO (2009)). Numerous recent studies have attempted to ‘weight’ climate models based on various measures of performance to produce more consistent or robust estimates of future change (see discussion in Section 2.3.1), but these studies do not necessarily endorse means over medians, or vice versa.

The climate simulations presented here included natural interdecadal variations that are present in the GCMs. These natural variations might present as a ‘wet decade’ or a ‘dry decade’ at any particular time for a given downscaled-GCM (as occurs in the historical record). When comparing a future period to an historical period for a downscaled-GCM, we risk showing changes that are caused more by inter-decadal oscillations (natural variability) than anthropogenic climate change. For this reason, we have chosen to average projections to define our central estimates. Averaging downscaled-GCMs has the effect of reducing inter-decadal variations present in the individual downscaled-GCMs, meaning that the changes shown are more likely to be caused by anthropogenic climate change.

The central estimate should not be considered in isolation, but should be considered alongside the entire ensemble of projections, as discussed in Section 1.4 over page.

Table 1.2 Model types and names used to produce runoff projections.

| Global climate models | Downscaling model | Runoff models | Hydro-electric system model | River models |
|-----------------------|-------------------|---------------|-----------------------------|--------------------|
| CSIRO-Mk3.5 | CSIRO-CCAM | AWBM | Temsim | CSIRO/Entura-TasSY |
| ECHAM5/MPI-OM | | IHACRES | | |
| GFDL-CM2.0 | | Sacramento | | |
| GFDL-CM2.1 | | Simhyd | | |
| MIROC3.2(medres) | | SMAR-G | | |
| UKMO-HadCM3 | | | | |

1.4 Interpreting projections presented in this report

The central estimate is used throughout this report to summarise projected changes in runoff and river flows, as well as to measure the performance of the simulations. However, the central estimate is no more or less plausible than any of the simulations by individual downscaled-GCMs. We have assumed that all simulations have equal weight (or plausibility) (see Section 2.3.1).

This implies that the entire range of projections should be considered by water managers and other interested parties before making any management

decisions. In instances where all (or most) of the projections agree, this task is not difficult. However, where projections diverge, we advise a precautionary approach. For example, if water managers wish to assess the viability of an irrigation scheme in a non-stationary climate, the precautionary approach would mean that the scheme should only be considered viable if it can supply water in the driest projection.

1.5 Regions referred to in this report

Regions referred to in this report are shown in Figure 1.6.

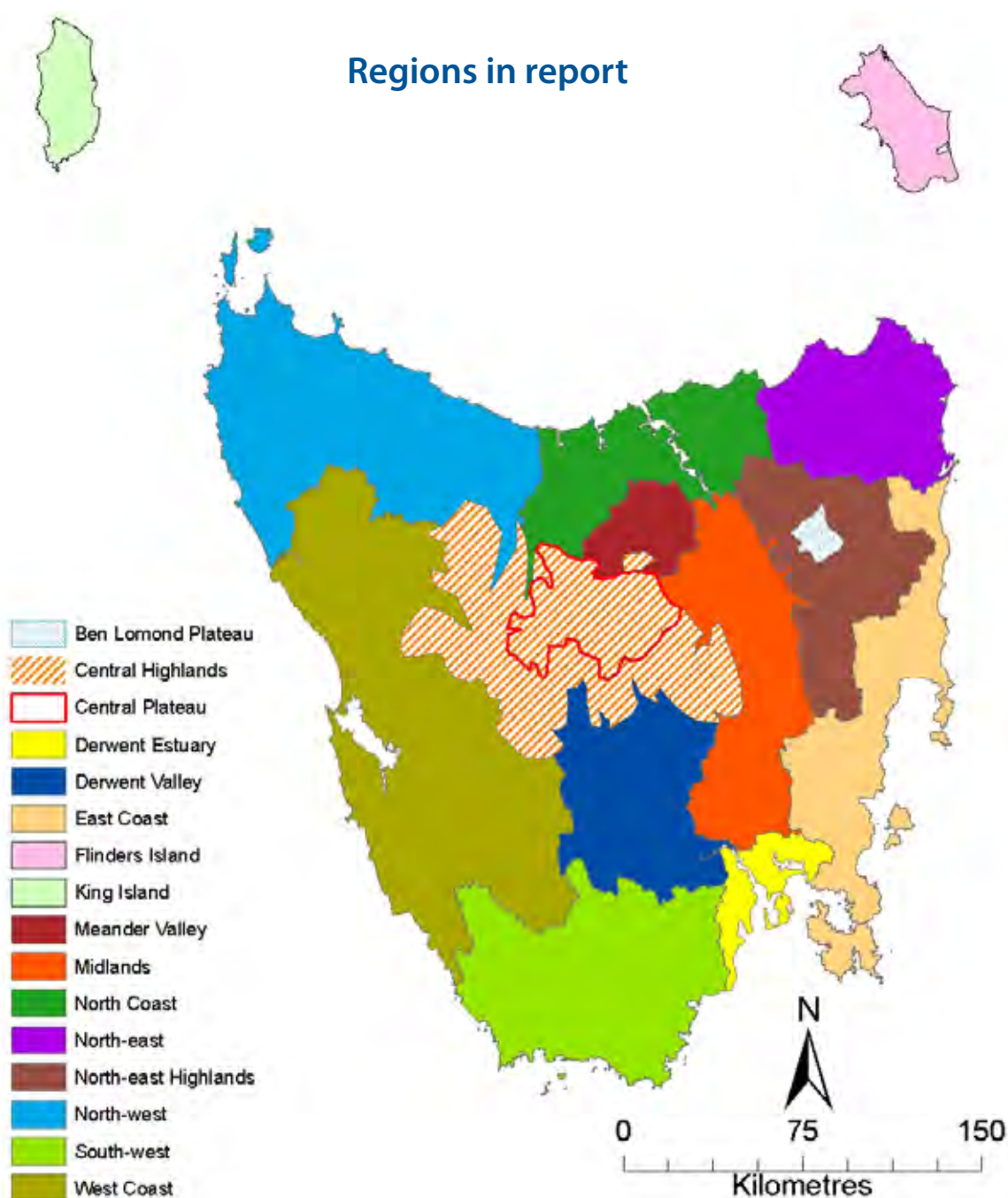
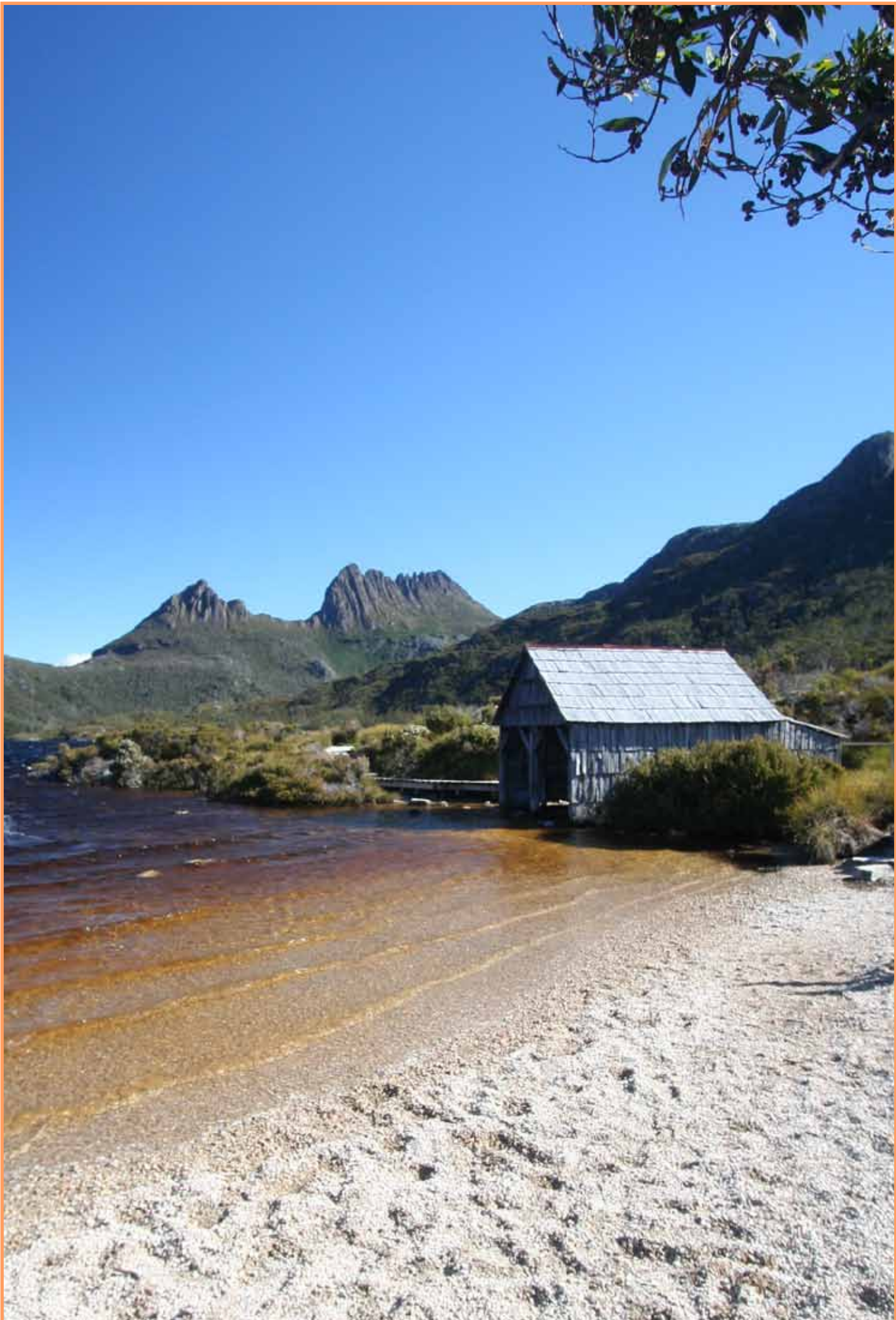


Figure 1.6 Regions referred to in this report.





2 Projecting future river flows

2.1 Modelling approach

Fine-resolution dynamical downscaling of global climate models (GCMs) provides a wealth of information on future changes to hydrological characteristics over catchment areas. Downscaled-GCMs not only project changes to mean rainfall and mean areal potential evapotranspiration (APET), but also project changes to climate drivers of rainfall/APET and the timing and duration of rainfalls. Duration of dry spells is also an important determinant of river flows, and changes to duration are projected by the downscaled-GCMs. The most direct way to use all the information provided by the downscaled-GCM projections to assess hydrological impacts is to use the downscaled-GCM projections as direct inputs to hydrological models.

Several studies have achieved realistic river flows using bias-adjustment of climate model variables (eg Wood et al (2004), Fowler and Kilsby (2007)). Fowler et al (2007) noted that in addition to incorporating temporal changes to rainfalls, the use of bias-adjusted downscaled-GCM projections as direct inputs to hydrological models has the benefit of preserving the “physical correlation between precipitation and temperature”. In order to make best use of the fine-resolution climate projections produced by Corney et al (2010) to assess hydrological impacts, we have chosen to use bias-adjusted downscaled-GCM projections directly in hydrological models. This approach to projecting river flows is not commonly used in Australia, and accordingly is carefully validated and tested using the simulations during the reference period (Section 2.3.6 and Section 3).

Corney et al (2010) showed that CCAM matched spatial and seasonal patterns of observed rainfall very well. CCAM's ability to replicate selected SILO rainfall characteristics is described in Section 2.3.6. Grose et al (2010) showed that projected regional changes in rainfall were consistent with changes to known regional climate drivers such as the position of the subtropical ridge of high pressure, the frequency of the southern annular mode and the incidence of atmospheric blocking.

Any bias-adjustment has the potential to constrain or disrupt the spatial and temporal relationships that CCAM maintains between (and within) climatic variables. For example, rain falling on a given day will affect APET (and vice versa) following CCAM's internally consistent physical processes. Because

Modelling approach

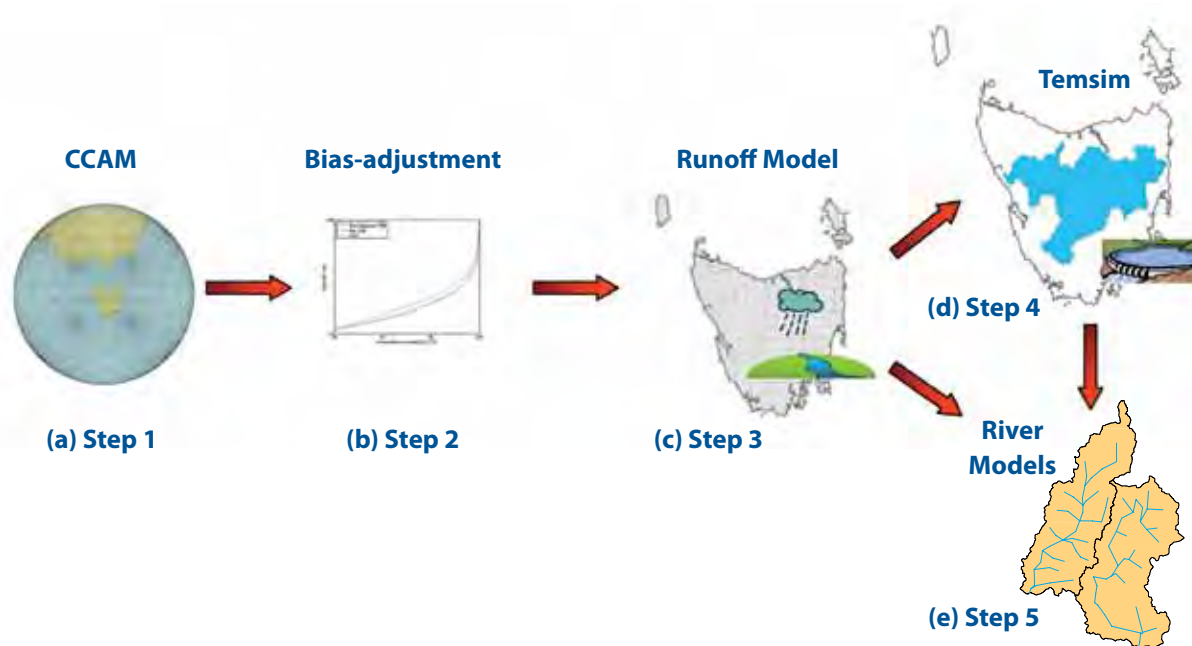


Figure 2.1 Steps taken to project future runoff and river flow: (a) dynamically downscaling GCM projections with CCAM (Section 2.3); (b) bias-adjusting CCAM outputs (Section 2.3.6); (c) runoff modelling (Section 2.4.1); (d) Temsim hydro-electric system modelling (Section 2.4.2); (e) river modelling (Section 2.4.3).

these variables are bias-adjusted independently, we risk altering their relationship in an unrealistic way. For this reason, it is important that bias-adjustment is kept as simple and as unintrusive as possible. We chose quantile-quantile bias-adjustment for the following reasons: it is simple, relatively easy to calculate and interferes minimally with climate model outputs (see Section 2.3.6). At the same time, it allows hydrological models driven by bias-adjusted climate model output to perform realistically (see Section 3).

2.2 Overview of the hydrological modelling program

Future river flows were modelled by adapting downscaled-GCM projections for use in existing hydrological models and aggregating runoff into river catchments. The hydrological models had been recently calibrated for the TasSY project by Viney et al (2009b). For convenience, we have broken the hydrological modelling program into the five steps shown schematically in Figure 2.1. Each step is described separately:

- Step 1 Figure 2.1a: GCM projections were dynamically downscaled using CCAM as described by Corney et al (2010) and reviewed in Section 2.3.
- Step 2 Figure 2.1b: downscaled-GCM projections were bias-adjusted and regridded to be compatible with the runoff models, described in Section 2.3.6.
- Step 3 Figure 2.1c: climate projections were converted to runoff, described in Section 2.4.1.
- Step 4 Figure 2.1d: runoff was aggregated to catchments used for Tasmania's hydro-electric system and used to model the future operation of the hydro-electric system, described in Section 2.4.2.
- Step 5 Figure 2.1e: runoff was aggregated to river subcatchments and combined with hydro-electric power station outflows to model river flows, described in Section 2.4.3.

2.3 Climate projections

2.3.1 Selection of GCMs

Corney et al (2010) selected the six GCMs listed in Table 1.2 primarily on how well they replicated Australian rainfall according to Smith and Chandler (2009). Smith and Chandler nominated five GCMs that scored well in a range of performance measures for replicating rainfall over Australia. Outputs from four of these GCMs, ECHAM5/MPI-OM, GFDL-CM2.0, GFDL-CM2.1 and UKMO-HadCM3, were available for downscaling by Corney et al (2010). The fifth GCM nominated by Smith and Chandler was MIROC3.2(hires), but outputs from this model were not available for the A2 emissions scenario. MIROC3.2(medres) was chosen instead. MIROC3.2(medres) has the same dynamical core as the hires version of MIROC3.2. While MIROC3.2(medres) did not rate highly in all the performance metrics used by Smith and Chandler, Smith and Chiew (2009) ranked MIROC3.2(medres) in their best five performing GCMs. The sixth GCM downscaled by Corney et al (2010), CSIRO-Mk3.5, was included because it was the premier Australian GCM available. CSIRO-Mk3.5 was not assessed by Smith and Chandler (2009) nor Smith and Chiew (2009); both these studies assessed the earlier CSIRO-Mk3 version of this GCM. Neither study ranked CSIRO-Mk3 highly. However, Gordon et al (2010) showed that CSIRO-Mk3.5 performed better than CSIRO-Mk3 in a number of metrics, such as improved replication of the El Niño Southern Oscillation (ENSO). Watterson (2008) ranked CSIRO-Mk3.5 slightly higher (12th) than CSIRO-Mk3 (=13th) on model skill, and gave CSIRO-Mk3.5 a similar skill score to UKMO-HadCM3 and MIROC3.2(medres). In short, there is no obvious reason to weight or exclude any of the six GCMs. In addition, since we are only using sea-ice and bias-corrected sea surface temperatures (SSTs) from the GCMs (see Section 2.3.3), no atmospheric information from the GCM is directly used in the downscaling process. Therefore, weighting or excluding the results based upon the GCMs performance is not appropriate. The range of results from the six GCMs allows a more realistic assessment of the uncertainty of future climate projections and impacts.

2.3.2 Selection of emissions scenario

Corney et al (2010) downscaled projections for two scenarios of future greenhouse gas emissions: a high emissions scenario (A2), and a lower emissions scenario (B1) (see Nakićenović & Swart (2000) for detailed descriptions of the emissions scenarios). Nakićenović & Swart developed one higher emissions scenario (A1FI), however projections from this scenario were not available for the six GCMs used in this project. We have used only the A2 greenhouse gas emissions scenario for the runoff and river flow projections, as it was only possible to run one set of projections through the hydrological models in

the time available for this study. The A2 emissions scenario is the highest emissions scenario for which IPCC GCM projections were available, and was chosen because it matches the observed rate of greenhouse gas emissions since 2000 better than the B1 emissions scenario (Allison et al 2009b).

2.3.3 Dynamical downscaling

Corney et al (2010) dynamically downscaled six IPCC AR4-class GCMs for the Tasmanian region. The six GCMs downscaled are listed in Table 1.2. Corney et al (2010) used the CSIRO Conformal Cubic Atmospheric Model (CCAM) to dynamically downscale these six GCMs to a fine resolution of 0.1 degrees, or approximately 10 km by 10 km grid cells, over Tasmania. CCAM is a global atmospheric model that uses a stretched grid to increase the grid resolution (and thus shrink the size of grid cells) over the region of interest. Because it is a global model, CCAM does not have lateral boundaries like nested limited-area dynamical models. CCAM has only one boundary: the ocean. CCAM was forced only by GCM sea surface temperatures (SSTs) and sea ice concentration. Biases inherent in GCM SSTs were removed using a simple additive bias-adjustment method that ensured that all GCMs were able to describe the observed climate during the reference period (Corney et al 2010). Removing GCM SST biases meant that the fine-resolution modelling could more accurately simulate mean sea-level pressure and the interaction of regional weather systems with local topography and land surfaces.

The dynamical downscaling method used by Corney et al (2010) offers three major benefits for our hydrological study:

1. Bias-adjusting the GCM SSTs before downscaling improves the representation of the current climate in the downscaled-GCMs while retaining the climate variability and climate change signal from the GCMs.
2. The downscaled-GCM outputs simulate spatial distributions of interpolated rainfall observations and other climate variables far better than GCM projections (Corney et al 2010).
3. CCAM simulates regional weather systems and their interaction with Tasmanian topography. In a warmer and more moist future, climate drivers of Tasmanian rainfall are free to vary in CCAM according to current understanding of meteorology and atmospheric physics (Grose et al 2010).

2.3.4 Ability of climate simulations to match recently observed statewide rainfall trends

Climate model simulations will replicate the natural variability of observations to some degree, however they will not replicate this variability in phase with observations. This means that natural variations in the models will not appear with the same timing as in observations. However, the downscaled-GCM simulations should respond to changes in greenhouse gas concentrations, direct aerosol effects and ozone – that is, a ‘climate change signal’ should be transmitted through the modelling outputs, to the extent that it is present. The central estimate of statewide rainfall simulations shows a small decline in Tasmanian total annual rainfall over the period 1961-2007, but this is less than the decline that appears in Bureau of Meteorology high-quality observations, particularly during autumn (Grose et al 2010). (A similar dissonance in observed and modelled trends is echoed in statewide annual runoff, described in Section 5.) There is some uncertainty in trends of statewide annual rainfall calculated from interpolated observations, as discussed in Section 4.1. The relative contributions of natural variability and climate change to the observed rainfall decline since the 1970s in south-east Australia and Tasmania (Figure 1.3) are still not clear and are the subject of ongoing research. The projections used in our study show no clear trend in statewide rainfall, even in future conditions where the effects of anthropogenic climate change are much stronger than experienced in the past 30 years (Grose et al (2010), and see Section 4). This indicates that the recent decline in statewide rainfall is not a harbinger of Tasmanian rainfall trends in the 21st century. Spatial and seasonal changes to rainfall are much more pronounced than statewide changes, however, and these are discussed in Section 4.

2.3.5 Downscaled-GCM variables used as inputs to hydrological models

The runoff models require two inputs: daily rainfall and daily areal potential evapotranspiration (APET). Daily rainfall is a direct output generated by CCAM. Pan evaporation is also generated by CCAM, but this variable is not suitable for use in the runoff models because Viney et al (2009b) calibrated the runoff models to Morton’s wet APET (Morton 1983).

Morton’s wet APET (mm) was calculated according to Equation 1:

Equation 1

$$APET = b_1 + b_2 \frac{\Delta_p}{\Delta_p + \gamma_p} R_p$$

where Δ_p (mbar.°C⁻¹) is the slope of saturation vapour pressure-temperature curve at equilibrium temperature, R_{np} (W.m⁻²) is the net radiation at

equilibrium, γ_p (mbar.°C⁻¹) is the psychrometric parameter, and b_1 and b_2 are empirically derived constants. The methods for the derivation of all parameters and constants are described by Morton (1983). In all instances, parameters and constants were identical to those used in the TasSY project (J Teng, pers comm, 9 July 2009). This ensured that APET values from CCAM were as similar as possible to APET values used to calibrate the hydrological models.

The inputs required to calculate all the parameters in Equation 1 are temperature, vapour pressure and solar radiation. Temperature and radiation are direct outputs from CCAM, however vapour pressure is not. Accordingly, vapour pressure was calculated at daily maximum temperature (Tmax) and daily minimum temperature (Tmin) by converting relative humidity simulated by CCAM according to Equation 2 and Equation 3:

Equation 2

$$e_{OT} = A \times \exp\left(K_1 \times \frac{T}{T + 273.16 - K_2}\right)$$

where e_{OT} is the vapour pressure (in kilopascals) at temperature T (°C), and A , K_1 and K_2 are empirically derived constants, defined as $A=0.611$, $K_1=17.27$, and $K_2=35.86$ (after Murray (1967)). Daily vapour pressure was then calculated from Equation 3:

Equation 3

$$e_d = \frac{RH_m}{\frac{50}{e_{OT \min}} + \frac{50}{e_{OT \max}}}$$

where RH_m is daily average relative humidity (%) taken from CCAM.

Morton’s wet APET does not account explicitly for wind. Wind is an important driver of evaporation and may explain recent declines in measured evaporation for continental Australia (Donohue et al 2010). The scarcity of wind observations over Tasmania makes the task of teasing apart the relative importance of wind on evaporation very difficult. The influence of wind on projections of evaporation generated by CCAM is unclear. Grose et al (2010) reported a slight decrease in the central estimate of wind over Tasmania by 2100. However, pan evaporation projections from CCAM, which account for changes in wind, showed much greater increases by 2100 than the Morton’s wet APET projections used in this report. This indicates that the decrease in mean wind speed had little effect on pan evaporation (in both absolute (mm) and proportional (%) terms – see Grose et al (2010)).

2.3.6 Bias-adjustment

Choice of interpolated observations

Other technical reports for this project use interpolated rainfall observations from the Australian Water Availability Project (AWAP) (Jones et al 2009). However, the runoff models used in our water and catchments study were calibrated to interpolated observations from the SILO dataset (Jeffrey et al 2001) (www.longpaddock.qld.gov.au/silo). Preliminary testing indicated that AWAP (accessed March 2009) was less compatible with the runoff models than SILO (not shown). This is unsurprising as SILO had been used to calibrate the runoff models. For compatibility with the hydrological models, SILO was used as the training dataset to create the bias-adjusted inputs to the runoff and river models.

SILO is interpolated from Bureau of Meteorology (BoM) weather stations. The accuracy of any interpolated dataset is limited by the number and spatial distribution of observations. BoM rain gauge stations have reasonably dense coverage in the east and north of the Tasmania, and there has been no substantial change in the number of BoM rainfall stations in Tasmania in the 1961-2007 period used to train the bias-adjustment (Figure 2.2). Coverage of unpopulated areas of Tasmania – the west coast, the south-west and the western part of the central highlands - is poor in relation to the rest of the state. SILO interpolated data may be less accurate in these areas.

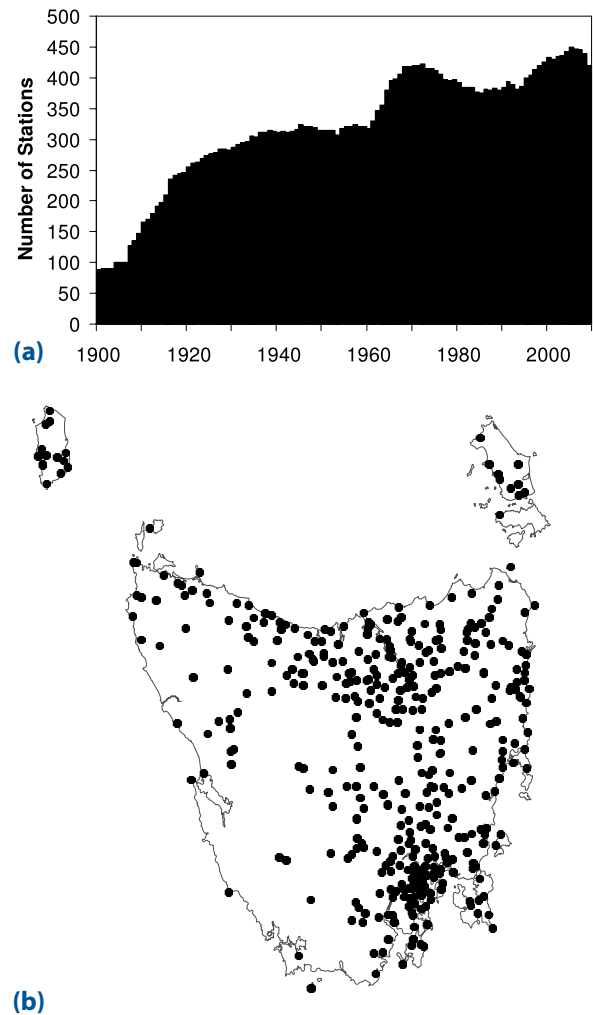
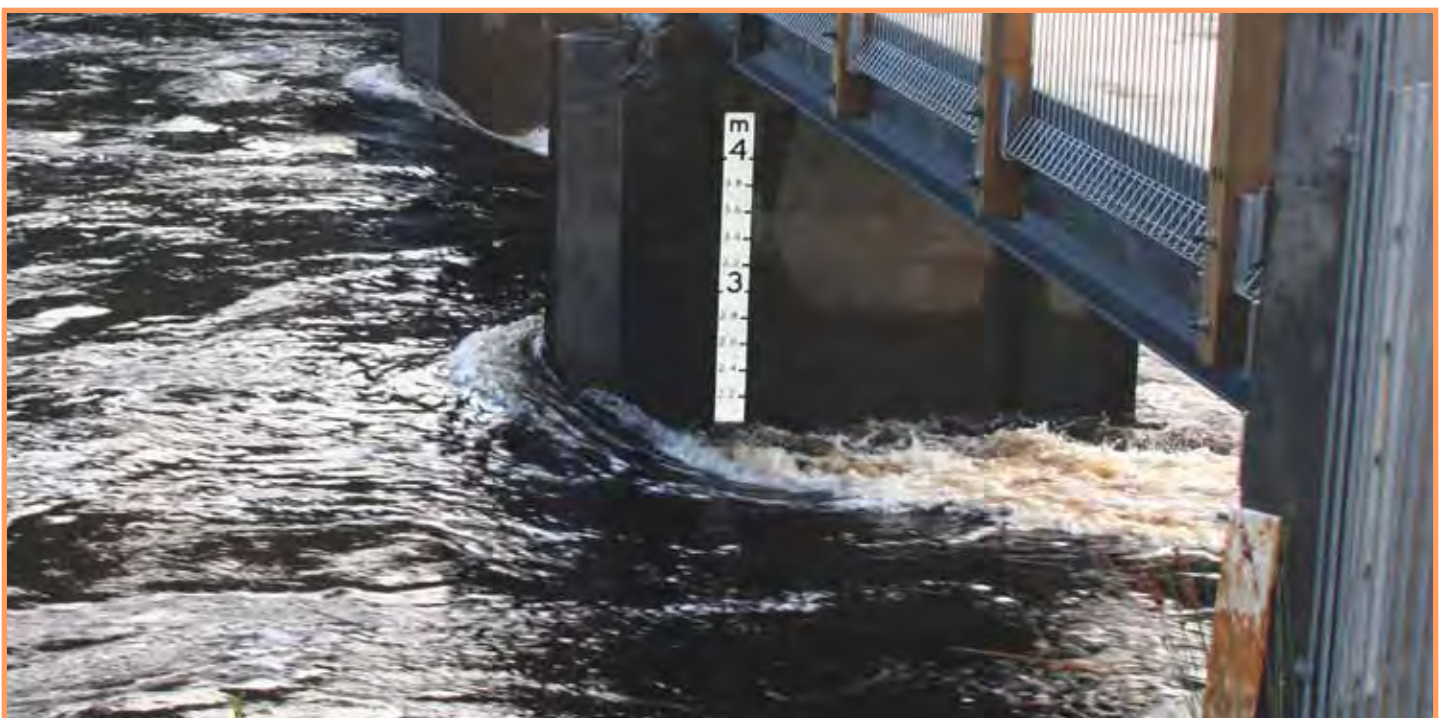


Figure 2.2 Bureau of Meteorology (BoM) rain gauge stations in Tasmania. Histogram (a) shows number of rain gauge stations operating in Tasmania since 1900, map (b) shows current extent of the BoM rain gauge network.



Quantile-quantile bias-adjustment

Downscaled projections replicate the general spatial distribution of SILO historical mean annual rainfall with a good degree of accuracy without any bias-adjustment (Figure 2.3a, Figure 2.3b and see Corney et al (2010) for comparisons of a number of relevant metrics to other interpolated observations). However, there are still substantial biases in annual and monthly rainfall totals in some regions. Biases of up to 150% in mean annual rainfall were present in some areas (notably in the Tamar basin, extending from the northern midlands to the Meander Valley and the north coast) (Figure 2.3c and see Corney et al (2010)). These biases preclude the use of climate modelling output as direct inputs to the hydrological models. To enable us to use the climate projections directly in the hydrological models, we bias-adjusted rainfall projections (Corney et al 2010).

APET calculated from downscaled variables had much smaller biases than those found for rainfall (not shown). However, for consistency we bias-adjusted both rainfall and APET to SILO gridded data using 1961-2007 as the training period.

Other studies have used a variety of techniques to bridge the divide between climate models and hydrological models. These range from relatively simple techniques such as explicitly correcting for the number of rain days and rainfall variability (van Pelt et al 2009) to complex statistical models like so-called 'weather generators' (see review by Maraun et al (2010)). Quantile-quantile bias-adjustment has the advantage of being relatively

simple to calculate, but also capable of successfully correcting (both implicitly and explicitly) important characteristics of rainfall.

Ines and Hansen (2006) pointed out that by correcting for intensity and frequency, the quantile-quantile adjustment corrects the quantity of rainfall implicitly (as the quantity simply equals intensity multiplied by frequency). They showed the method could be successfully applied to daily GCM rainfall outputs. Quantile-quantile bias-adjustment has also been shown to correct implicitly for temporal characteristics of rainfall and has been applied successfully to correct regional climate model daily rainfall outputs over Europe (Piani et al 2010).

Quantile-quantile bias-adjustment forces the frequency distributions of modelling outputs over the training period to be very similar to the frequency distributions of observed climate. Our method assumes:

1. Adjustments for the training period are the same in future periods.
2. The choice of training period will not substantially affect the future variable values.
3. Any adjustment could alter projected changes to frequency distributions of climate variables.

We address each of these assumptions on the following page.

Rainfall biases

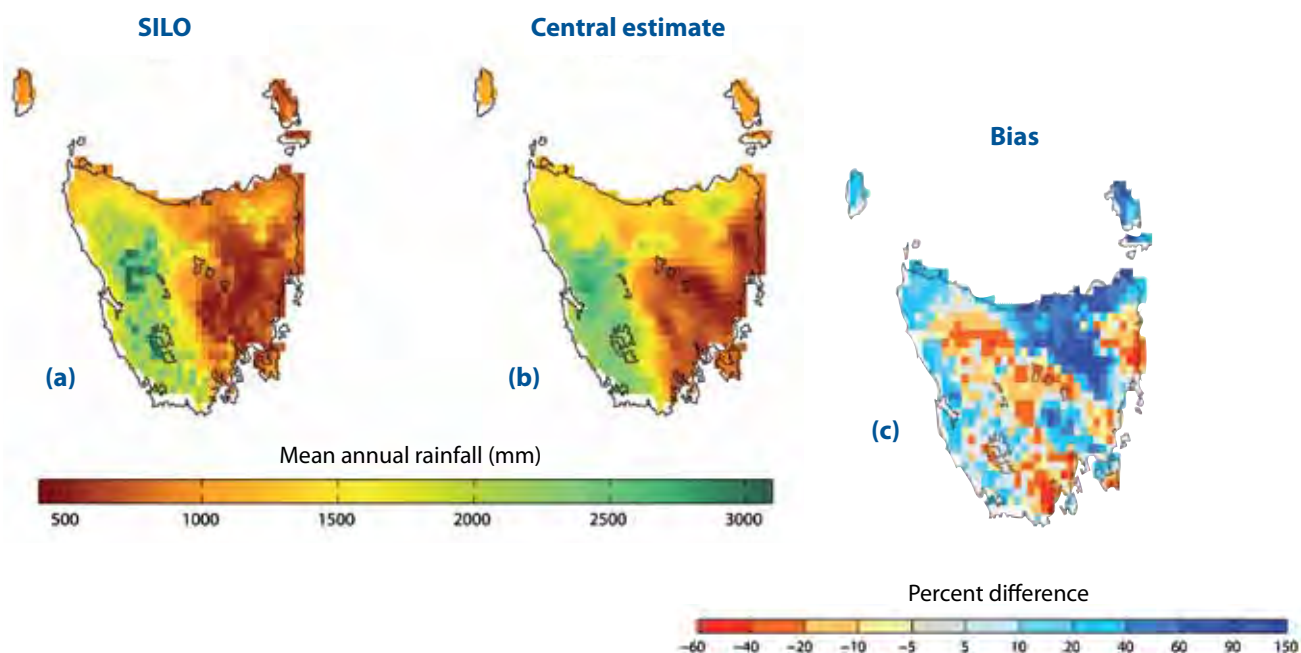


Figure 2.3 Mean annual rainfall 1961-2007 represented by (a) SILO (regridged to 0.1-degree grid) and (b) Unadjusted central estimate (0.1-degree grid). Climate model bias is shown in (c).

To ensure that any changes in frequency distributions of rainfall and evaporation were preserved, we chose a quantile-quantile bias-adjustment similar to that described by Wood et al (2004). The adjustment was performed independently for each downscaled-GCM. Our method followed these steps:

1. SILO data were regridded from a 0.05-degree grid to a 0.1-degree grid to be compatible with the 0.1-degree gridded climate modelling outputs. This step was taken as it was significantly computationally and logistically simpler than adjusting the climate data to 0.05-degree SILO data, and still yielded acceptable results (see Section 2.3.7 and Section 3). However, it had the disadvantage of reducing the spatial variability inherent in the SILO 0.05-degree dataset. Consequently, this reduced the spatial variability of the bias-adjusted modelling outputs. This problem is discussed further in Section 2.3.7.
2. Adjustments were carried out for each season. We split observed and modelled time series for each grid cell into summer (December, January, February), autumn (March, April, May), winter (June, July, August) and spring (September, October, November).
3. We calculated percentile values for each grid cell for both observed and modelled seasonal data (including no-rain days) from the period 1961-2007. Each modelled percentile value was multiplied by a factor so that it exactly matched the corresponding observed percentile value. These factors are called 'adjustment factors' for convenience. The result was a table of 100 adjustment factors for each downscaled-GCM, for each variable, for each season and for each grid cell.
4. To avoid eliminating any climate trends from the climate simulations with the adjustment, we detrended all (140-year) modelled time series by subtracting 30-year running means. All detrended time series values were then assigned to a percentile 'bin'. Each bin was one percentile wide and centred on each half percentile value. For example, the bin for the 50.5th percentile contained any values falling between the 50th percentile and the 51st percentile. Each value was assigned an index identifying the bin in which it fell, and the index was transferred to the original (undetrended) time series. Adjustment factors were not calculated for the zeroth and 100th percentiles.
5. Values falling in each bin were multiplied by the corresponding adjustment factor. Zeroth percentile values were scaled by the adjustment factor calculated for the 0.5th percentile, while values at the 100th percentile were scaled by the adjustment factor calculated for the 99.5th

quantile. Figure 2.4a gives an example of a rainfall non-exceedance probability curve adjusted to better match observed data and Figure 2.4b shows how the projection was adjusted for a future period.

Bias-adjustment

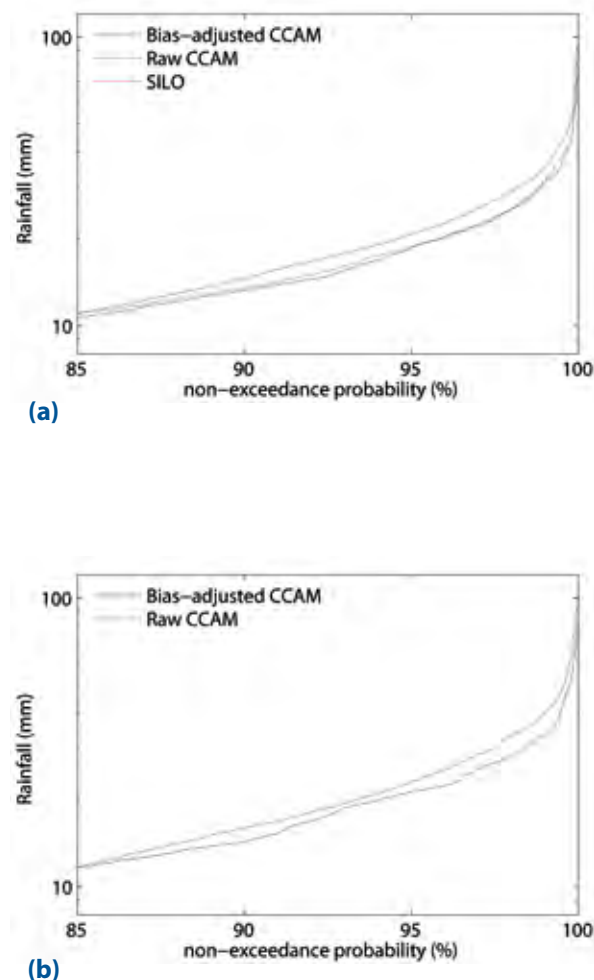


Figure 2.4 Examples of bias-adjusted annual exceedance curves compared to unadjusted CCAM rainfall for a single grid cell located at Launceston Airport for the GFDL-CM2.1 downscaled-GCM. Only higher rainfalls (>85% non-exceedance probability) are shown to illustrate the effect of the bias-adjustment: (a) adjustment of exceedance curve for the historical period 1961-1997 (b) adjustment of rainfall exceedance curve for the period 2070-2099.

The frequency distribution of daily rainfall data is skewed because of the many days on which no rain falls. Matching the tails of rainfall frequency distributions, as our method of bias-adjustment attempts to do, can present problems at lower percentiles where modest differences can require large adjustments because of the small magnitudes of rainfall. For example, if the 60th percentile of observed rainfall at a given site is 0.1 mm and the modelled value is 0.01 mm, this would require an adjustment factor of 10, despite an insignificant amount of rainfall. Any future changes at the 60th percentile would then be unjustifiably magnified by the bias-adjustment.

To mitigate this problem, rainfall values of less than 0.2 mm were set to zero in all modelled and observed datasets, both before and after the bias-adjustment. The 0.2 mm threshold was chosen as this is the limit of resolution for BoM rain gauges (a day with less than 0.2 mm of rain will not be recorded as a rain day by the BoM). Because SILO is interpolated from BoM observations, it is reasonable to apply this resolution limit to the SILO dataset. The same limit was applied to the downscaled-GCM outputs for consistency.

The bias-adjustment partly ameliorates differences in the number of rain days in the downscaled-GCM output and in the observations. Whenever there are more rain days in the downscaled-GCM output, these are forced to become no-rain days by the bias-adjustment. However, bias-adjusted rainfall simulations can still overpredict the number of rain days during the training period (1961-2007), because the adjustment is applied to rainfall distributions calculated from 140 years of simulations (Step 4), while the adjustment factors were calculated only from the training period (Step 3). In instances where SILO has more rain days than the downscaled-GCM output, a small difference in rain days could persist in the bias-adjusted downscaled-GCM output. However, there is close agreement between the number of rain days in the bias-adjusted downscaled-GCM simulations and the number of rain days in SILO (Figure 2.5). Differences in both annual and seasonal number of rain days were less than $\pm 3\%$ for much of the state. Central estimate biases in the number of rain days shown in Figure 2.5 were of similar magnitudes and extents to those calculated for individual downscaled-GCMs (not shown).

Bias in number of rain days

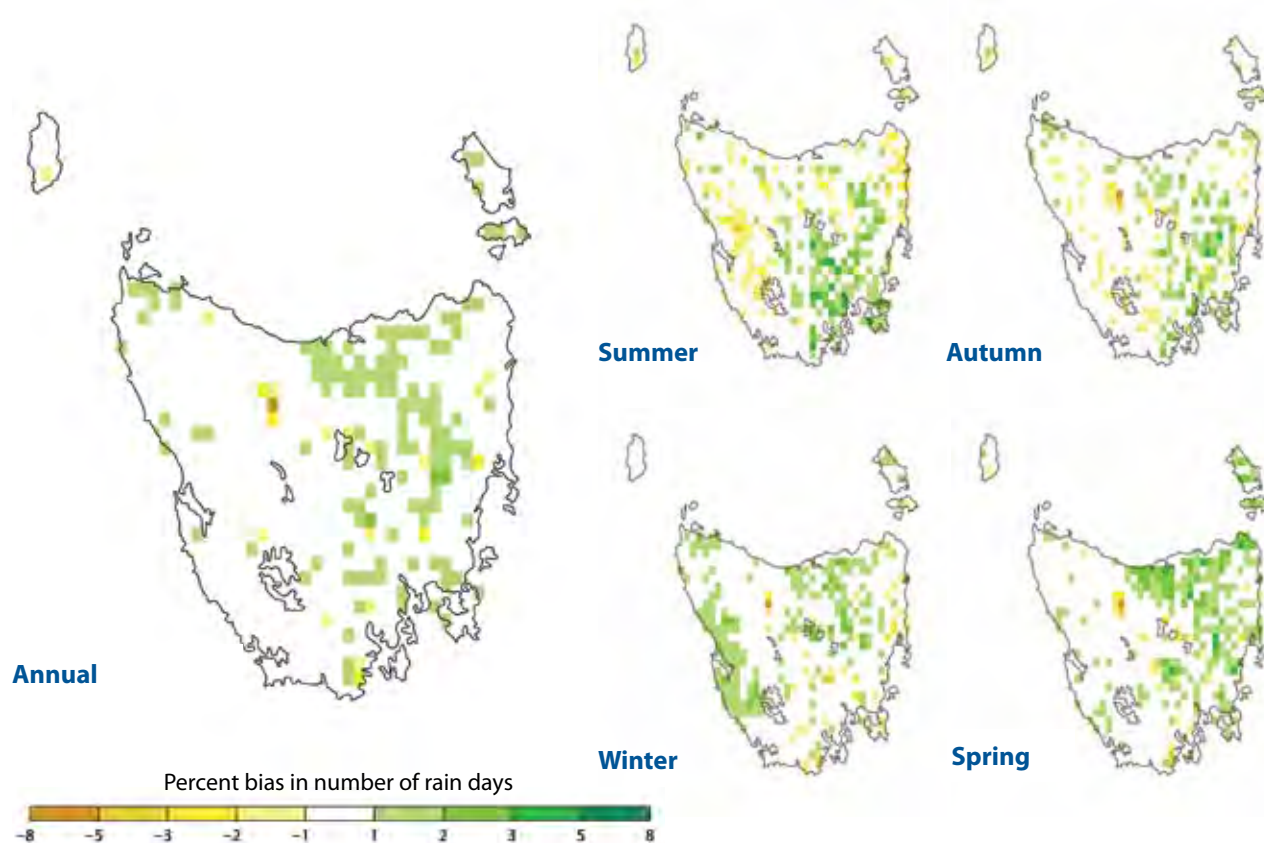


Figure 2.5 Bias in number of rain days (defined as days with precipitation > 1 mm) for the period 1961-2007, calculated from the central estimate of the downscaled-GCM ensemble against SILO interpolated observations.

Removing trends from the projections (Step 2) before the bias-adjustment was designed to stop any longer-term trends being 'adjusted' out of the projections. For example, if there were significant increases in rainfall by 2100, then daily values towards the end of the time series would be over-represented in the higher percentiles and consequently adjusted down disproportionately, flattening the trend. Testing showed that projected changes in the unadjusted downscaled-GCM rainfalls were very similar to those derived from the bias-adjusted projections (Appendix A). Cross-validation testing showed that while the period chosen to train the bias-adjustments changed the adjustment factors, the choice of training period had little impact on projected changes to rainfall (Appendix A).

Importantly, our quantile-quantile adjustment method allowed us to transfer as much of the information provided by climate simulations to the hydrological models as possible. This information includes projected changes in rain-bearing weather systems and changes to the spatial and temporal distribution of rainfall.

Limitations of quantile-quantile bias-adjustment for hydrological studies

Any form of bias-adjustment will change the dynamical balance of the climate modelling output. Rainfall and APET were adjusted independently and thus the simulated climate system is no longer in balance. In extreme cases, bias-adjustment could limit the utility of modelling output. The bias-adjustment process was designed to minimise the adjustments to the dynamical balance of the modelling output (Corney et al 2010). Nonetheless, some potential limitations in the process remain and these are discussed below.

Bias-adjustment at each cell was independent of surrounding cells. This means that spatial relationships of rainfall could be altered by the bias-adjustment. Rain from a single storm will often fall over multiple cells, depositing different quantities of rain in each grid cell. This means that rain from a single storm that falls in one grid cell can be

classified into a different percentile bin than rain in a neighbouring cell and could be adjusted differently.

Positive biases tended to decrease at higher percentiles and more cells tended to be negatively biased at higher percentiles (Figure 2.6). Thus biases in lower quantiles were usually adjusted down more than biases at higher quantiles. If an unusually large storm (say, a 99th percentile storm on a catchment basis) sweeps across a set of cells in a catchment, the bias-adjustment may treat the storm as if it is less unusual in some cells (perhaps in the 90th percentile). In those cells, the rainfall will be adjusted down more than in other cells, reducing the overall size of the event.

Larger events will tend to be adjusted down more than smaller events in this way. This is because an unusual event in a single grid cell will be unlikely to correspond with a similarly unusual catchment-wide storm. For example, a 99th percentile event in one SILO grid cell does not necessarily occur on the same date as the 99th percentile event in a neighbouring grid cell. A catchment-wide rainfall total at the 99th percentile is unlikely to register as the 99th percentile event in many (or any) individual grid cells – in most cells rain will register in a lower percentile bin. A greater proportion of rain is converted to runoff from larger rainstorms than from smaller storms. This is because the size of the surface and soil water stores in the hydrologic model remains constant, regardless of storm size. Accordingly, if larger rain events are adjusted down proportionately more than smaller rain events, runoff will be systematically reduced (negatively biased). It should be noted, however, that the reverse can also occur, and could result in more runoff (positively biased) in a given catchment.

Changes in the spatial relationships of rainfall that result from the bias-adjustment are difficult to estimate directly for a given catchment. The outcome is determined by a complex set of conditions, including the size of adjustment factors at different percentiles for a given cell in the catchment, the spatial relationships of the adjustment factors to those in other cells, and the parameters of a particular rainfall-runoff model.

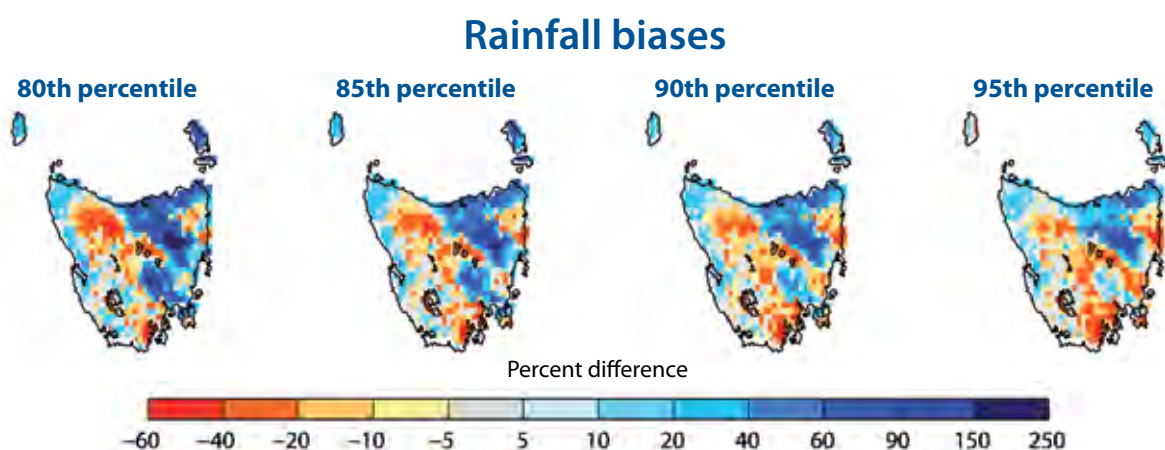


Figure 2.6 CCAM rainfall biases (central estimate compared to SILO) at four percentiles for the period 1961-2007.

Effect of bias-adjustment

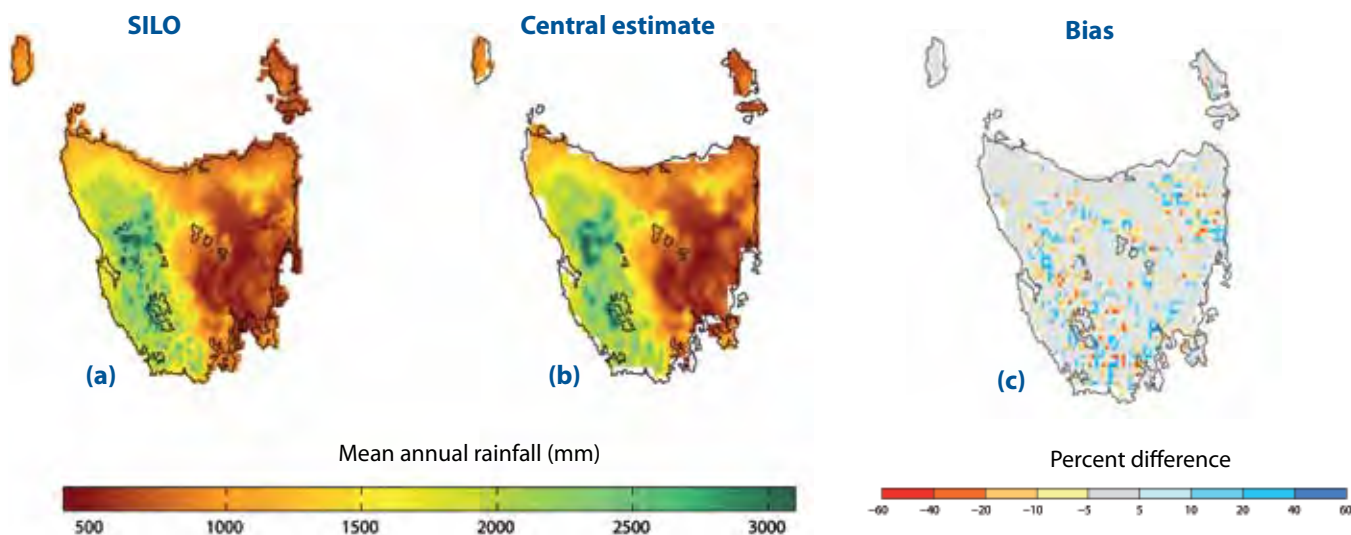


Figure 2.7 Mean annual rainfall 1961-2007 represented by (a) SILO (0.05-degree grid) and (b) Bias-adjusted central estimate regridded to 0.05-degree grid. Climate model bias is shown in (c).

2.3.7 Regridding climate projections

Influence of regridding on spatial variability of SILO data

Climate modelling outputs were downscaled to a 0.1-degree grid. The runoff models (Section 2.4.1) were configured to accept 0.05-degree inputs. Accordingly, climate simulations were regridded from a 0.1-degree to a 0.05-degree grid using a cubic spline interpolation. As noted in Section 2.3.6, SILO data were regridded from a 0.05-degree grid to a 0.1-degree grid for the bias-adjustment. Regridding from a finer to a coarser resolution and back again inevitably leads to a loss of fine-scale variability. The bias-adjusted 0.05-degree modelling outputs therefore do not have the same spatial variability as the 0.05-degree SILO data. However, spatial patterns and quantities of annual rainfall of 0.05-degree observations (Figure 2.7a) and bias-adjusted 0.05-degree climate simulations (Figure 2.7b) still show good agreement. Bias was near zero for much of the state, however in regions where SILO shows high spatial variability (notably along the mountainous west coast) larger biases are present in some cells (Figure 2.7c).

Land-ocean boundaries

One of the major advantages of CCAM over GCMs is CCAM's superior resolution of land-ocean boundaries. When grid cells are large relative to the land mass being modelled, as is the case when using GCMs to model Tasmania, the land-ocean boundaries can be both incorrectly located (by 100s of km, in worst cases) and incorrectly shaped (Tasmania becomes a square or a rectangle at GCM resolution). Unpublished analyses show that changes in land-ocean boundaries from GCMs and CCAM could result in the sign of rainfall change being reversed between a given GCM and its

downscaled-GCM cousin (notably in the north-east of Tasmania).

CCAM ocean cells were not suitable for use in runoff models and were excluded from the regridding interpolation. A given 0.1-degree (10 km by 10 km) ocean cell can reach as much as 5 km inland. This meant that several 0.05-degree cells near the coast did not have climate projections available for use in river models (Figure 2.8). For each of these 'missing' cells runoff from the nearest neighbouring cell was assigned. Because these cells were always coastal, they were always located at the terminus of catchments, meaning they had little effect on modelled catchment outflows.

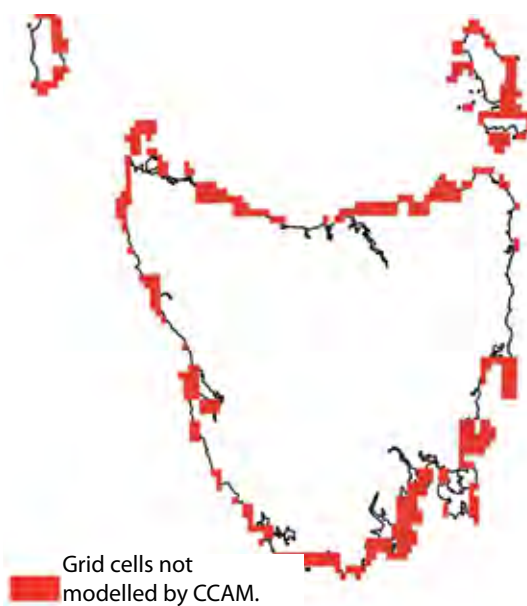


Figure 2.8 Cells used in river models but not modelled by CCAM (red). Runoff from the nearest neighbouring cell was assigned to each of these cells.

2.4 Hydrological modelling

Hydrological models built for the Tasmania Sustainable Yields Project (TasSY) were used for our project (see Box 2, page 14, for a description of TasSY). The TasSY surface water models used for our study have three components:

1. A statewide gridded runoff model that generates runoff for each 0.05-degree grid cell over Tasmania.
2. The Hydro Tasmania system model Temsim that projects future power station outflows into rivers.
3. River models that aggregate runoff by watersheds and power station outflows (when present) to produce river flows, and accounted for water extractions and diversions for agriculture and other uses.

Each of these components is described separately.

2.4.1 Runoff models

Runoff models used for this study were originally calibrated and used by TasSY. This section gives an overview of these models – for more detail refer to the TasSY runoff technical report by Viney et al (2009b).

Viney et al (2009b) calibrated five different rainfall-runoff models: AWBM (Boughton 2004), IHACRES (Croke et al 2006), Sacramento (Burnash et al 1973), Simhyd (Chiew et al 2002) with Muskingum routing (Tan et al 2005), and SMAR-G (Goswami et al 2002), but chiefly used the Simhyd model for its hydrological projections.

The TasSY runoff models were adapted specifically to study climate change and offer a number of benefits to our study:

1. These models produce runoff time series distributed to a 0.05-degree grid for the entire state. Attenuation of river flows is implicitly calculated by the runoff models. Gridded 0.05-degree runoff from the models can be aggregated to synthesise flow at any point in Tasmania.
2. The models were calibrated recently (May 2009) to 90 high-quality stream flow records spanning 1975-2007.
3. The calibration objective function combined Nash-Sutcliffe efficiency (NSE) (Nash & Sutcliffe 1970) and a novel log-bias constraint (Viney et al 2009a) to accurately represent stream flows.
4. In catchments where water extractions were judged a significant proportion of flows, estimates of these extractions were added to the flow records to synthesise a 'natural' flow record.
5. The models run on the easy-to-use, robust software ICYME (Yang 2009).

Viney et al (2009b) calibrated the TasSY runoff models to 90 catchments across Tasmania (Figure 2.9). Gridded interpolated SILO rainfall (Jeffrey et al 2001) and gridded Morton's wet evapotranspiration (Morton 1983) calculated from SILO variables were used as inputs to the models. Viney et al (2009a) showed that the five runoff models generally calibrated well (Figure 2.10). Median catchment NSEs were above 0.7 for all runoff models. As is to be expected, models of regions with less variable rainfall and runoff (for example in north-west Tasmania) performed better than models of catchments with more variable rainfall and runoff (such as occur along the east coast).

All runoff models except Sacramento exhibited an absolute bias of less than 5% for the vast majority of catchments; absolute biases at the 10th and 90th percentile catchments were less than 5% for the AWBM, IHACRES and Simhyd models. Sacramento showed higher biases and generally tended to underpredict flows, but even here median bias was less than 5%.

Calibration sites

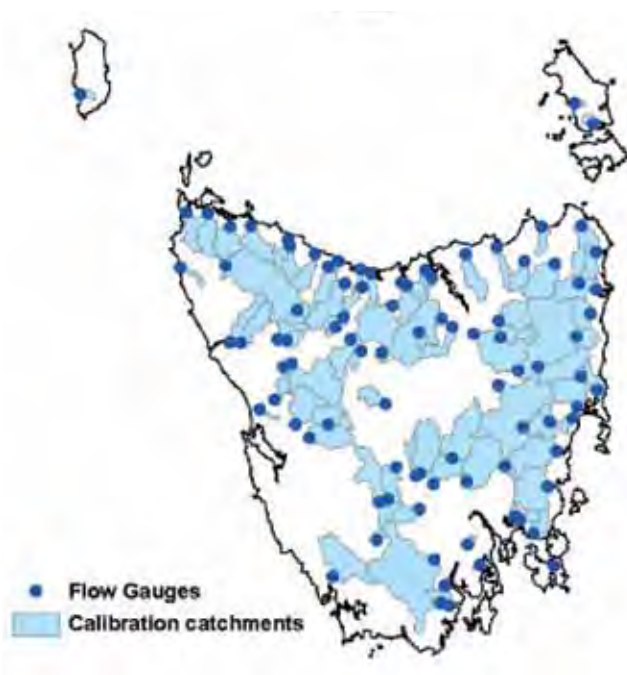


Figure 2.9 Catchments and flow gauge stations used to calibrate the TasSY runoff models that were used for our study.

Runoff model calibration

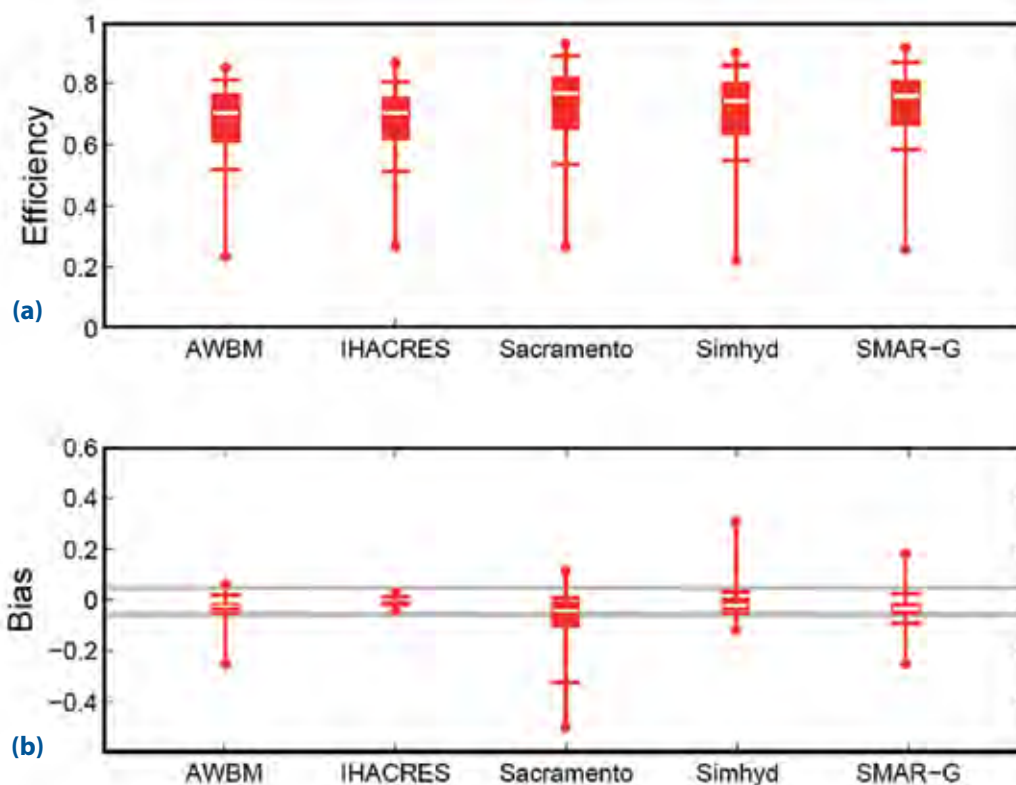


Figure 2.10 Box plots of (a) calibration Nash-Sutcliffe efficiency (Nash & Sutcliffe 1970) and (b) bias for the five TasSY runoff models for 90 calibration catchments. The boxes indicate the 25th, 50th and 75th percentile catchments, the whiskers indicate the 10th and 90th percentile catchments, and the dots indicate the extrema (adapted from Viney et al (2009a)). Grey lines in (b) mark $\pm 5\%$.

Viney et al (2009b) assigned model parameters to ungauged catchments from their nearest gauged neighbour. This method assumes that neighbouring catchments are similar enough to allow the hydrological model to generate stream flows for the ungauged catchment with acceptable accuracy. Viney et al (2009a) tested this assumption by transferring the parameter set from a given catchment to its nearest gauged neighbour. Viney et al (2009a) repeated this cross-verification test for each of the calibration catchments. Only parameter sets from non-nested catchments were transferred to gauged neighbouring catchments.

Catchment models performed less well under cross-verification. Median NSEs for all models dropped to 0.65 or lower and absolute biases increased, though median biases for all models remained less than 5%. Absolute biases for the IHACRES model increased most, though this can be attributed in part to the low absolute biases attained with this model during calibration. Viney et al (2009b) argued that the Simhyd model, the primary model used for TasSY and our study, performed acceptably well under cross-verification: median efficiency was 0.64 and three-quarters of catchments had absolute biases less than 25%.

Limitations of runoff modelling in a non-stationary climate

When describing 140-year runoff simulations we have implicitly assumed that the runoff models perform consistently through the entire period. This assumption may not be justified for a non-stationary climate: some part of the projected changes to runoff may be magnified (or reduced) by poor runoff model performance under different rainfall or APET regimes. Vaze et al (2010) found that performance of rainfall-runoff models declined markedly in periods where average annual rainfall was 15% lower (or less) or more than 20% greater than annual rainfall in the calibration period. Vaze et al (2010) also found that runoff model performance decreased more in dry conditions than in wet conditions.

Vaze et al's (2010) findings indicate that the runoff models should perform reasonably well in the conditions simulated by the downscaled-GCMs used in our study. Differences in simulated mean annual rainfall during the reference period (1961-1990) and SILO mean annual rainfall during the calibration period (1975-2007) were between -15% and +20% for most of the state (Figure 2.11). Individual grid cells had differences outside the limits of the -15% to 20% range prescribed by Vaze et al (2010). Most of these cells were located in the west coast and south-west.

These cells are not well covered by stream flow gauges (Figure 2.9), making the impacts of these differences on runoff model performance difficult to measure. These differences are a result of the regridding undertaken for the bias-adjustment, described in Section 2.3.7. Differences between simulated future mean annual rainfall from downscaled-GCMs and SILO mean annual rainfall during the calibration period (1975-2007) were also generally within -15% and +20% (Figure 2.11), although some individual downscaled-GCMs projected larger changes than the central estimate in certain regions.

Two downscaled-GCMs (CSIRO-Mk3.5 and MIROC3.2(medres)) projected reductions in mean annual rainfall of up to 20% over the central plateau, while UKMO-HadCM3 projected increases in mean annual rainfall of more than 35% for the Derwent Valley and along parts of the east coast. Nonetheless, rainfall changes were not large enough in most regions and for most downscaled-GCMs to be likely to cause serious deterioration in runoff model performance.

2.4.2 Tamsim

Discharges from Tasmania's hydro-electric system (see Box 3, page 31) into Tasmanian rivers are not simply a function of inflows but a function of energy demand and prices, maintenance schedules, environmental regulations and national electricity market (NEM) operating rules. All of these factors contribute to the operation of the system and need to be considered when projecting power station operation and river flows. These complex elements are all accounted for by Hydro Tasmania's Tasmanian electricity market simulation model (Tamsim). Tamsim optimises system operation to meet demand for electricity and to maximise financial return by trading in the NEM. The catchments and storages that are used for hydro-electricity generation are operated as a total system rather than as individual catchments.

In its standard configuration, Tamsim uses historical inflows and models the Hydro Tasmania system 20 years into the future.

Rainfall variation from runoff model calibration period

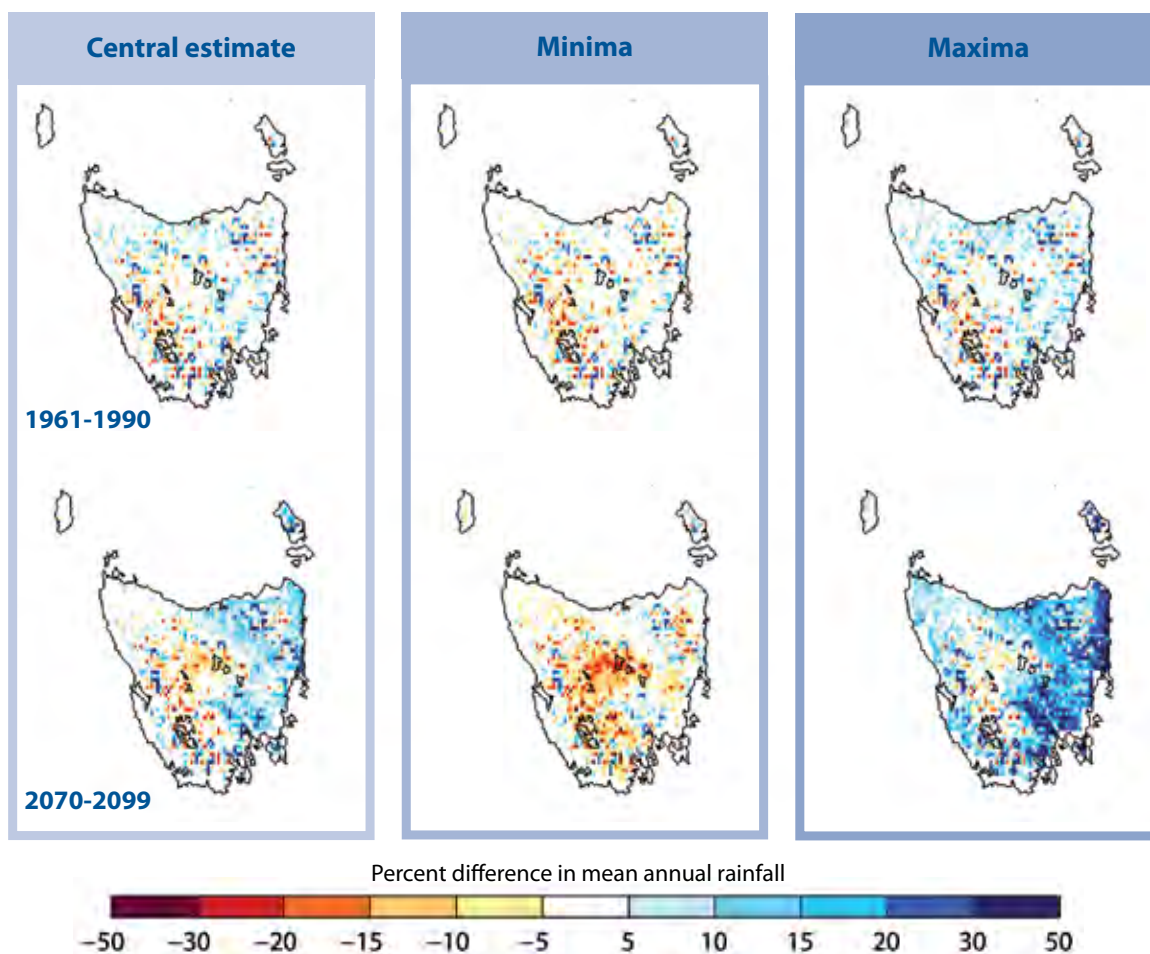


Figure 2.11 Comparison of SILO mean annual rainfall during the runoff model calibration period (1975-2007) to mean annual rainfall from downscaled-GCMs for the reference period (top row) and end-of-century (bottom row). Left column shows percent difference of SILO (1975-2007) from central estimate. Middle and right columns show range of differences of SILO (1975-2007) from individual downscaled-GCMs at each grid cell. Middle column shows lowest percent differences, right column shows highest differences.

The historical inflows are calculated from power station outflows, storage levels and extrapolations from stream flow gauges. We adapted Tamsim to accept inflows generated solely from the rainfall-runoff models used in our study. The use of inflows generated from rainfall-runoff models (rather than from historical records) as inputs did not materially reduce Tamsim performance (Appendix B). In addition, Hydro Tasmania adapted Tamsim to be run for 140 years (1961-2100). Simulating the operation of the hydro-electric system for 140 years implies the ability to predict electricity prices and demand for the coming 90 years. Our study has not undertaken any detailed analyses to generate these predictions. The assumptions of electricity demand and prices used for Tamsim's standard 20-year configuration were applied to the whole 140-year projection.

Although Tamsim models catchments in the eastern half of the state – the South Esk Basin, the Ouse River and the Clyde River – these catchments are duplicated by the TasSY river models. Whenever catchments are duplicated, TasSY river models are used to report changes to river flows. Catchments whose inflows are simulated by Tamsim are shown in Figure 2.13. Power station outflows projected by Tamsim are used as inputs to six of the river models: Forth River, Mersey River, Brumbys Creek, Lake River, Ouse River and the Derwent River.

Box 3

Hydro-electricity in Tasmania

Tasmania's hydro-electric system covers a large proportion of the western and central areas of Tasmania (Figure 2.12). The system stores significant quantities of water in reservoirs and diverts the courses of several rivers, including transferring water between catchments.

The system includes Australia's largest and sixth largest lakes: Lake Gordon/Pedder (11,000 GL) and Great Lake (3,000 GL). Power stations are operated according to inflows to the system, to electricity demand, to market drivers, to maintenance schedules and to operational and environmental constraints. These factors vary in importance from power station to power station. For example, run-of-river power schemes, such as the Pieman River Scheme on the west coast, cannot store significant quantities of water. This means that this scheme is essentially operated according to seasonal fluctuations in rainfall – when inflows are high, power is generated. Conversely, larger reservoirs buffer the system during seasonal or even multi-year droughts.

River flows downstream of power stations can be radically altered from their natural state, particularly in systems that feature interbasin water transfers or have large storages. Diversions are frequently important to downstream water users: for example, the significant proportion of the Derwent River catchment that supplies Great Lake is now diverted north into the Tamar basin, where irrigators have come to rely on the regular supply of diverted water.

Hydro-electric schemes

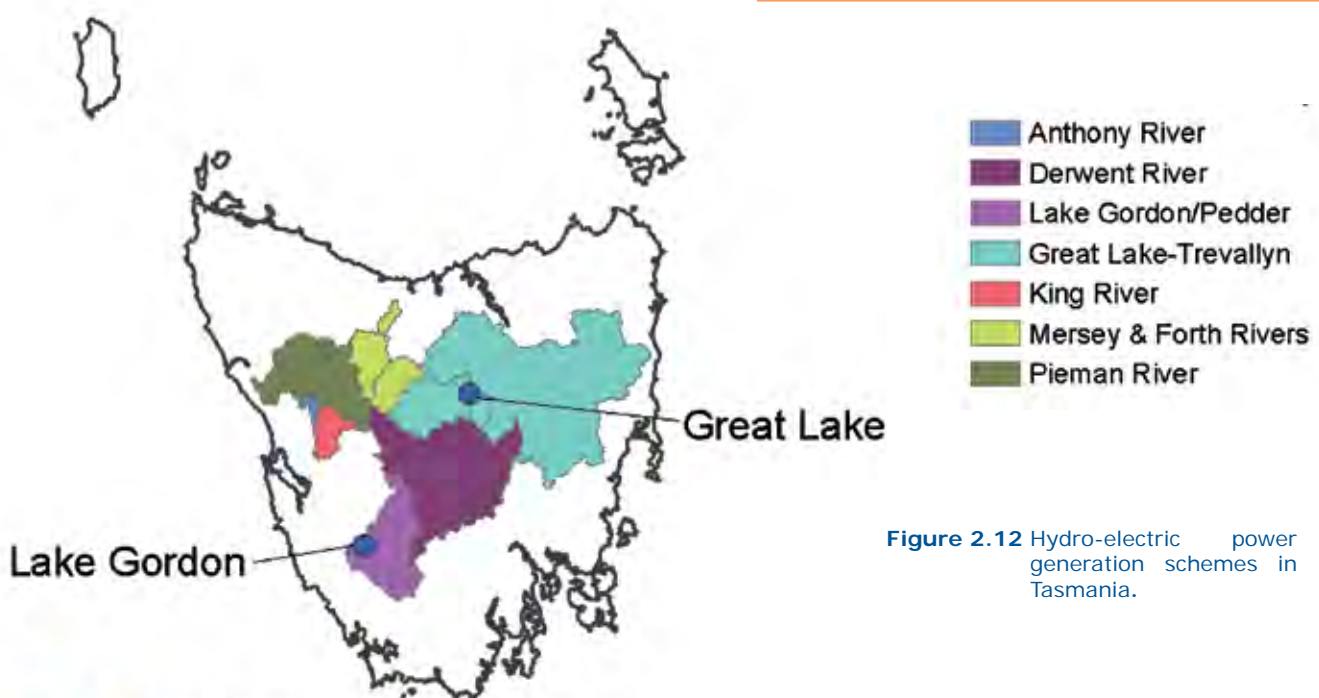


Figure 2.12 Hydro-electric power generation schemes in Tasmania.

2.4.3 River models

The runoff models measure water availability at each grid cell. This measure is made tangible by aggregating it to river flows. This aggregation of runoff is the function of the 78 river models used in this project. The names and locations of all river catchments modelled in our project are given in Appendix C. Most (62) of these river models were inherited from the TasSY study, however 16 catchments for which existing catchment delineations were available were added for this project (green coloured catchments in Figure 2.13). These 16 catchments are free-flowing rivers in remote areas that have negligible water extractions for human use and thus are simple systems that do not require complex catchment delineations or water accounting rules. Accordingly, these catchments are not divided into sub-areas. These 16 catchments are modelled for areas upstream of gauge sites. Sometimes these gauge sites are near the terminus of the catchment (for example the Savage River), while for other catchments, the gauge sites are higher in the catchment (for example the Franklin River). The 62 river models used by the TasSY project (referred to hereafter as the TasSY river models) were created by Ling et al (2009a, b, c, d, e) (Figure 2.13). The TasSY river models generate flows for each catchment by aggregating runoff and accounting for infrastructure (diversions and dams), water demands and water management rules current at 31 December 2007. Infrastructure, water demands and water management rules vary from catchment to catchment. What follows is an overview of the general functions of the TasSY river models - for details of each of the 62 TasSY river models refer to Ling et al (2009a, b, c, d, e).

Catchment delineations and routing

River catchments are broken into sub-areas. Each sub-area is a calculation and reporting point, where the flows are aggregated and losses subtracted. Where possible, the TasSY river models used sub-area delineations from the Department of Primary Industries, Parks, Water and Environment's (DPIPWE) TasCatch project (Bennett et al 2009). These delineations are compatible with existing DPIPWE water management software. Sub-area breaks are positioned at major confluences and at other points determined by DPIPWE. Sub-areas in a given catchment are usually of a similar size. Routing length between catchment centroids is representative of the river length. Attenuation and lag is implicitly calculated by the runoff models and no additional attenuation or lag is added.

Catchments modelled

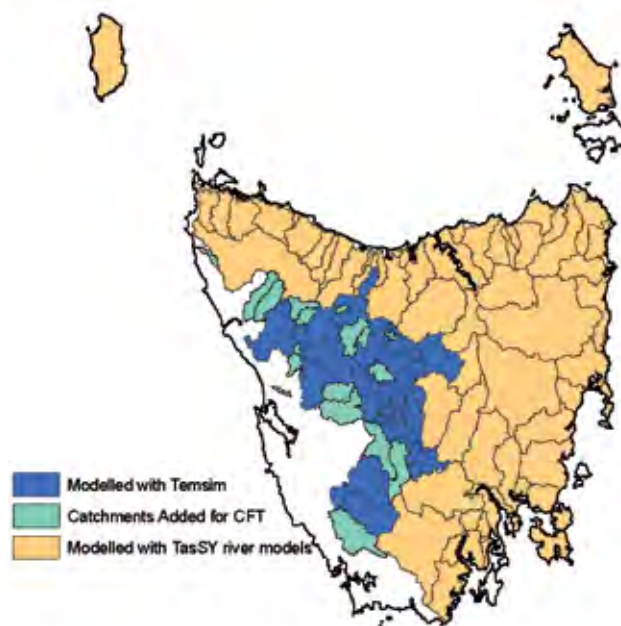


Figure 2.13 Catchments reported in this study. Tan colour shows regions modelled with TasSY river models. Regions modelled with Temsim are shown in blue. Only changes to inflows to Temsim catchments are described. Green-coloured catchments are free-flowing rivers reported in our study, but not by TasSY. White areas are not covered by the river models.

Water extractions

Water extractions for agriculture and other uses are rarely monitored in Tasmania. Water use for TasSY was estimated from DPIPWE water licensing information held on its Water Information Management System (WIMS) database. Farm dams smaller than 1 ML do not need to be licensed in Tasmania. Detailed estimates of unlicensed small farm dams and other unlicensed water extractions were included in water extraction estimates for each sub-area, as described by Ling et al (2009a, b, c, d, e) and references therein.

Major storages

The TasSY models incorporated 14 major irrigation and water supply storages (Table 2.1). Storages are modelled according to operating rules current at 31 December 2007. To be able to compare reference period river flows to future river flows, these operating rules were applied for the entire 140-year simulation (1961-2100). For example, construction of the Meander Dam was completed only in 2007, but the river models assume it has been in place since 1961. Inflow, evaporative loss, spill and storage volume was calculated for each of the 14 storages. Only inflows to storages are reported in this study, but time series of all other metrics are available to researchers and other interested parties (see Section 7).

Table 2.1 List of irrigation storages modelled

| Storage name | Effective volume (ML) | Catchment | Operation described by |
|----------------------|-----------------------|------------------|------------------------|
| Cascade Reservoir | 3,250 | Ringarooma R | Ling et al (2009c) |
| Companion Dam | 1,350 | Emu R | Ling et al (2009a) |
| Craigbourne Dam | 12,400 | Coal R | Ling et al (2009e) |
| Curries Dam | 11,500 | Pipers R | Ling et al (2009c) |
| Frome Dam | 1,960 | Ringarooma R | Ling et al (2009c) |
| Guide Reservoir | 1,600 | Cam R & Emu R | Ling et al (2009a) |
| Lake Crescent/Sorell | 80,730 | Clyde R | Ling et al (2009e) |
| Lake Isandula | 625 | Leven R | Ling et al (2009b) |
| Lake Leake | 18,800 | Macquarie R | Ling et al (2009d) |
| Lake Mikany | 2,770 | Duck R | Ling et al (2009a) |
| Meander Dam | 40,450 | Meander R | Ling et al (2009d) |
| Pet Reservoir | 2,500 | Cam R & Emu R | Ling et al (2009a) |
| Talbots Lagoon | 2,750 | Arthur R & Emu R | Ling et al (2009a) |
| Tooms Lake | 21,050 | Macquarie R | Ling et al (2009d) |

Box 4

Summary of methods used to model future river flows

- Future river flows are modelled by adapting downscaled-GCM projections for use in runoff models and aggregating flow into river catchments. Daily rainfall and daily APET are required inputs for the hydrological models. Daily rainfall is a direct output generated by the downscaled-GCM simulations. Morton's wet APET is calculated from temperature, radiation and relative humidity generated by the downscaled-GCM simulations.
- Rainfall and APET inputs were bias-adjusted to match the SILO interpolated dataset using quantile-quantile bias-adjustment.
- Five different rainfall-runoff models are used for hydrologic modelling: AWBM, IHACRES, Sacramento, Simhyd with Muskingum routing and SMAR-G. Simhyd is used to present river flow projections.
- Catchments and storages within Tasmania's hydro-electricity system are modelled using Hydro Tasmania's system model, Temsim, with inflows generated from rainfall-runoff models run with bias-adjusted downscaled-GCM simulations regridded to a 0.05-degree grid as inputs.
- River flows are generated using river system models that aggregate runoff and account for infrastructure (diversions and dams), water demands and water management rules. Runoff generated by the hydrologic models and storage releases generated by Temsim are inputs to the river system models.

3 Performance of runoff models

Assessment of hydrological model performance usually involves assessing a combination of bias and correlation efficiency at matching observed hydrographs (such as Nash-Sutcliffe Efficiency (NSE) (Nash & Sutcliffe 1970)). Measures of efficiency assume that observed and modelled hydrographs are synchronised. The downscaled-GCM simulations are not synchronised with observations; that is, rain in the downscaled-GCM simulations falls on different days than in the observed record. It follows that streams modelled from GCM outputs rise and fall at different times than is recorded in historical hydrographs. This means that the efficiency of our hydrological modelling cannot be tested with conventional methods and we rely on other measures of model performance.

We have relied chiefly on assessing biases of annual and seasonal flows (that is, proportional differences of simulated flows from observations) to test our runoff models, and have considered variance of daily flows, frequency of cease-to-flow events (less than 0.1 ML/d) and high flows (5% exceedance probability) and low flows (95% exceedance probability). Simhyd is the model we have used as the basis for our flow projections and accordingly most of our measures of hydrological model performance are performed on Simhyd simulations.

3.1 Performance of runoff models with downscaled-GCM inputs compared to SILO inputs

Flows generated from bias-adjusted simulations and SILO inputs are compared to observations available at 86 flow gauges for the period 1961–2007. The flow gauges were all used by Viney et al (2009b) to calibrate the hydrological models used for this project (location map shown in Figure 2.9).

Four of the flow gauges used by Viney et al (2009b) to calibrate the runoff models are removed for our analysis. These four gauges (Ouse River at 3b Weir, Mersey River at Kimberley, Wilmot River above Forth River and Dee River above Derwent River) are all downstream of hydropower diversions. Viney et al (2009b) were able to utilise these sites by synthesising ‘natural’ flow records by subtracting historical outflows from upstream hydropower stations from gauged flows. We could not follow this method, as modelled hydropower outflows generated by our project are subject to system operating rules current at 1 January 2008. These operating rules can be markedly different from historical operation and hence these four gauges were unsuitable

for simulating ‘natural’ flow records following the method used by Viney et al (2009b).

A strength of our study is the use of multiple runoff models to test the efficacy of bias-adjusted climate modelling simulations as direct inputs to hydrological models. All of the runoff models showed larger biases when run with downscaled-GCM bias-adjusted rainfall and APET inputs than when they were run with SILO inputs (Figure 3.1a). All runoff models showed a tendency to underpredict flows with downscaled-GCM inputs compared to SILO inputs, and all showed increased absolute biases (Figure 3.1b). Some degradation in performance is expected with downscaled-GCM inputs, as the runoff models were calibrated using SILO inputs. The more negative biases for all models may be caused by inherent limitations of the bias-adjustment method when applied to rainfall, the regridding of SILO variables or unrealistic simulations of rainfall or APET characteristics by CCAM. Bias-adjusting each cell independently may result in the spatial relationships of rainstorms being modified (see Section 2.4.1), while aggregating SILO from 0.05-degree grid to a 0.1-degree grid is likely to reduce rainfall in cells that produce more rainfall than their neighbouring cells (see Section 2.3.7).

Simhyd was the least biased hydrological model when combined with downscaled-GCM inputs: Simhyd median bias was -3%, while catchments at the 25th and 75th percentile had biases within $\pm 10\%$ (Figure 3.1). While the Simhyd biases are worse than calibration biases, they are acceptably small for the purposes of our study. AWBM, Sacramento and SMAR-G all showed slightly larger median biases. IHACRES was the least biased model with SILO inputs, but was clearly the worst performing model with CCAM inputs (median bias of -21%).

With the exception of IHACRES, the runoff models showed small biases with downscaled-GCM simulations as inputs. Simhyd, in particular, performed reasonably well with downscaled-GCM inputs (see also Section 3.2). The degradation in performance of IHACRES echoes the reduced performance of the same model under spatial cross-verification tests carried out by Viney et al (2009a). Viney et al (2009a) attributed this to an IHACRES parameter that effectively scales rainfall. The problem may be peculiar to Tasmania: rainfall here can vary greatly over small distances and it may be more difficult to apply a parameterised rainfall scaling factor to neighbouring catchments.

Viney et al (2009c) used the same suite of five runoff models for a study of south-eastern Australian rivers and there IHACRES performed well under spatial cross-verification tests. The IHACRES model presents an interesting test for our method of using downscaled-GCM simulations directly in runoff models.

Diagnosing the reduced performance of IHACRES with downscaled-GCM inputs is outside the scope of this report, but will be the subject of future research. We speculate that the rainfall-scaling identified by Viney et al (2009a) is the likely cause for the reduced performance of IHACRES with downscaled-GCM inputs.

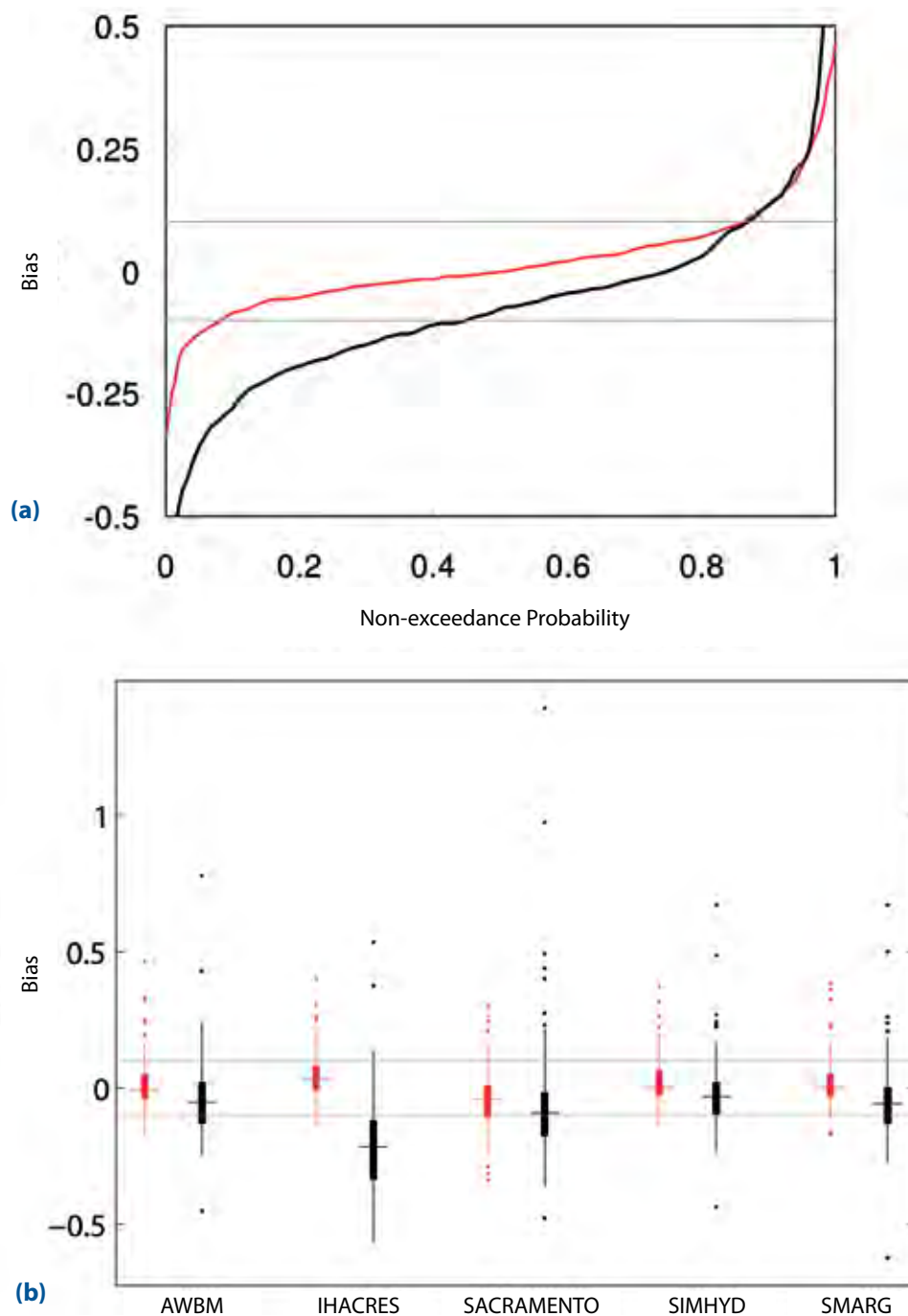


Figure 3.1 Biases of runoff models with downscaled-GCM inputs (black) and SILO inputs (red) at 86 stream flow gauge sites for 1961-2007. Biases are proportional differences between simulated average annual flow volumes and observations, and are dimensionless. (a) combined non-exceedance probabilities of bias for all five runoff models; (b) box plots of biases for each hydrological model – boxes indicate 25th, 50th and 75th percentiles, whiskers approximate two standard deviations from the mean, points are outliers. Grey lines in both plots mark biases of $\pm 10\%$.

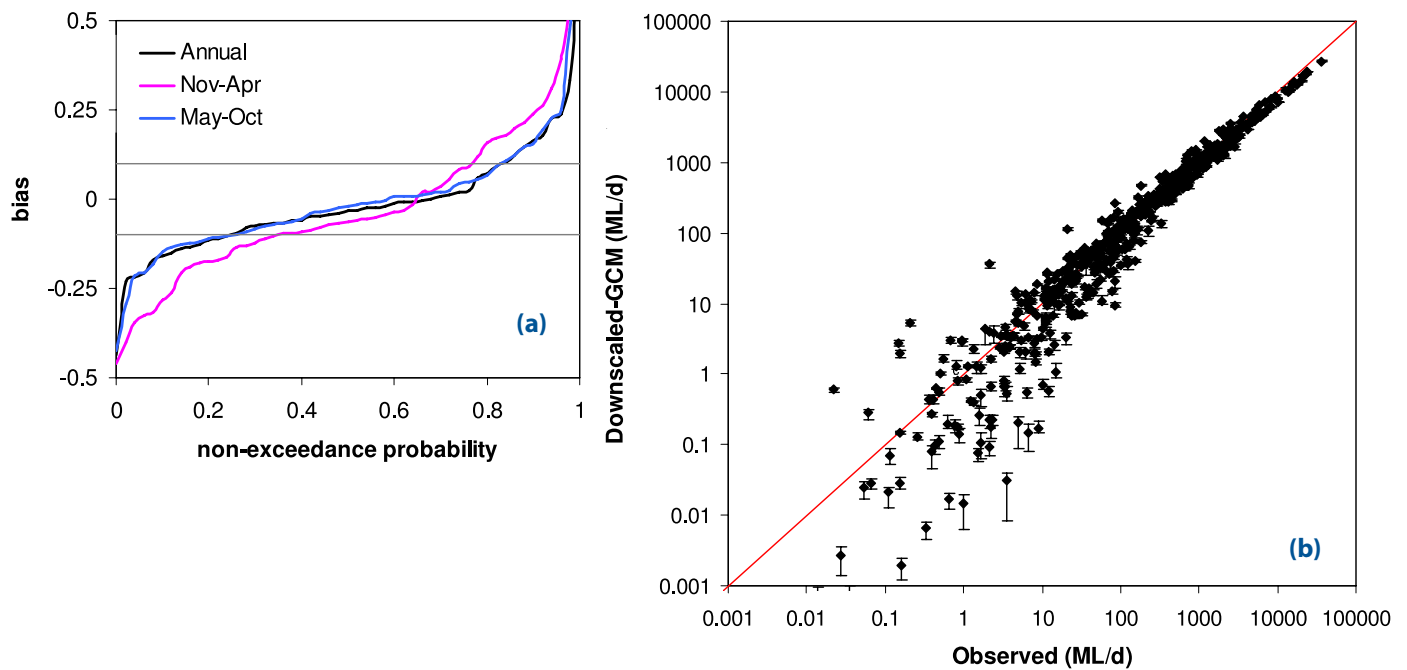


Figure 3.2 Simhyd central estimate flows compared to observations at 86 flow gauge sites for 1961-2007: (a) non-exceedance probabilities of Simhyd bias for all months (black), wetter months (May-Oct) (blue) and drier months (Nov-Apr) (pink) (biases are proportional differences of simulated average flow volumes from observations and are dimensionless); (b) quantile-quantile log-log plot of daily flows at all sites from 2nd to 98th percentile. Error bars in (b) show downscaled-GCM range (where visible).

3.2 Performance of Simhyd runoff model with downscaled-GCM inputs

Simhyd showed reasonable performance with downscaled-GCM inputs. The downward shift in bias displayed in other runoff models is also present in Simhyd, but is not as pronounced (Figure 3.1b). Bias-exceedance curves for Simhyd are similar for wetter and drier months, with a slight negative shift in bias for the drier months (Figure 3.2a). The negative bias was also reflected in a quantile-quantile plot (Figure 3.2b), particularly at lower flows, although the log-log scale of the plot emphasises discrepancies at lower flows. This is confirmed when viewing low flows in isolation (Figure 3.3a) and particularly cease-to-flow days (Figure 3.3d), neither of which show the strong agreement found between Simhyd and observed high flows (Figure 3.3b) and mean flows (Figure 3.3c). Simhyd also showed a slight tendency to underpredict high flows, particularly at high flow sites (Figure 3.3b).

Observed variance in flows is reasonably well replicated by flows simulated by Simhyd with downscaled-GCM inputs. Daily coefficients of variation (CV) are lower for flows simulated by Simhyd with downscaled-GCM inputs than observed flows at many of the gauge sites (Figure 3.4a). However, this is largely caused by the reduction in variance of flows inherent in the runoff models. This can be seen by comparing daily CV of daily flows simulated by Simhyd with downscaled-GCM inputs with daily CV of daily flows simulated by Simhyd with SILO inputs (Figure 3.4b), which show good agreement.

Comparing flows generated from downscaled-GCMs to flows generated with SILO isolates the effects of the downscaled-GCM rainfall and APET inputs.

A negative bias occurs in nearly all seasons for each of the six downscaled-GCMs (Figure 3.5). Generally, the negative biases are least noticeable in winter. Median seasonal biases range from zero to -10%. The negative biases could be caused by the spatially uneven bias-adjustment of rainstorms (see Section 2.3.6), or by a reduction of rainfall in high-rainfall cells through the regridding of SILO data (see Section 2.3.7).

In addition, biases could be caused by inaccuracies in the replication of characteristics of rainfall/APET by CCAM. For example, spatial and temporal differences between downscaled-GCM rainstorms and SILO rainstorms could cause some of the outliers in Figure 3.1b and will be the subject of future research.

Despite the downward shift in bias, Simhyd gives a reasonable replication of historical flow characteristics with downscaled-GCM rainfall and APET as inputs. More than 60% of catchments have absolute biases of less than 10% (that is, they are within $\pm 10\%$). Catchments with larger absolute biases tend to be located in the east of the state (Figure 3.6i). Profiles of seasonal flows are also reasonably well represented (Figure 3.6a-f), particularly in the north-west of the state (Figure 3.6a, b). The range in the downscaled-GCM simulations during 1961-2007 tends to increase to the east of the state (Figure 3.6c, e, h), in keeping with the more sporadic and inherently less predictable rainfalls that occur in eastern catchments.

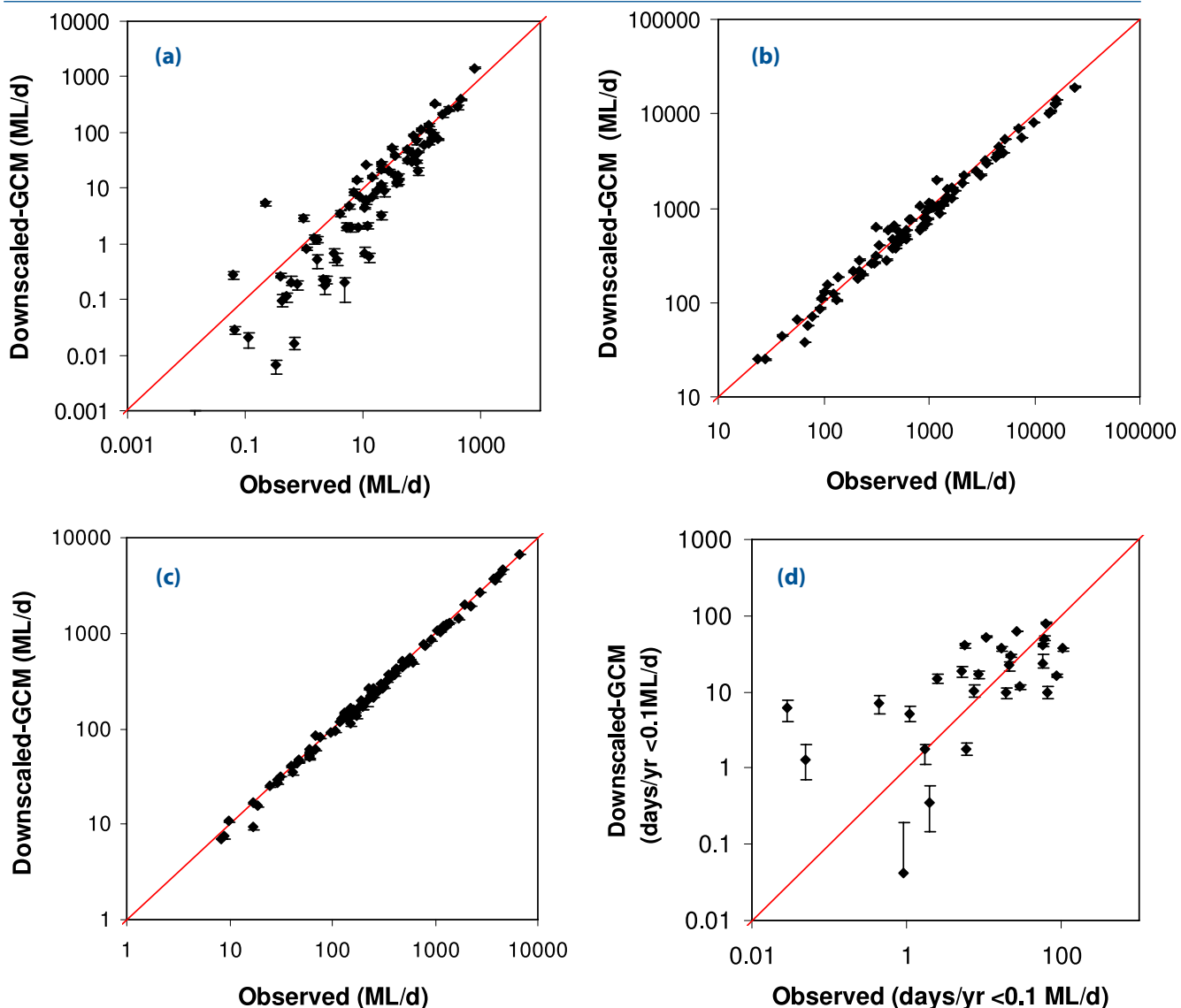


Figure 3.3 Log-log plots comparing Simhyd flows generated with downscaled-GCM inputs (vertical axes) to available observed flows (horizontal axes) at 86 calibration sites for 1961-2007: (a) low flows (exceeded 95% of the time); (b) high flows (exceeded 5% of the time) (c) mean flows; (d) cease-to-flow days per year, defined as flows < 0.1 ML/d. Points show central estimates, while error bars (when visible) give downscaled-GCM range.

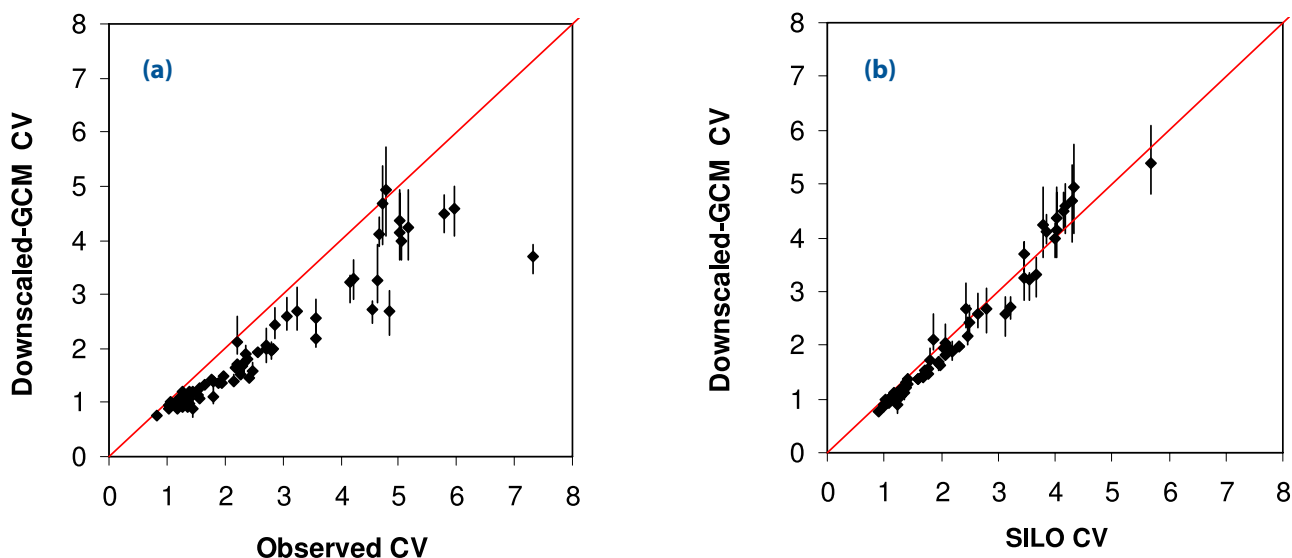


Figure 3.4 Coefficients of variation (CV) of Simhyd daily flows generated with downscaled-GCM inputs (vertical axes) compared to (a) CV of observed daily flows and (b) CV of Simhyd daily flows generated with SILO inputs at 86 calibration sites for 1961-2007. Points show central estimates, while error bars give downscaled-GCM range.

Simhyd performance

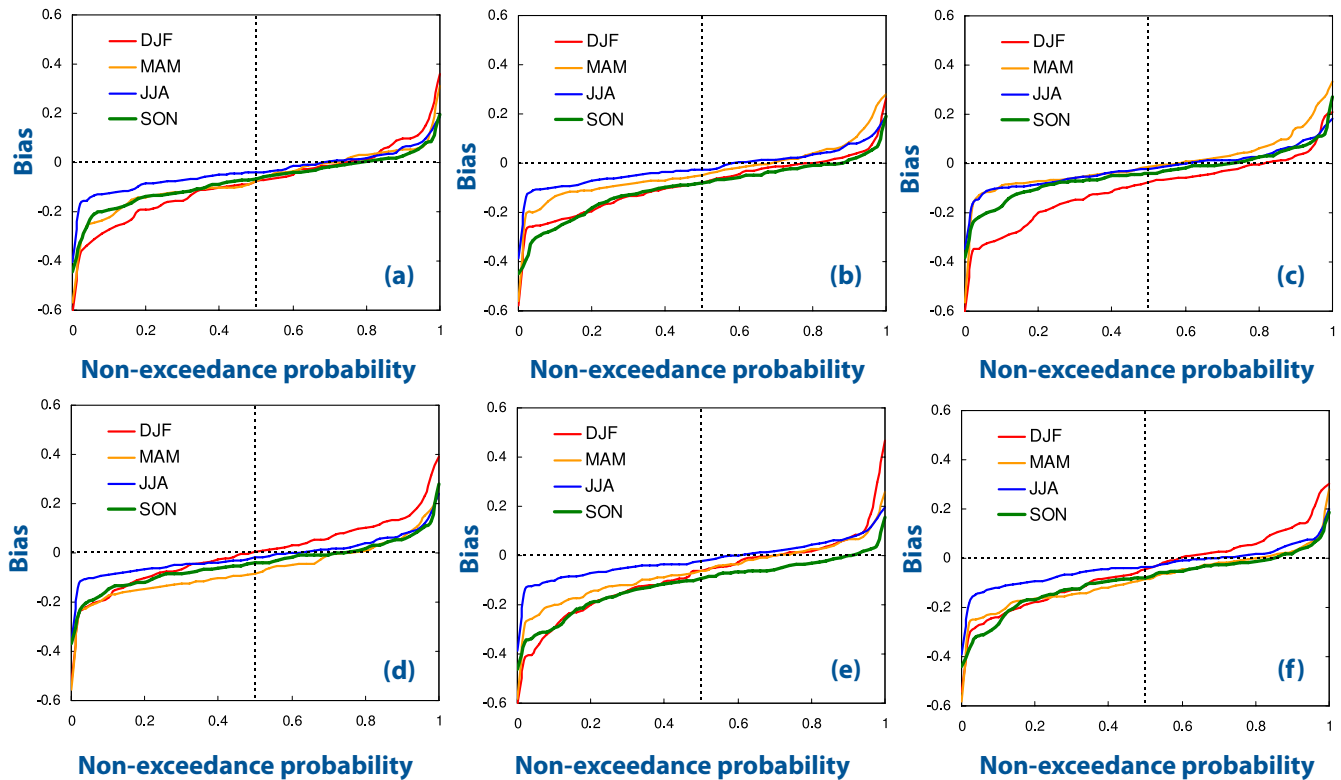


Figure 3.5 Non-exceedance probabilities of bias of seasonal Simhyd flows simulated with downscaled-GCM inputs compared to Simhyd flows simulated with SILO inputs at 86 sites. Biases are proportional differences of simulated average flow volumes from observations, and are dimensionless. Abbreviations in legend signify seasons: DJF (December, January, February) is summer, MAM (March, April, May) is autumn, JJA (June, July, August) is winter, SON is spring (September, October, November).

The performance of all runoff models, including Simhyd, decrease with the use of downscaled-GCM rainfall and APET inputs compared to the use of SILO inputs. The reduction in performance of the runoff models must be weighed against the benefits of our method, such as including the effects of projected changes to the timing and duration of rainfall events and dry spells.

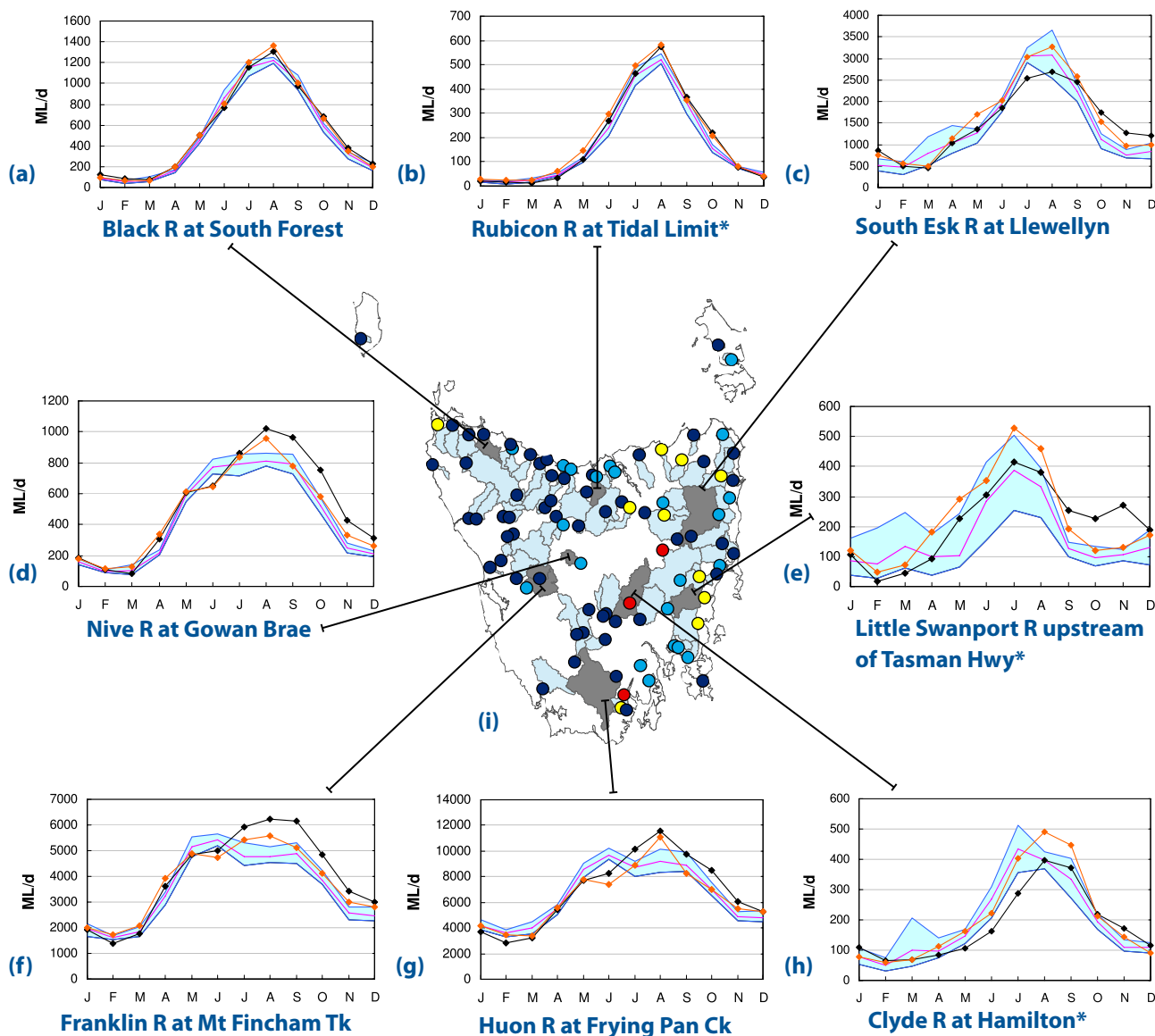
Similar results may have been achieved using simpler methods, such as 'simple perturbation', which perturbs historical rainfall and APET data by anomalies. However, the benefits of the method used here, such as the inclusion of changes to climate drivers of rainfall and the inclusion of changes to the length of dry and wet spells in runoff projections (Grose et al 2010; White et al 2010), makes this method a worthwhile alternative to more traditional perturbation methods.

Box 5

Summary of performance of runoff models

- Flows generated from downscaled-GCM inputs and SILO inputs are compared to observations available at 86 stream flow gauges for the period 1961-2007. Hydrological model results show larger biases with downscaled-GCM rainfall and APET inputs compared to SILO inputs.
- The AWBM, Simhyd, Sacramento and SMAR-G runoff models show acceptable biases when run with downscaled-GCM inputs. Biases are largest in the IHACRES model with CCAM inputs.
- Simhyd is the least biased hydrological model when combined with downscaled-GCM inputs: Simhyd median bias is -3%, while the 25th and 75th percentile biases are within $\pm 10\%$.
- The direct use of downscaled-GCM inputs with the Simhyd model allows projected changes to the quantities and characteristics of Tasmanian rainfall to be generated.

Simhyd performance



Monthly flows

- ▭ Range
- Central estimate
- ◆ SILO
- ◆ OBS

Absolute bias

- 0 - 10
- 10 - 20
- 20 - 40
- >40

Annual and seasonal bias at featured sites

| Site | Annual | Nov-Apr | May-Oct |
|------|--------|---------|---------|
| a | -0.04 | -0.19 | -0.02 |
| b | -0.07 | -0.17 | -0.09 |
| c | -0.05 | -0.17 | 0.01 |
| d | -0.15 | -0.27 | -0.12 |
| e | -0.22 | -0.12 | -0.26 |
| f | -0.11 | -0.09 | -0.13 |
| g | -0.04 | 0.02 | -0.07 |
| h | 0.07 | -0.11 | -0.15 |

* Observations synthesised by adding estimates of water extractions to gauged flows

Figure 3.6 Performance of Simhyd with downscaled-GCM inputs at 86 flow gauge sites for the period 1961-2007: (a)-(h) central estimates of monthly flows predicted by Simhyd featured at eight stream flow gauge sites (pink) and downscaled-GCM range (blue). Also plotted are Simhyd flows generated with SILO inputs (orange) and observations (black). Central map (i) gives spatial distribution of absolute bias of Simhyd with downscaled-GCM inputs at all 86 sites. Annual and seasonal biases for the eight featured sites are given at bottom right.

4 Changes to rainfall and areal potential evapotranspiration

This section is intended only as an overview of the rainfall and areal potential evapotranspiration (APET) inputs to the hydrological models used in this project. For a more expansive description of the downscaled-GCM rainfall projections, including a discussion of changes to the climatic drivers of rainfall in Tasmania, refer to Grose et al (2010).

4.1 Historical rainfall

Historical rainfall and APET are represented by the reference period 1961-1990. Figure 4.1 shows the steep west-to-east gradient that characterises Tasmanian rainfall. Western Tasmanian rainfall is strongly seasonal, falling mostly in winter and the surrounding months. Rainfall in the drier east is less seasonal.

Determining trends in historical Tasmanian statewide rainfall is difficult, as evidence from different interpolated datasets is not consistent (Figure 4.2). These inconsistencies are probably the result of the poor coverage of rain gauges in some of the wettest areas of the state (the south-west and west coast), particularly in the earlier part of the 20th century. The gridded rainfall datasets each use different methods of interpolation. Where observations are sparse differences in interpolation methods become more noticeable.

Figure 4.2 shows smoothed statewide rainfall trends for three interpolated rainfall datasets for Tasmania - AWAP, the Bureau of Meteorology high-quality (BoM-HQ) dataset (Della-Marta et al 2004), and SILO. AWAP and BoM-HQ both show a clear, near-linear decline in rainfall throughout the 20th century. SILO, conversely, shows no strong trend since the 1930s, due to a marked low-rainfall period from 1930 to the mid-1940s, which is not present in the other datasets.

The three datasets show better agreement from 1960 onwards. Tasmania is often stated to be in rainfall decline since the mid-1970s, but examination of post-1970 ignores the low rainfall period of the early 1960s. However, even when the dry early-1960s period is considered, BoM-HQ and AWAP indicate that the period after 2000 is the driest period in these records. SILO, conversely, indicates that the most recent decade is dry, but is not unprecedented in the record (SILO shows drier periods in early 1960s and in the 1920s and 1940s).

4.2 Projected changes to rainfall

Statewide annual rainfall is not projected to change markedly by the end of the century (Grose et al 2010), however seasonal and spatial distributions of rainfall are projected to shift.

The central estimate of statewide annual rainfall is almost constant by end-of-century (projected increase of 0.1%) relative to natural variability (Table 4.1). This follows a slight decrease in the near future and medium-term future. The central estimate of annual rainfall reduces over the central highlands by the end of the century and increases in the east (Figure 4.3). The increase in rain in the east occurs predominantly in summer and autumn. Mean annual west coast rainfall shows little change, however there are marked seasonal changes: rainfall is projected to reduce in summer and increase during winter. Grose et al (2010) showed that these rainfall changes are consistent with projected changes to known regional climate drivers of rainfall.

Table 4.1 Central estimates of statewide mean annual rainfall for the reference period and three future periods. Range of changes from individual downscaled-GCMs is shown in the right hand column.

| Period | Statewide mean annual rainfall (mm) | Change from reference period (mm) | Change from reference period (%) | Downscaled-GCM range of change (%) |
|-----------|-------------------------------------|-----------------------------------|----------------------------------|------------------------------------|
| 1961-1990 | 1346 | - | - | - |
| 2010-2039 | 1341 | -5 | -0.4 | -4.4 to 7.3 |
| 2040-2069 | 1333 | -13 | -1.0 | -7.2 to 7.7 |
| 2070-2099 | 1348 | 2 | 0.1 | -3.6 to 9.9 |

Modelled historical rainfall

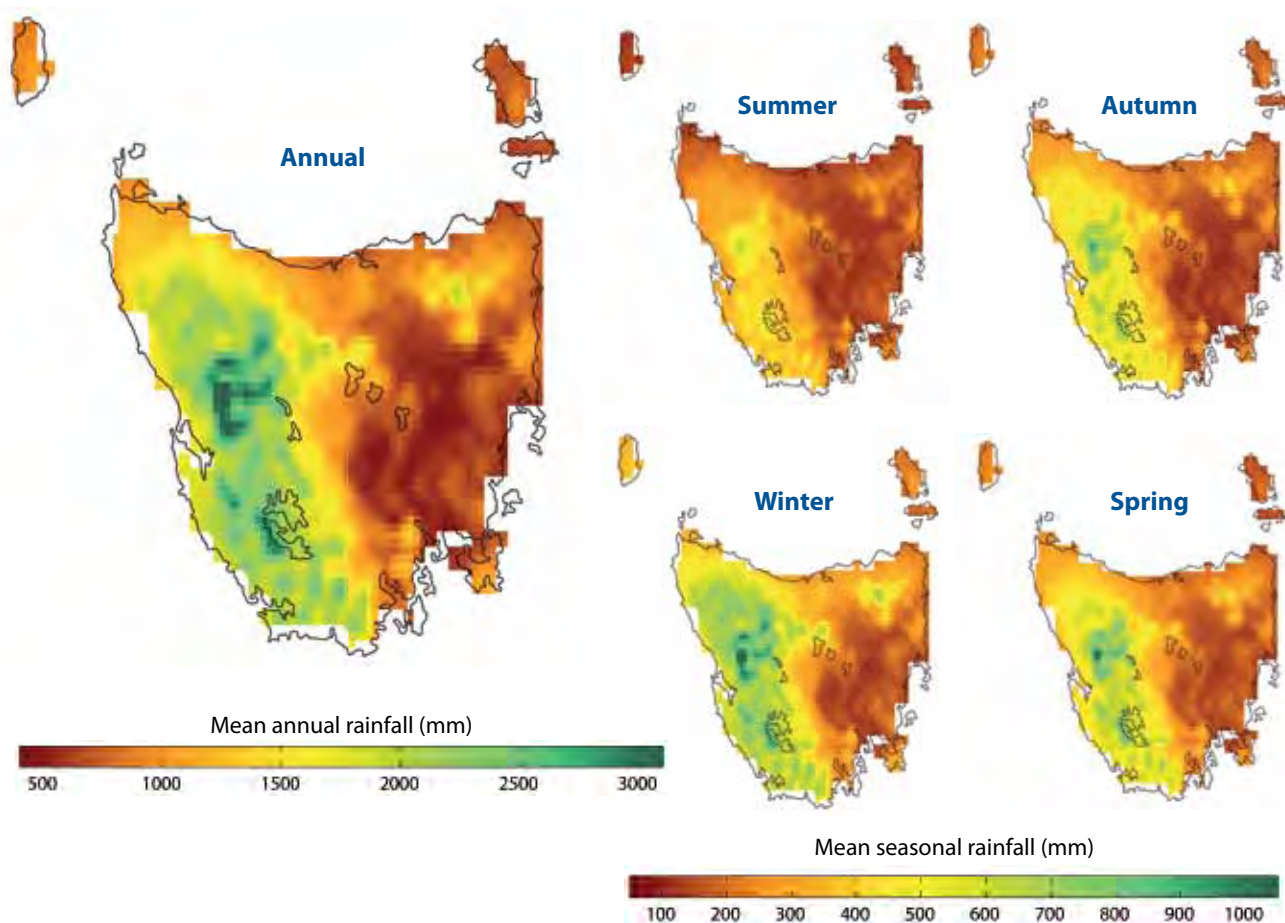


Figure 4.1 Mean annual and seasonal rainfall during the reference period (1961-1990) (central estimate).

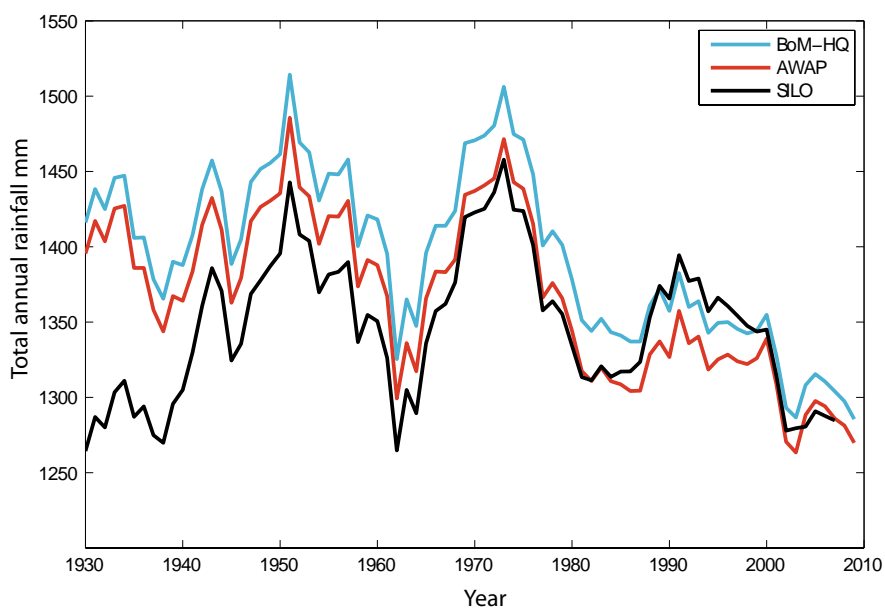


Figure 4.2 Tasmanian statewide mean annual rainfall for three observation datasets from 1930-2008. The three curves are smoothed with an 11-year centred moving average.

Change in rainfall

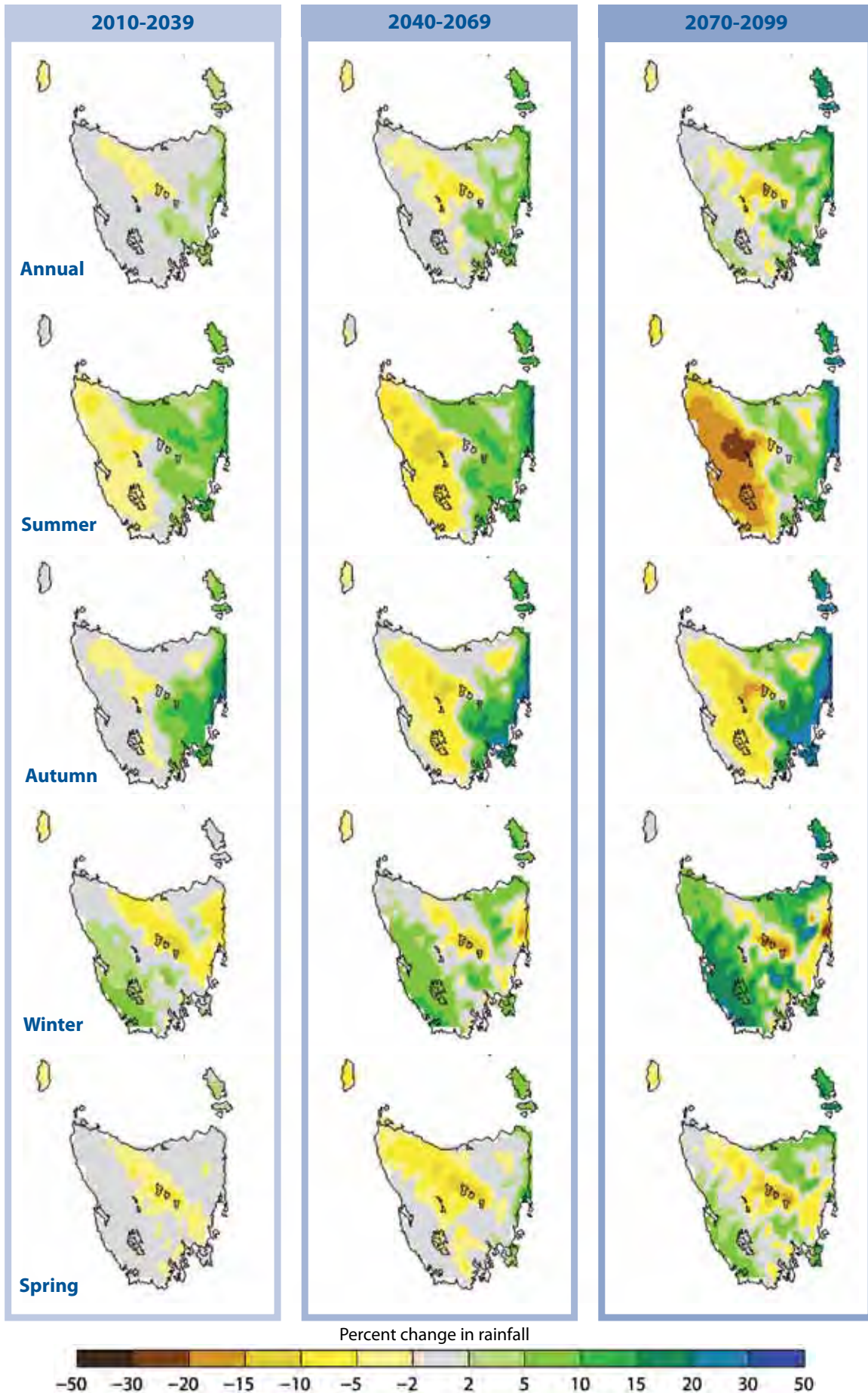


Figure 4.3 Changes in mean annual and seasonal rainfall from the reference period (1961-1990) for three future periods: 2010-2039, 2040-2069, 2070-2099 (central estimate).

4.3 Areal potential evapotranspiration (APET)

Historical mean annual areal potential evapotranspiration (APET) shows a north-south gradient, as well as a more gradual east-west gradient (Figure 4.4a). Projected changes to APET vary much less between seasons than rainfall and, accordingly, only the projected changes to APET are presented. Projected annual APET increased more in the western and central highlands than over the remainder of the state (Figure 4.4b).

The central estimate shows a very similar range of changes as the individual downscaled-GCMs (not shown). Even the largest end-of-century projected changes were moderate (<11% for all seasons and all downscaled-GCMs), while annual APET is projected to change very little in the east (Figure 4.4b).

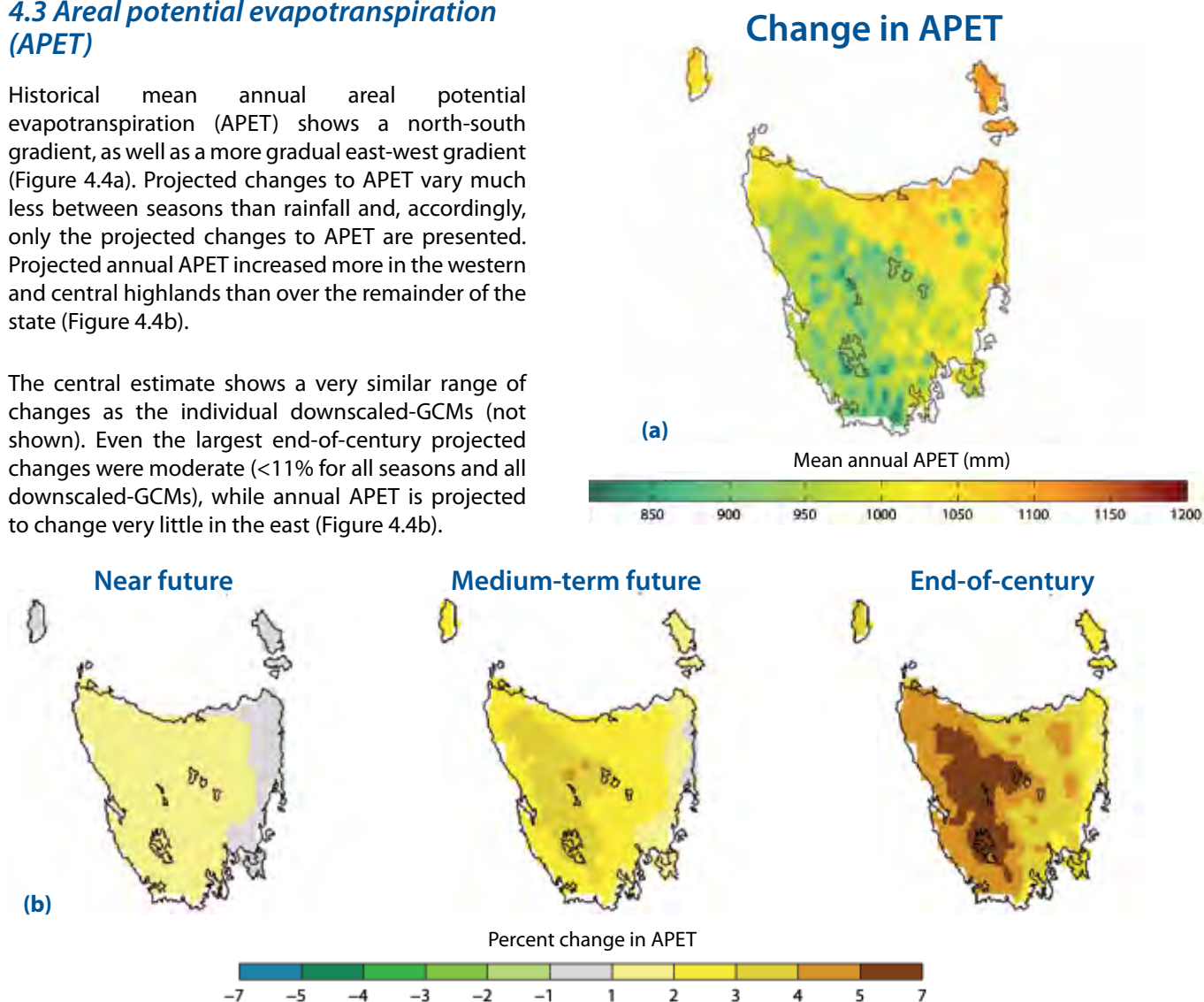


Figure 4.4 (a) Reference period (1961-1990) mean annual areal potential evapotranspiration (APET) and (b) change to mean annual APET for three future periods (central estimate shown).

Box 6

Summary of changes to rainfall and areal potential evapotranspiration

- Mean annual rainfall for the central highlands is projected to decrease by the end of the century.
- Mean annual rainfall is projected to increase in the east of the state.
- The projected increase in rain in the east occurs predominantly in summer and autumn.
- Annual west coast rainfall shows little change.
- West coast rainfall is projected to reduce in summer and increase during winter.
- Annual APET is projected to increase more in the western and central highlands than over the remainder of the state.
- Even the largest end-of-century APET changes are moderate. This applies to both the central estimate and to individual downscaled-GCMs.

5 Changes to runoff

5.1 Runoff during the reference period (1961-1990)

Tasmanian runoff distribution closely follows rainfall, exhibiting a steep west-to-east gradient (Figure 5.1). Runoff during the reference period (1961-1990) from the Simhyd model varied from more than 3000 mm in some areas over the western mountains to less than 20 mm in some areas in the east. The statewide annual mean runoff is 737 mm (50,091 GL). Winter has more runoff than any other season for almost the entire state (Figure 5.1); 39% of annual statewide runoff occurs in winter. Summer produces the least runoff in most areas of the state (Figure 5.1), accounting for 14% of annual statewide runoff.

The spatial pattern of annual runoff for a particular runoff model (eg Simhyd) does not vary greatly between the downscaled-GCMs during the reference

period (Figure 5.2). Likewise, seasonal runoff during the reference period does not vary greatly between downscaled-GCMs for a given hydrological model, as shown by the Simhyd runoff model (Figure 5.3). By contrast, there are marked differences in patterns of runoff between some of the runoff models. As discussed in Section 3, IHACRES simulated flows are much lower than the other models used with downscaled-GCM inputs (Figure 5.2, Figure 3.1b). This is particularly noticeable on the south-west coast and west coast, where IHACRES produces less than 1200 mm annual runoff for most cells, while the other runoff models produce more than 1500 mm annual runoff for the same cells (Figure 5.2). The models Simhyd, AWBM and SMAR-G produce similar results, while Sacramento is slightly drier than these three runoff models (Figure 5.2). Simhyd produces the highest statewide runoff during the reference period.

Modelled runoff 1961-1990

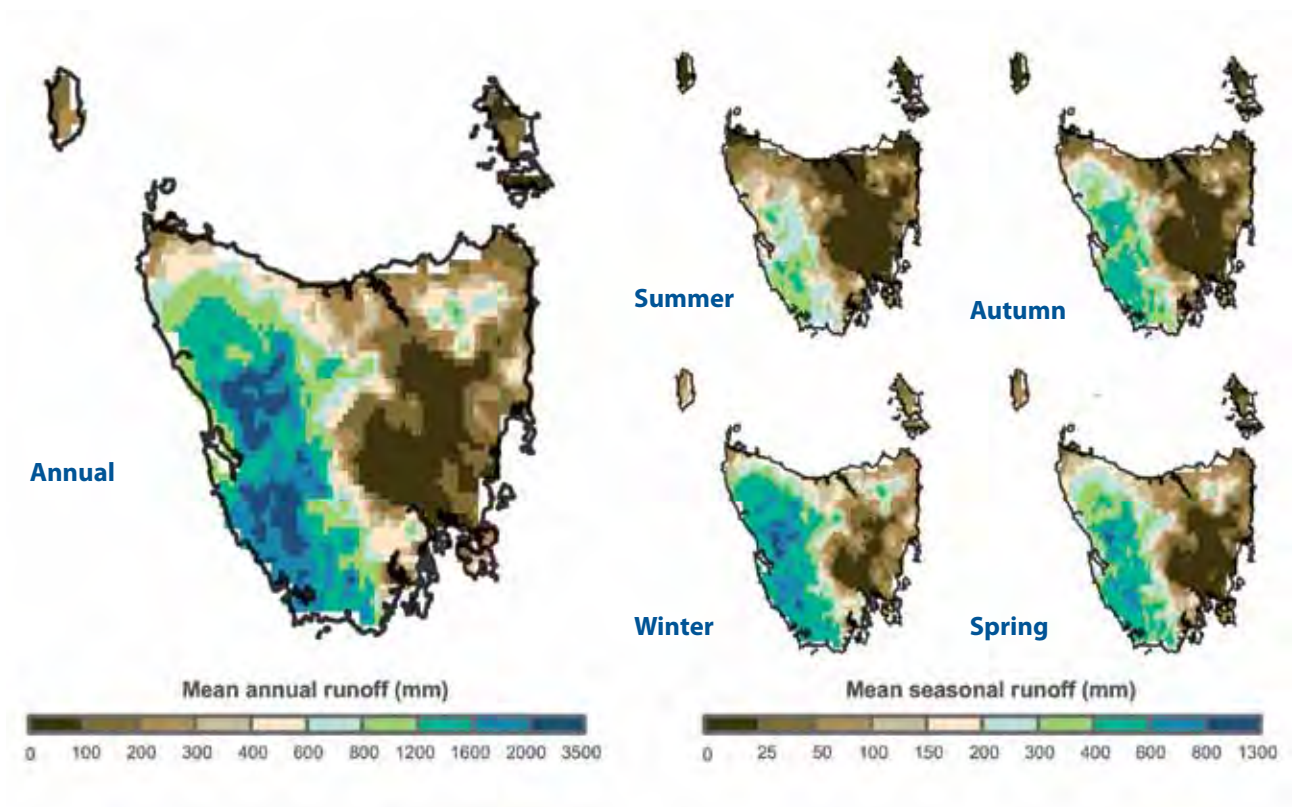


Figure 5.1 Simhyd annual and seasonal runoff for the reference period (1961-1990) (central estimate shown).



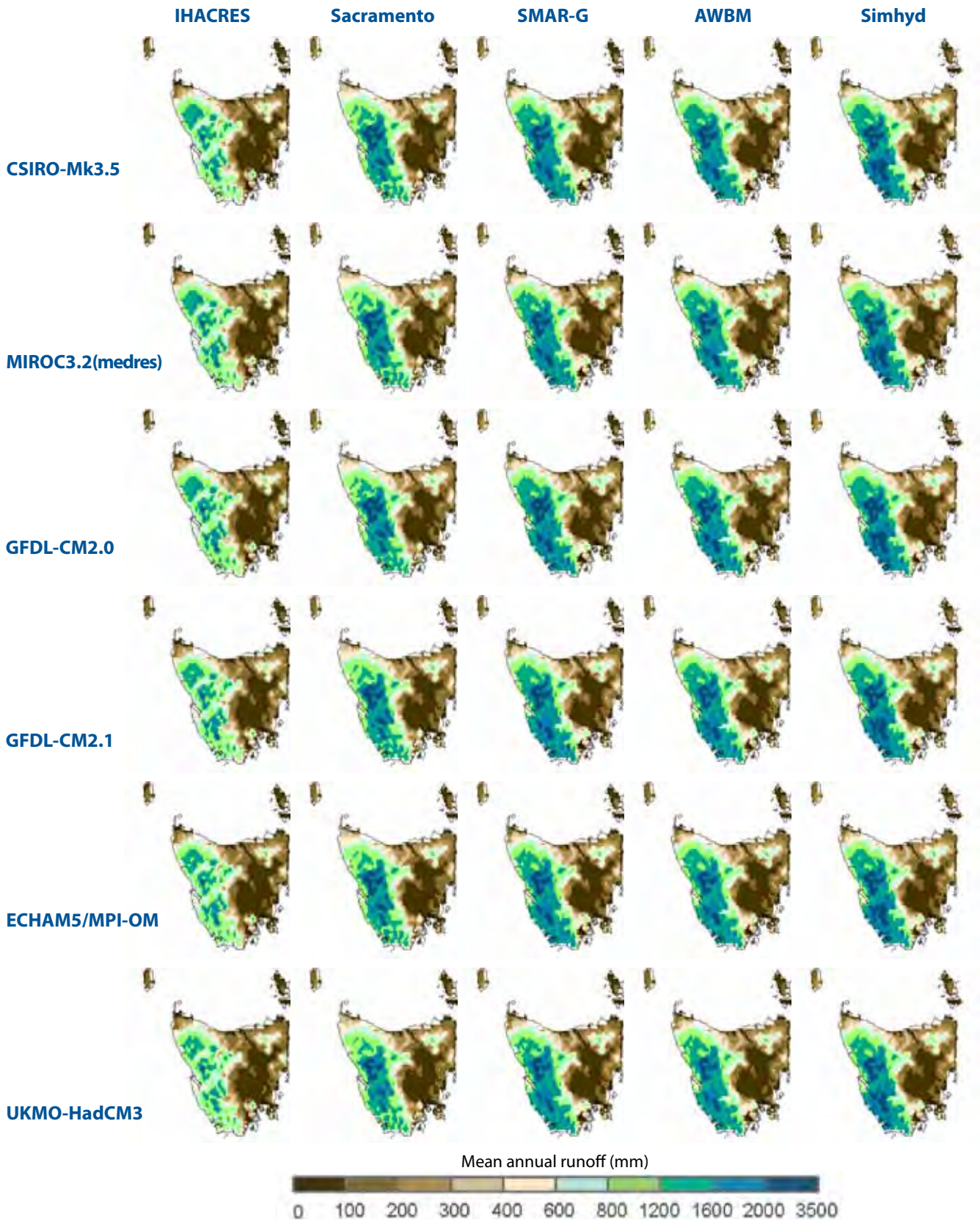


Figure 5.2 Mean annual runoff for the reference period (1961-1990) from all downscaled-GCMs and all runoff models. Runoff models are ordered left to right from lowest statewide runoff (IHACRES) to highest statewide runoff (Simhyd).

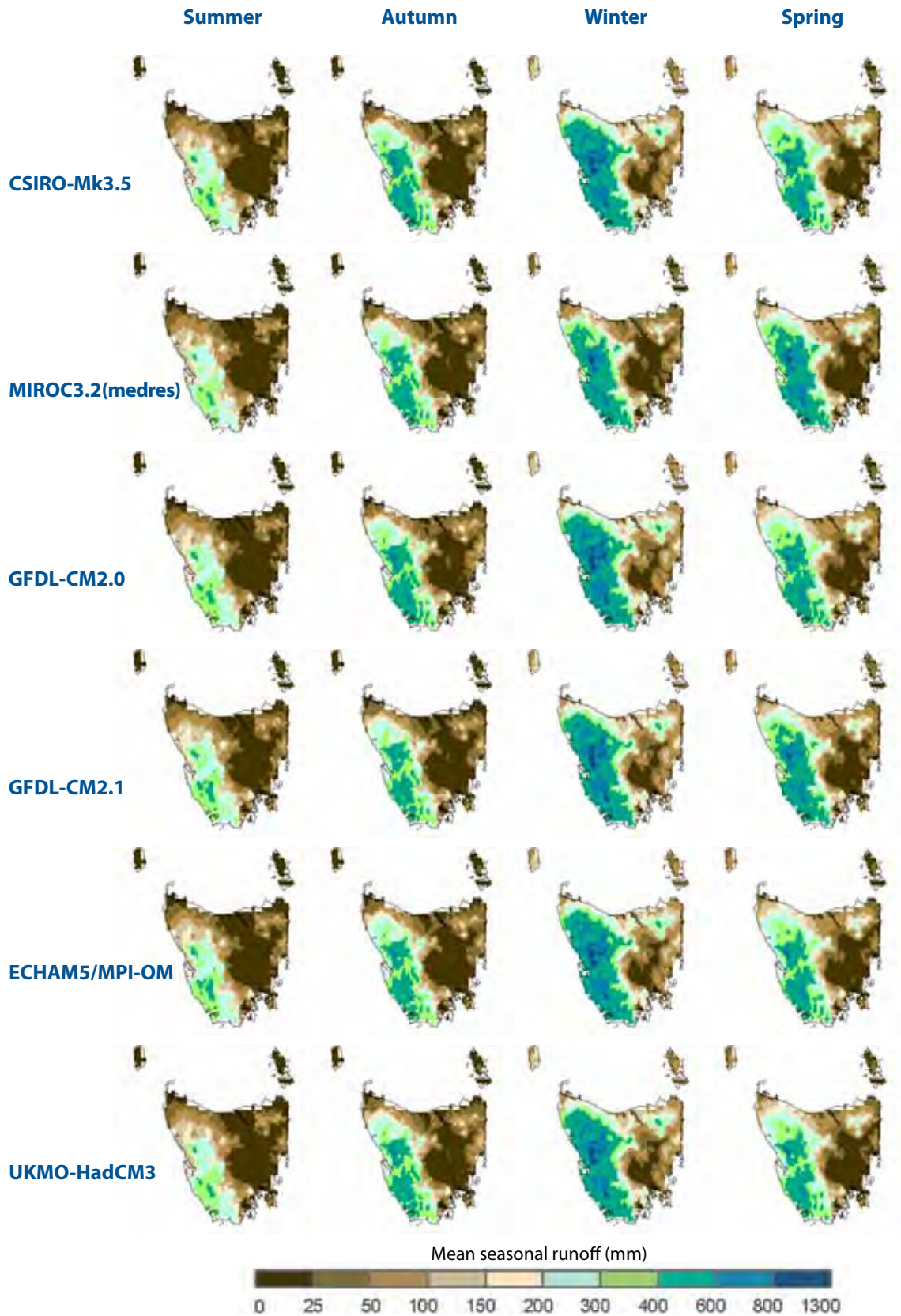


Figure 5.3 Simhyd mean seasonal runoff for the reference period (1961-1990) for all downscaled-GCMs.

5.2 Variation in runoff projections

Climate change projections of future runoff vary considerably between downscaled-GCMs, and to a lesser degree between runoff models (Figure 5.5). That is, the most uncertainty in future runoff comes from the differences between the simulations of future climate rather than from the differences between the hydrological models. The Sacramento, SMAR-G, AWBM and Simhyd runoff models show generally consistent changes for a given downscaled-GCM. IHACRES, however, generally projects wetter futures than the other runoff models. The high sensitivity of IHACRES to changed inputs (discussed in Section 3.1) means that this model is probably not a reliable predictor of future runoff in this project. Simhyd was chosen to represent all river model projections (Section 6) because Simhyd shows the lowest biases of all the runoff models, and because changes projected by Simhyd are consistent with all other runoff models (excepting IHACRES). Thus, Simhyd is used for all runoff and river flow projections from this point in the report.

Projections of end-of-century (2070-2099) change in annual runoff range between downscaled-GCMs from near statewide wetting (UKMO-HadCM3) to marked drying for much of the north and centre of the state (CSIRO-Mk3.5). Nonetheless, some spatial patterns are consistent for all downscaled-GCMs: the central highlands dry proportionately more than the remainder of the state, little change is expected along the west coast, and the eastern half of the state is generally projected to have greater percentage runoff increases than the western half.

We have used central estimates and downscaled-GCM ranges to represent projected changes. Central estimates summarise changes, however the variability between the downscaled-GCMs (and accompanying uncertainty) must be considered as a range of the possible projections of runoff. For this reason, changes in runoff projected by all downscaled-GCMs are described alongside the central estimates of changes, and downscaled-GCM ranges are assigned to river flow projections in Section 6.

5.3 Future runoff

The observed mean annual statewide runoff generated from SILO inputs shows a decline since the mid-1970s (Figure 5.4). The longer-term trend in SILO-forced historical runoff is positive for the 20th century, although century-scale rainfall trends from the SILO dataset are inconsistent with AWAP or BoM-HQ datasets (see Section 4.1). The recent decline in statewide runoff is not projected to continue through the 21st century (Figure 5.4), consistent with the absence of any significant trend in projected statewide rainfall (described in Section 4). Simhyd projected a slight increase of 1.1% in statewide annual runoff (559 GL.yr⁻¹) for the central estimate by the end of next century (Table 5.1). This increase is not monotonic and includes decadal variations, although changes are monotonic for particular regions, such as the reduction in runoff in the central highlands. Statewide runoff is projected to decrease in both the near future (2010-2039) and the medium-term future (2040-2069), before rising again by century's end (Table 5.1).

A part of these near future and medium-term future changes will be caused by natural variability while some part will be caused by anthropogenic climate change. Natural variability is likely to play a greater role in changes described for the near future and medium-term future. This is because the strength of the effects of anthropogenic climate change increase throughout the 21st century. There is considerable difference between individual downscaled-GCMs on both the sign and the magnitude of change to statewide runoff, reflected in the large ranges shown in the right-hand column of Table 5.1 and in the ranges shown in Figure 5.4. This large range implies high uncertainty in statewide runoff changes and that statewide runoff change is insignificant relative to uncertainty. More confidence can be expressed in those regional and seasonal changes on which the downscaled-GCMs show strong agreement.

Table 5.1 Central estimates of statewide mean annual rainfall for the reference period and three future periods. Range of changes from individual downscaled-GCMs is shown in right hand column.

| Period | Statewide mean annual runoff (mm) | Statewide annual runoff (GL) | Change from reference period (GL) | Change from reference period (%) | Downscaled-GCM range of change (%) |
|-----------|-----------------------------------|------------------------------|-----------------------------------|----------------------------------|------------------------------------|
| 1961-1990 | 737 | 50,091 | - | - | |
| 2010-2039 | 732 | 49,733 | -358 | -0.7 | -6.0 to 10.4 |
| 2040-2069 | 726 | 49,351 | -739 | -1.5 | -9.7 to 10.0 |
| 2070-2099 | 745 | 50,650 | 559 | 1.1 | -4.2 to 14.6 |

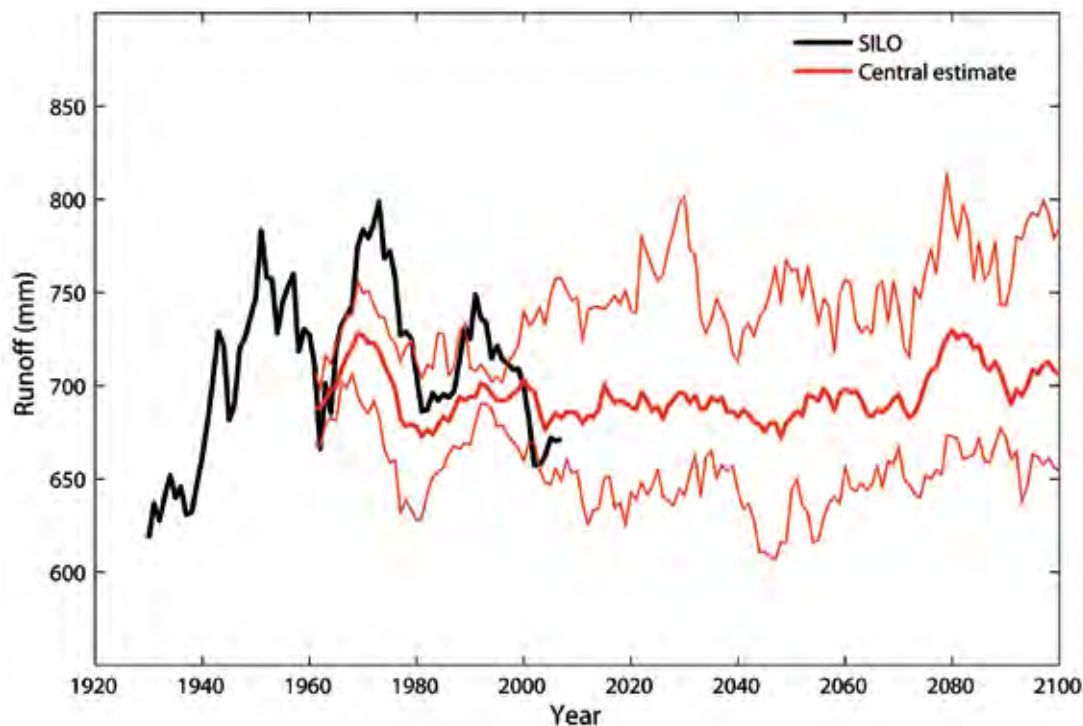


Figure 5.4 Observed and projected statewide runoff from 1930-2100. Curves are smoothed with an 11-year centred moving average. Black line shows Simhyd runoff with SILO inputs, calculated from outputs generated by Viney et al (2009b). Lighter red lines show range of downscaled-GCM projections, dark red line shows central estimate from the ensemble of six downscaled-GCMs.

The small statewide annual changes mask more significant seasonal and spatial variations in runoff across Tasmania. Summer runoff on the west coast and the north-west is projected to decrease throughout the 21st century, culminating in decreases of more than 20% for much of the north-west (Figure 5.6). Summer runoff in the east of the state is projected to increase (by as much as 100% in the north-east) by the end of the century. Autumn is projected to experience even greater increases in runoff in the east of the state: runoff increases by more than 100% in the Derwent Valley and to the east of the Derwent Valley. Autumn runoff is projected to decrease in the west, while winter runoff is projected to increase over most of the state. The notable exception to winter runoff increases is the central plateau. Indeed, the central plateau is the only region for which a decrease in runoff is projected for every season, and in every future period. Changes in annual and seasonal runoff in millimetres are given in Appendix D.

Annual runoff changes are not spatially uniform: decreases are projected for the central plateau in near, medium-term and end-of-century periods, while the eastern half of the state gets progressively wetter through the course of the century (Figure 5.6). Changes for the near future period are compared to projections produced for the TasSY project in Box 7, page 52.

The range of seasonal and annual runoff changes calculated from the Simhyd simulations is given for the end-of-century (2070-2099) in Figure 5.7. There is considerable variation in runoff projections between downscaled-GCMs. The CSIRO-Mk3.5 projection

of runoff is the driest of the downscaled-GCMs by 2070-2099. UKMO-HadCM3 is distinguished from the other downscaled-GCMs by projecting consistently wetter futures for all periods and all seasons. However, UKMO-HadCM3 consistently projects decreased runoff on the west coast during summer for all three future periods, as well as decreased runoff on the central plateau. GFDL-CM2.1 is notable for its similarity to the central estimate: for the end-of-century period this model strongly resembles the central estimate in both the spatial distribution and quantum of annual and seasonal runoff changes.

Despite some differences among the projections of the six downscaled-GCMs, certain spatial and seasonal changes are present in most of the projections (Figure 5.8). By 2070-2099, at least five of the six downscaled-GCMs agree on:

1. Decreased runoff in the central highlands in all seasons.
2. Increased runoff in the Derwent Valley in spring, winter and autumn.
3. Increased runoff in the lower South Esk River and lower Macquarie River catchments.
4. Decreased runoff in the western part of the state during summer.
5. Increased runoff along the west coast during winter.

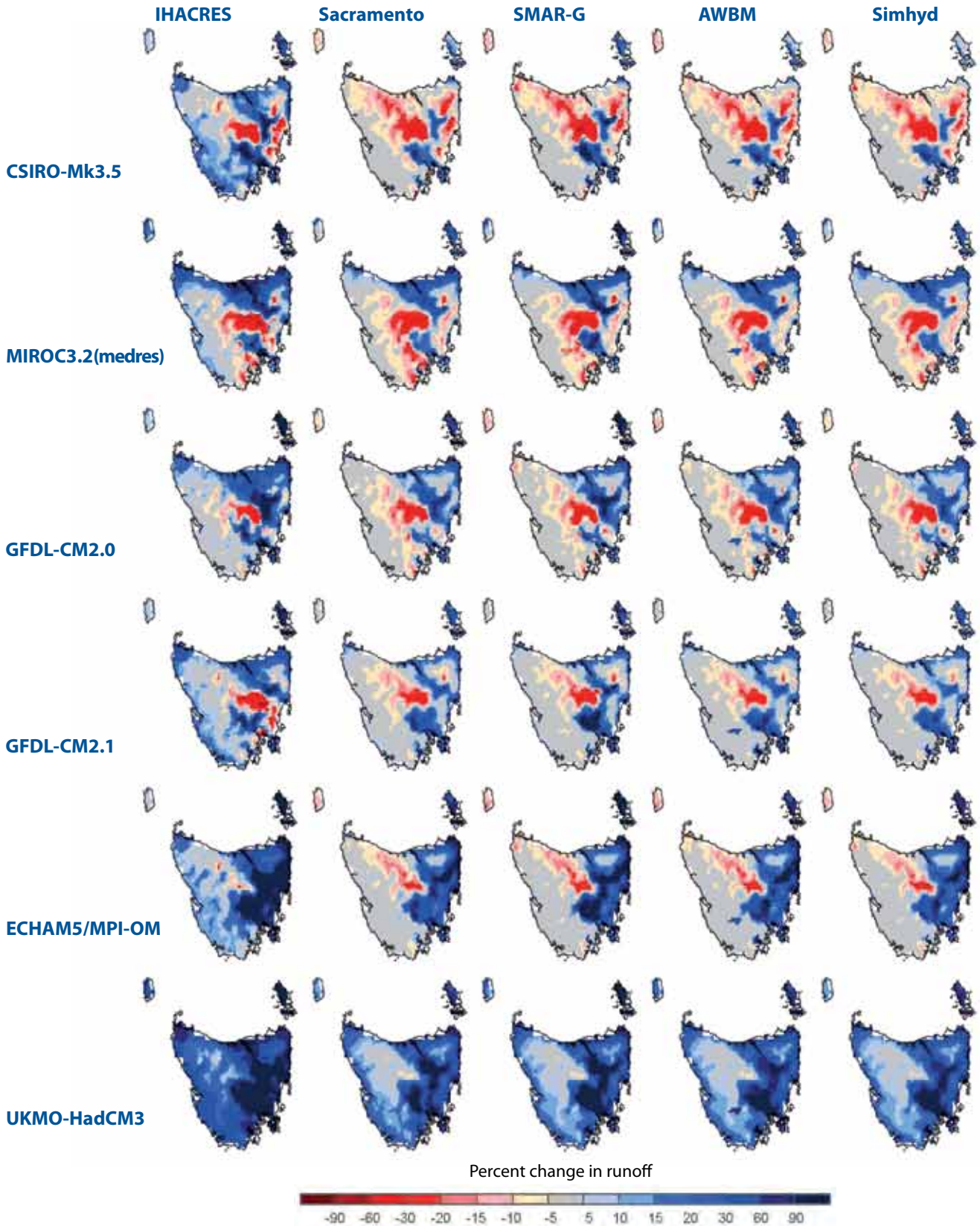


Figure 5.5 End-of-century (2070-2099) change in mean annual runoff compared to reference period (1961-1990) for all downscaled-GCMs and runoff models. Downscaled-GCMs are ordered top to bottom from driest statewide projection (CSIRO-Mk3.5) to wettest statewide projection (UKMO-HadCM3).

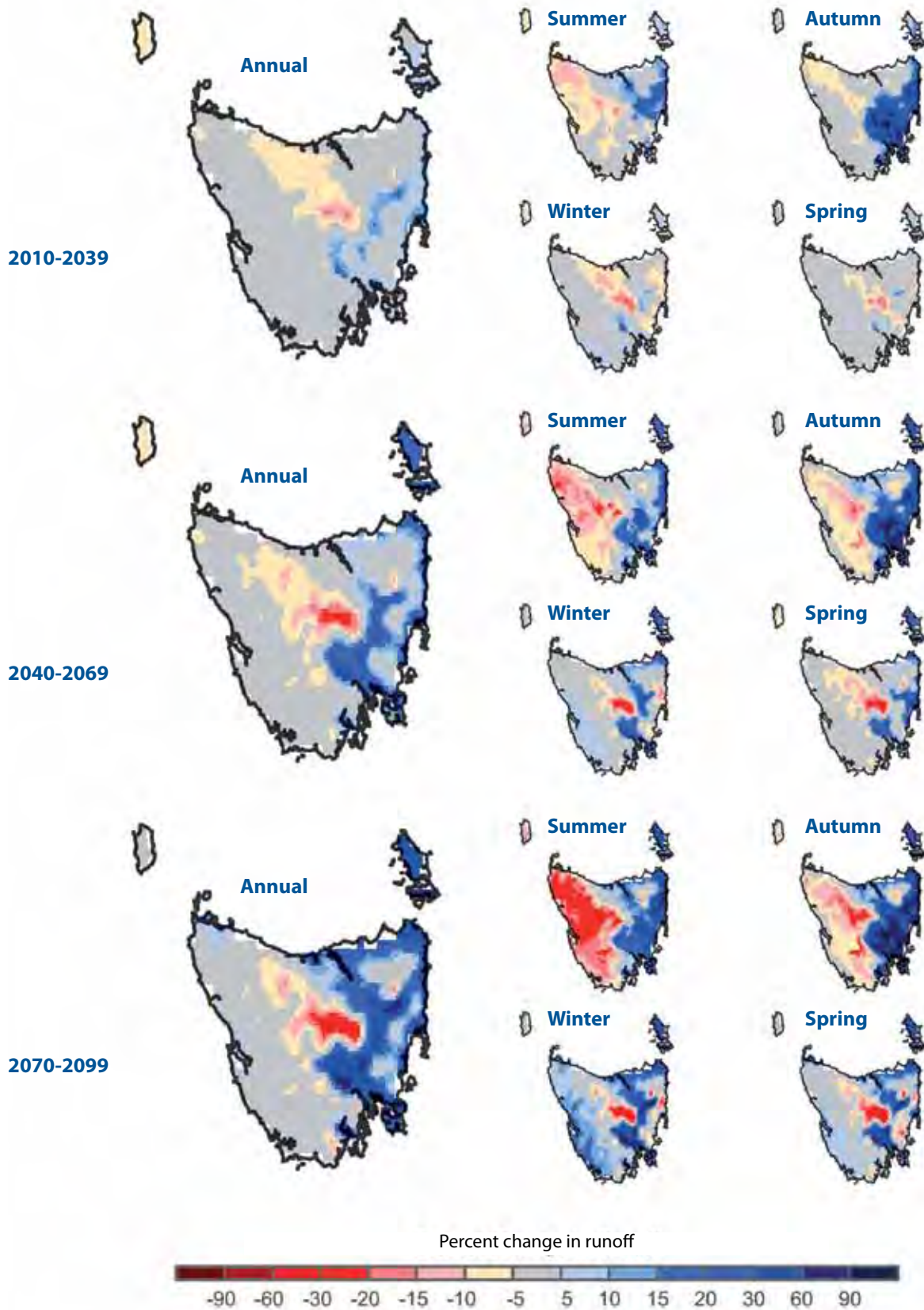


Figure 5.6 Percent change in mean seasonal runoff and mean annual runoff for three future periods compared to the reference period (1961-1990) from the Simhyd projections (central estimates).

Box 7

Comparison with the Tasmania Sustainable Yields Project

The *Tasmania Sustainable Yields Project* (TasSY) produced runoff projections for the year 2030. This timeframe approximates the period described as the near future (2010-2039) in our study. There are many similarities between annual runoff projections produced by Viney et al (2009b) for the TasSY median scenario (Figure 1.5) and those shown in our study (Figure 5.6) for the near future period. Both TasSY and our study project a statewide reduction in runoff (by 2% and 0.7%, respectively) in the near future. Both studies show marked reductions in runoff in the central highlands, and reduced runoff for a band extending from the central highlands to the north-west. Both studies showed little change in the west coast and south-west regions of the state.

There are clear differences between the studies for the east coast, however. Where we find little change in the north-east (Figure 5.6), Viney et al's (2009b) median scenario showed marked drying. Differences between the two studies in the north-east of the state are even more pronounced in projections of seasonal changes. Further, the projected increases in autumn runoff in the midlands, Derwent Valley and the east coast (Figure 5.6) are not present in Viney et al's (2009b) median scenario, which projected decreases in the midlands and Derwent Valley and only slight increases along the east coast.

Differences between the TasSY study and this project are caused by a number of factors. Differences stem from the downscaling methods employed, the different number (and different) GCMs used in both studies, and the different reference periods. We speculate that the most significant differences between the studies are caused by the fundamentally different downscaling techniques and the different GCMs used by the two studies. For example, Post et al's (2009) method preserves the magnitude of rainfall changes taken directly from GCMs, while our study does not. Unpublished analyses show that the bias-adjustment of sea surface temperatures (SSTs) and fine-resolution downscaling could reverse the sign of rainfall change of a given GCM over the north-east of the state from drying to wetting. In addition, Post et al (2009) used 15 GCMs to produce the TasSY climate scenarios while our study uses six downscaled-GCMs. Importantly, despite using fewer GCMs, our study includes some GCMs not included by the TasSY project. The most notable of these is the UKMO-HadCM3 downscaled-GCM, which consistently produces the wettest future projections in our project.

Changes in runoff are not necessarily caused by changes in average precipitation alone. For example, White et al (2010) showed that there was a larger increase in peak rainfall intensities in the south-east. Preliminary analyses (not shown) indicate that increases in the Derwent Valley are likely to be caused by increases in average daily rainfall intensities as much as by increases in mean seasonal or annual rainfall (not shown).

Changes to high daily runoff events (daily runoff that is exceeded on less than 2% of days) calculated from central estimates of Simhyd simulations follow a similar spatial pattern to mean runoff (Figure 5.9). However, high runoff events are likely to increase proportionately more than mean runoff in regions where mean runoff increases (Figure 5.9), for example the western parts of the west coast and north-west regions. The largest increase in high runoff events occurs in the east, particularly in the lower Macquarie and South Esk Rivers, and in the lower Derwent Valley. The only region projected to experience a decrease in high runoff events is the central highlands plateau. Changes in high daily runoff events essentially reflect changes to rainfall extremes. For a discussion of changes to rainfall extremes, see White et al (2010). The underlying causes of the runoff changes, including the meteorological drivers and changes in the frequency of rainfall, will be explored in subsequent research.

Low daily runoff events (daily runoff that is exceeded on more than 95% of days) show marked regional differences to changes in mean runoff. Most of the state shows decreases in low flows by end-of-century (Figure 5.10). This applies to regions such as the Derwent Valley, even as that region experiences increases in mean and high runoff events.

In summary, by end-of-century much of the state exhibits decreased or little-changed low runoff events and increases to high runoff events, even in regions that show little change to average runoff. This points to possible changes to the shape and character of stream flows: hydrographs may rise faster, to higher peaks, and drop more quickly in a warmer world. The central highlands are again exceptional, as this is the only region that shows clear decreases in low flows as well as in high flows. Changes to characteristics of stream flow could have important implications for fluvial geomorphology and water quality caused by changed regimes of erosion and deposition of sediments, and other environmental impacts. Exploring these implications is outside the scope of our study.

Annual and seasonal runoff

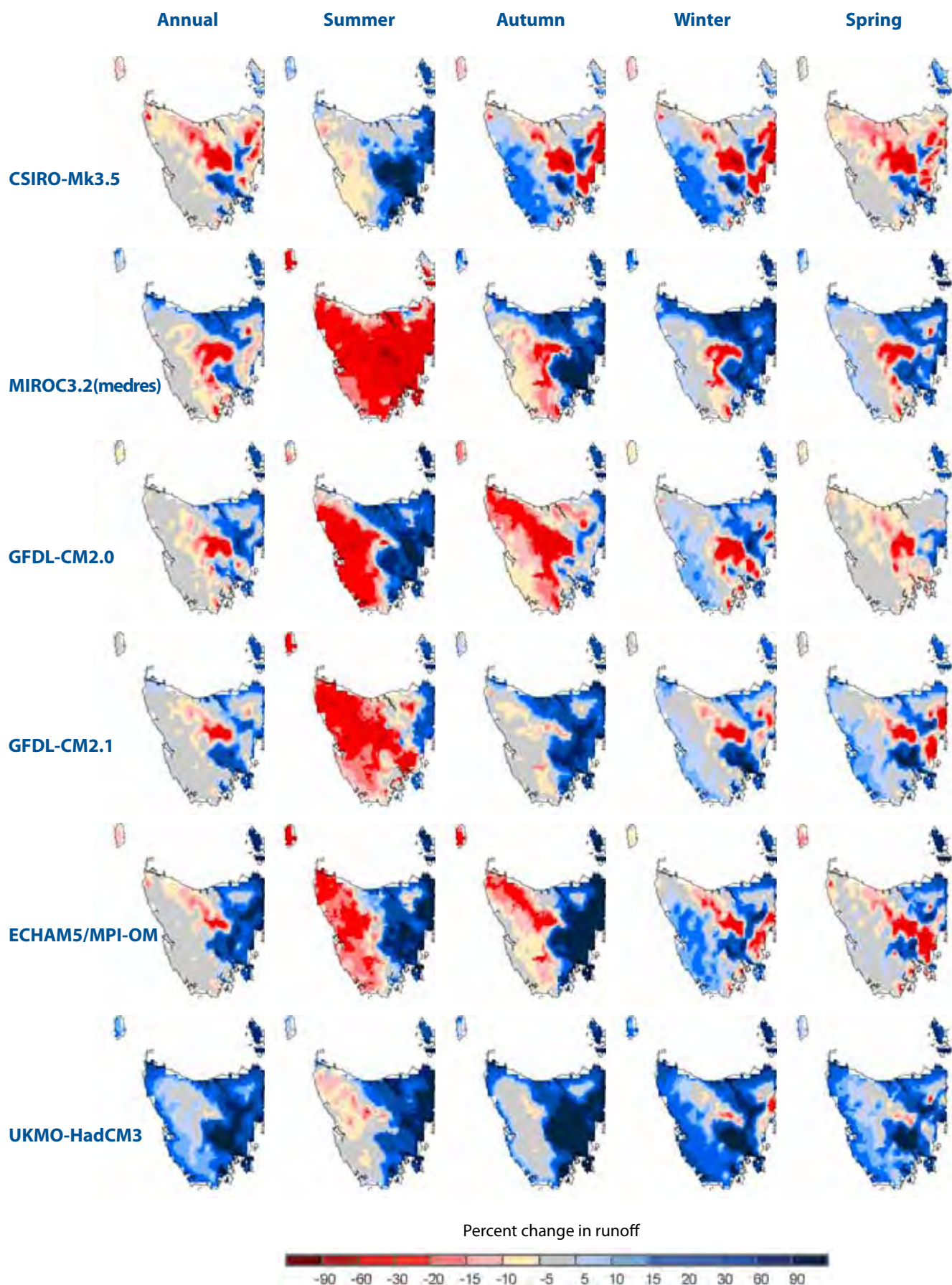


Figure 5.7 Change in mean annual runoff and mean seasonal runoff from the reference period (1961-1990) to end-of-century (2070-2099), calculated for all downscaled-GCM Simhyd projections.

Climate model agreement

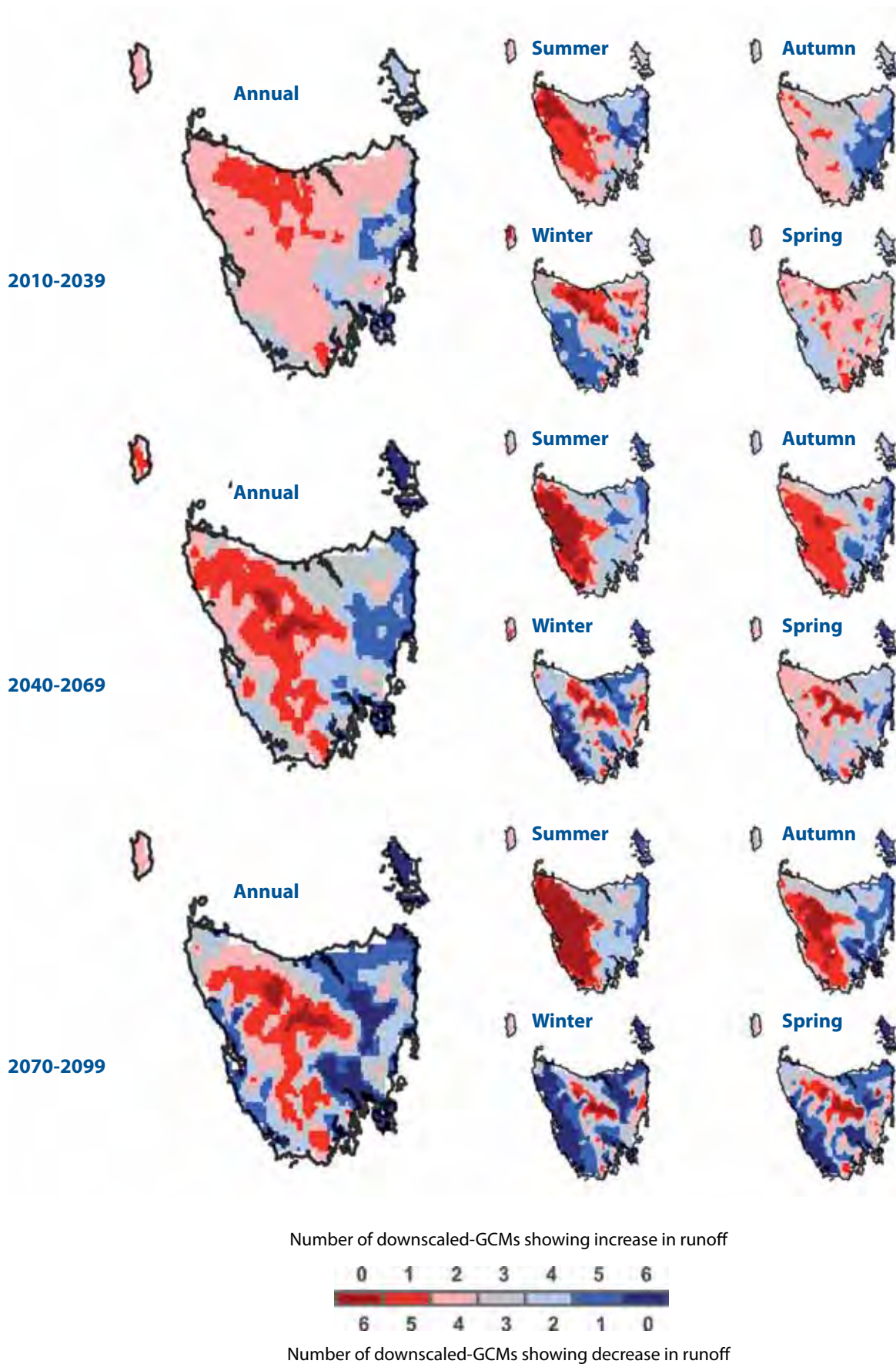


Figure 5.8 Number of downscaled-GCMs showing annual and seasonal increases or decreases in mean runoff for three future periods, calculated from Simhyd projections.

High and low runoff events

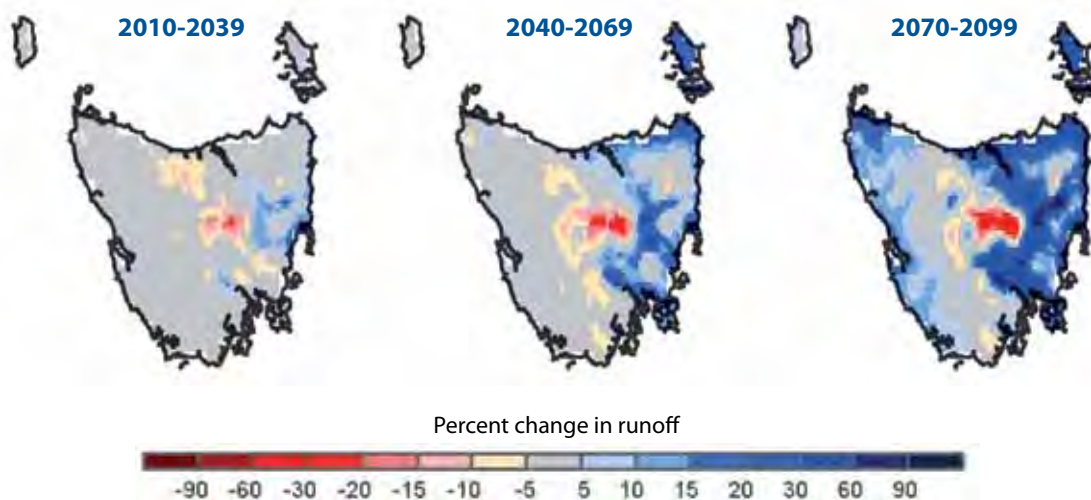


Figure 5.9 Change in high daily runoff (runoff with a 2% exceedance probability) for three future periods compared to the reference period (1961-1990) generated from central estimates of Simhyd projections.

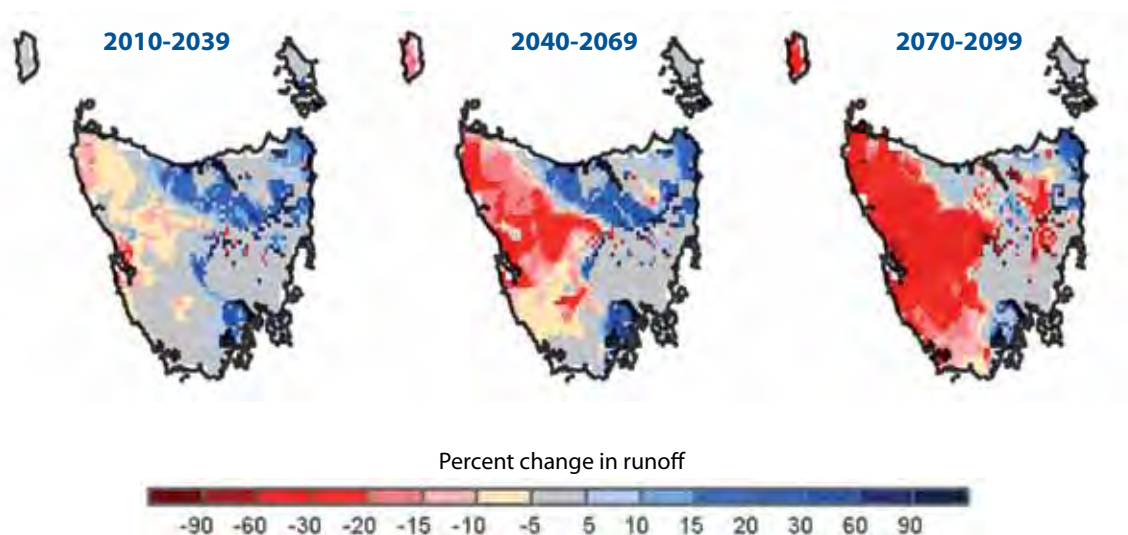


Figure 5.10 Change in low daily runoff (runoff with a 95% exceedance probability) for three future periods compared to the reference period (1961-1990) generated from central estimates of Simhyd projections.

Box 8

Summary of changes to runoff

- Statewide runoff shows little change for the 21st century.
- There are substantial changes to the seasonal and spatial distributions of runoff.
- By 2070-2099, at least five of the six downscaled-GCMs show:
 - Decrease in runoff in the central highlands in all seasons.
 - Increase in runoff in the Derwent Valley and surrounds in spring, winter and autumn.
 - Increase in runoff in the lower South Esk River and lower Macquarie River catchments.
 - Decrease in runoff in the western part of the state during summer.
 - Increase in runoff along the west coast during winter.



6 Changes to river flows

Projections of river flows described in this section are flows remaining after all water extractions, diversions and other losses (where applicable) have been taken into account. Extractions, diversions and other losses are calculated according to operating rules and water licences that were current at 31 December 2007. No account has been taken of future changes to land use or water management practices that could affect projected river flows. The projected river flows presented here are therefore the changes caused only by a changing climate and rising greenhouse gases, and not caused by changes to the catchments through other human activities or practices.

Changes in central estimates of flow varied between the three future periods. During the 21st century, there is a progressive rise in the number of rivers showing increased flows. Thirty percent of the 78 modelled catchments show a clear increase in central estimates of annual flows in the near future (2010-2039). This fraction increases to 50% of catchments for the medium-term future (2040-2069) and at the end-of-century (2070-2099) flows increase in 64% of catchments (50 of 78 catchments) (Figure 6.1a). By end-of-century (2070-2099), only 35% of catchments (28 of 78 catchments) are projected to have clear decreases in flow. There are marked changes projected in annual flows for a number of rivers by end-of-century. Absolute changes of more than 10% in central estimates of annual flows are projected for 32 of 78 catchments (40% of catchments) (Figure 6.1b). Absolute changes of more than 10% are projected for 20% of catchments in the medium-term future and 2% of catchments in the near future (Figure 6.1b). Changes to central estimates of flows are listed for each catchment and future period in Appendix E, alongside the range of changes projected by individual downscaled-GCMs by end-of-century (2070-2099). The ranges of plausible changes to river flows by end-of-century (Appendix E) can be significantly higher than the mean changes, and also significantly lower. In the highest case, 59 rivers change by more than $\pm 10\%$ and in the lowest case only 24 rivers change by more than $\pm 10\%$.

There is considerable variation around the central estimates of river flows from the ensemble of downscaled-GCMs. Changes in river flows from the reference period are plotted for four example rivers in Figure 6.2. Three of the four rivers show increases in central estimates of annual flow by end-of-century (the exception is the Black River, which shows little change). However, each of the downscaled-GCMs shows large decadal variations in trends in river flows over the 21st century.

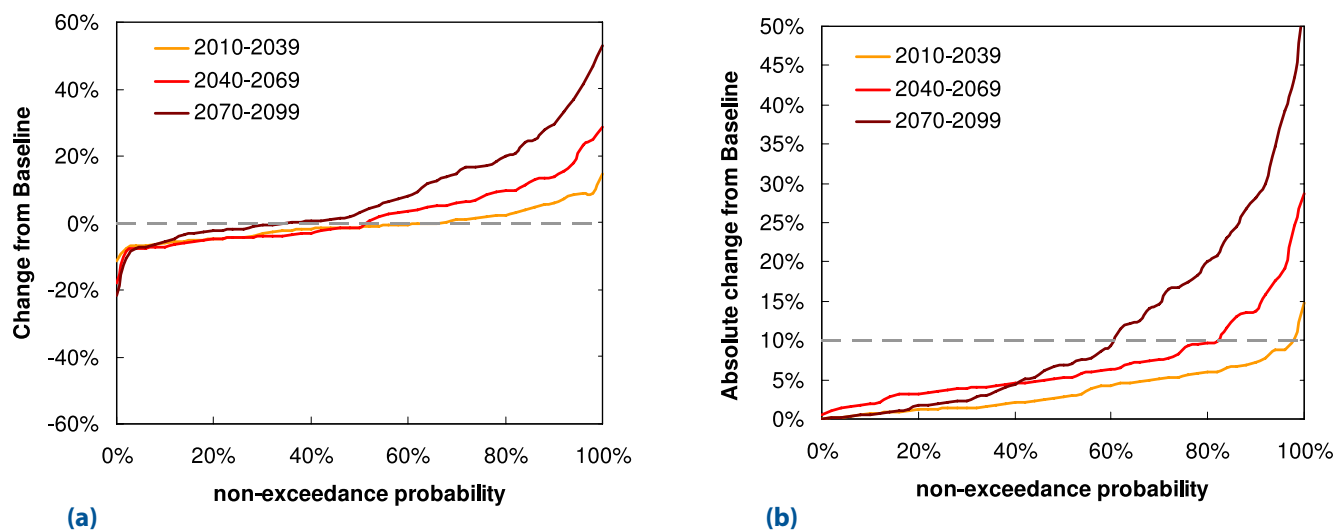


Figure 6.1 Non-exceedance probabilities of (a) percent change in river flow and (b) absolute percent change in river flow for 78 river catchments (central estimates). Grey dashed lines show (a) no change and (b) 10% change.

These variations are created by the slow variations in the ocean sea surface temperatures from the GCMs. The decadal variations are not spatially uniform. For example, MIROC3.2(medres) shows decreases in flow in the Rubicon River until about 2060, after which it shows a marked increase in flows and projects the wettest end-of-century future. Conversely, MIROC3.2(medres) shows a reduction in flow for the entire century in the Little Swanport River and gives the driest end-of-century projection for this river. UKMO-HadCM3 shows clear increases in all four example catchments, but the changes are not necessarily synchronised. For example, UKMO-HadCM3 projects large increases in flows for both the Little Swanport and Clyde Rivers around 2050 (Figure 6.3c,d), and these increases are not present in the Black River or Rubicon River (Figure 6.3a,b).

At end-of-century, four of the six downscaled-GCMs, ECHAM5/MPI-OM, GFDL-CM2.0, GFDL-CM2.1, and MIROC3.2(medres), project increases in about half of the 78 catchments, while CSIRO-Mk3.5 shows moderate decreases for about 70% of catchments. The UKMO-HadCM3 model is something of an exception to the other downscaled GCMs, as it projects increases in all catchments for the near future period (Figure 6.3a) and for almost all catchments for the medium-term future and end-of-century (Figure 6.3b, Figure 6.3c). UKMO-HadCM3 skews the central estimate towards increased flows, particularly for the medium-term future and end-of-century.

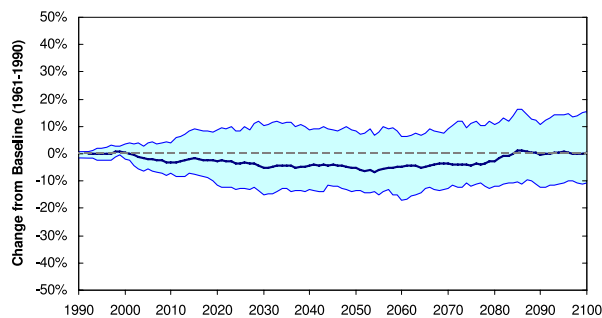
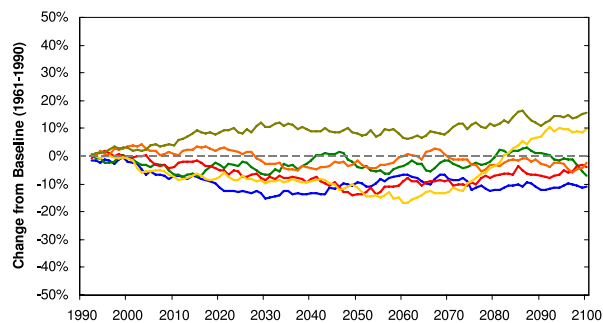
Spatial distributions of annual and seasonal changes to central estimates of river flows for the end-of-century are given in Figure 6.4. Central estimates of seasonal

flows at eight example catchments for this period are shown by Figure 6.4a-h. Spatial changes in flows for all downscaled-GCMs are given in Appendix H. The spatial distribution of changes to flows in free-flowing rivers approximates the changes described for runoff in Section 5. This includes a progressive reduction in flows in all seasons in the central highlands just east of the central plateau and in the only river modelled in the central highlands region, the Nive River, particularly in summer (Figure 6.4d). Flows in the rivers in the state's north-west progressively declined in summer by up to 22% at end-of-century, as shown by the Black River (Figure 6.4a). Flows in north-west and north coast rivers increased above flows during the reference period by end-of-century (Figure 6.4a,b). Similar seasonal changes were also experienced by western and south-western rivers, shown by the Franklin River and the Huon River (Figure 6.4f,g).

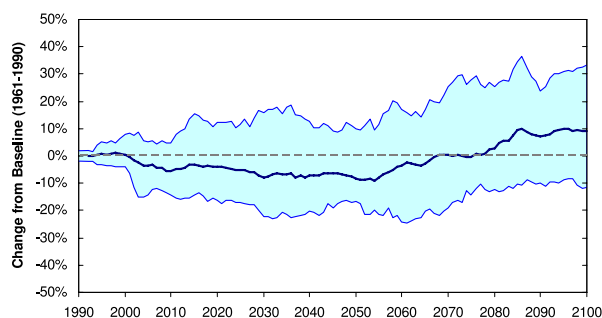
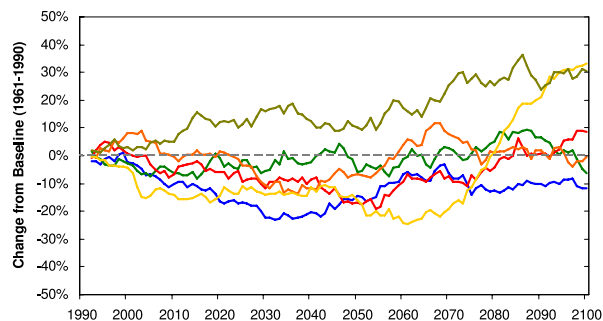
Rivers on the east coast and midlands generally showed progressively increasing flows for the 21st century, particularly during summer and autumn (Figure 6.4c,e,h). Substantial proportions of the South Esk, Clyde and Little Swanport catchments are presently used for agriculture, and the increased river flows and runoff projected for these basins could have important implications for agricultural practices in these catchments. The changes to the central estimates of the river flows tend to be smaller than the range of projected flows from the ensemble of downscaled-GCMs. That is, the ranges of future and reference flows projected by the downscaled-GCMs overlap in all eight rivers for all periods. The ranges tend to be wider for the eastern rivers in both the reference and future periods.

River flows

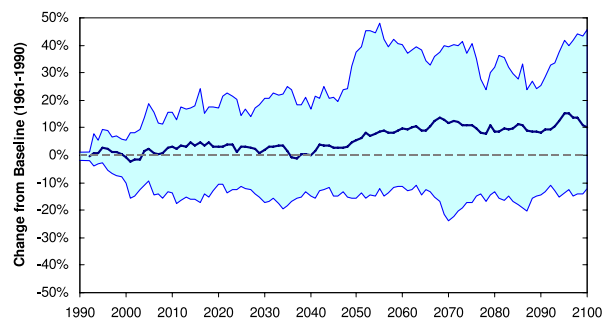
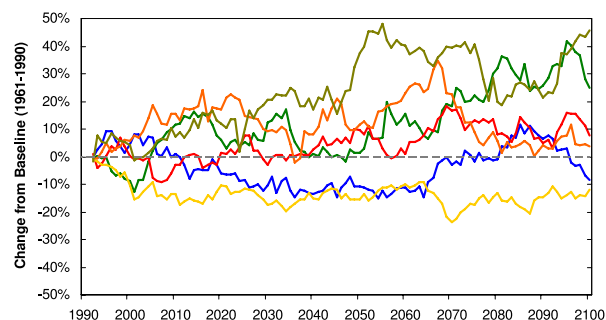
Black R at South Forest



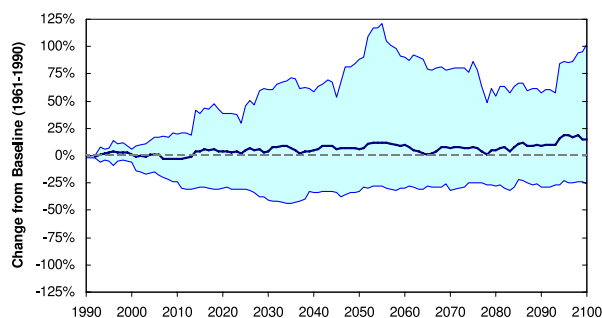
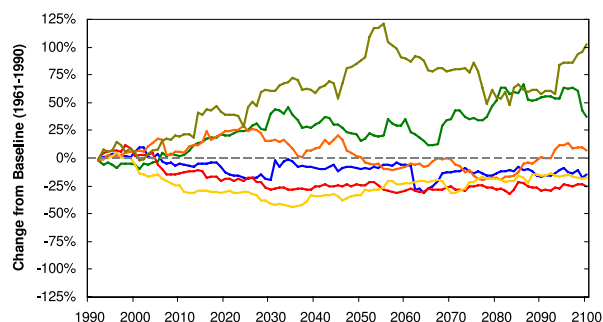
Rubicon R at tidal limit



Little Swanport R upstream Tasman Hwy



Clyde R at Hamilton



— CSIRO-Mk3.5
 — ECHAM5/MPI-OM
 — GFDL-CM2.0
 — GFDL-CM2.1
 — MIROC3.2(medres)
 — UKMO-HadCM3

Range
 Central estimate

Figure 6.2 Change in river flows for four example rivers at existing gauge sites. Changes plotted are percent change of 30-year trailing moving average flows from the reference period (1961-1990). Plots on left give change for each downscaled-GCM, plots on right show changes to central estimates and the range of the downscaled-GCMs. Gauge site locations are shown in Figure 6.4.



River flows

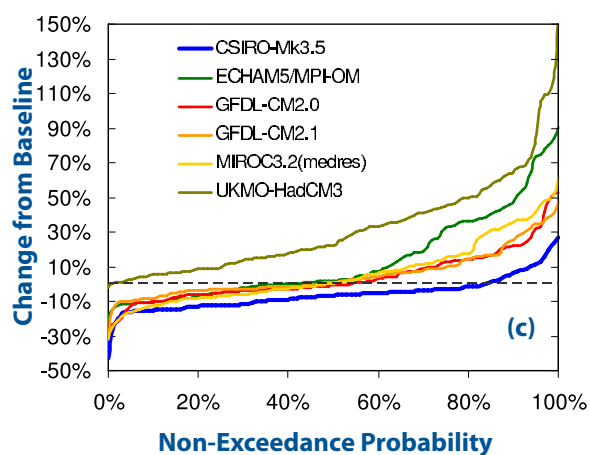
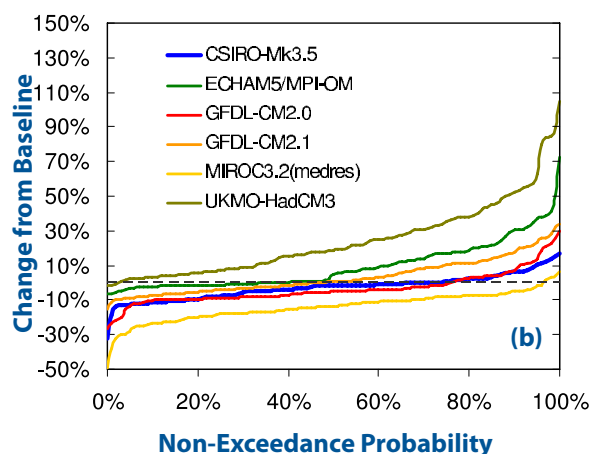
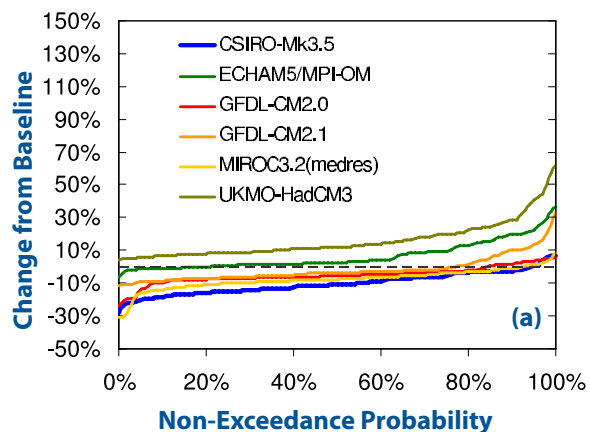


Figure 6.3 Number of catchments showing a given percent change in flows (expressed as non-exceedance probabilities) for all downscaled-GCMs for (a) the near future (2010-2039), (b) the medium-term future (2040-2069) and (c) end-of-century (2070-2099). Grey dashed lines show no change.

River flows

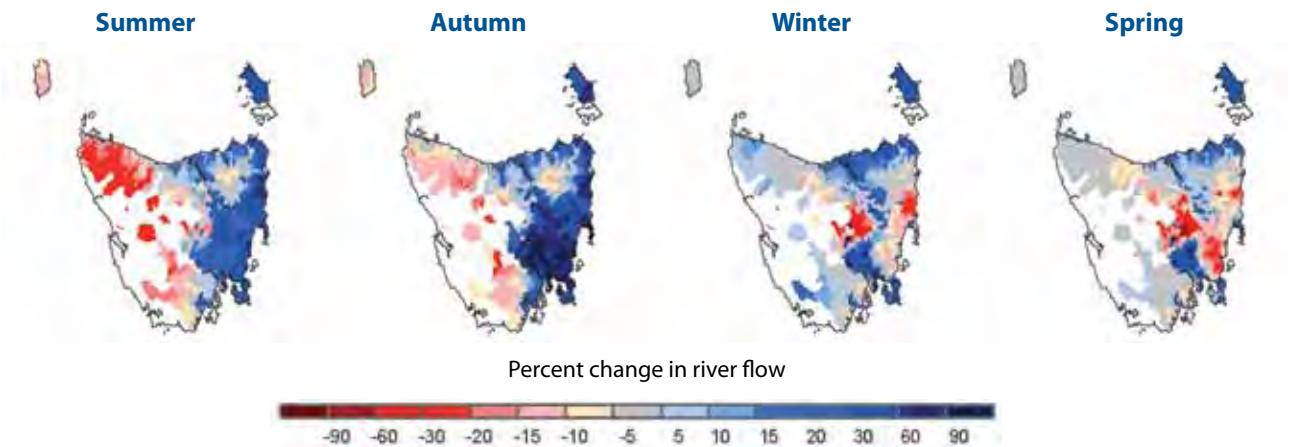
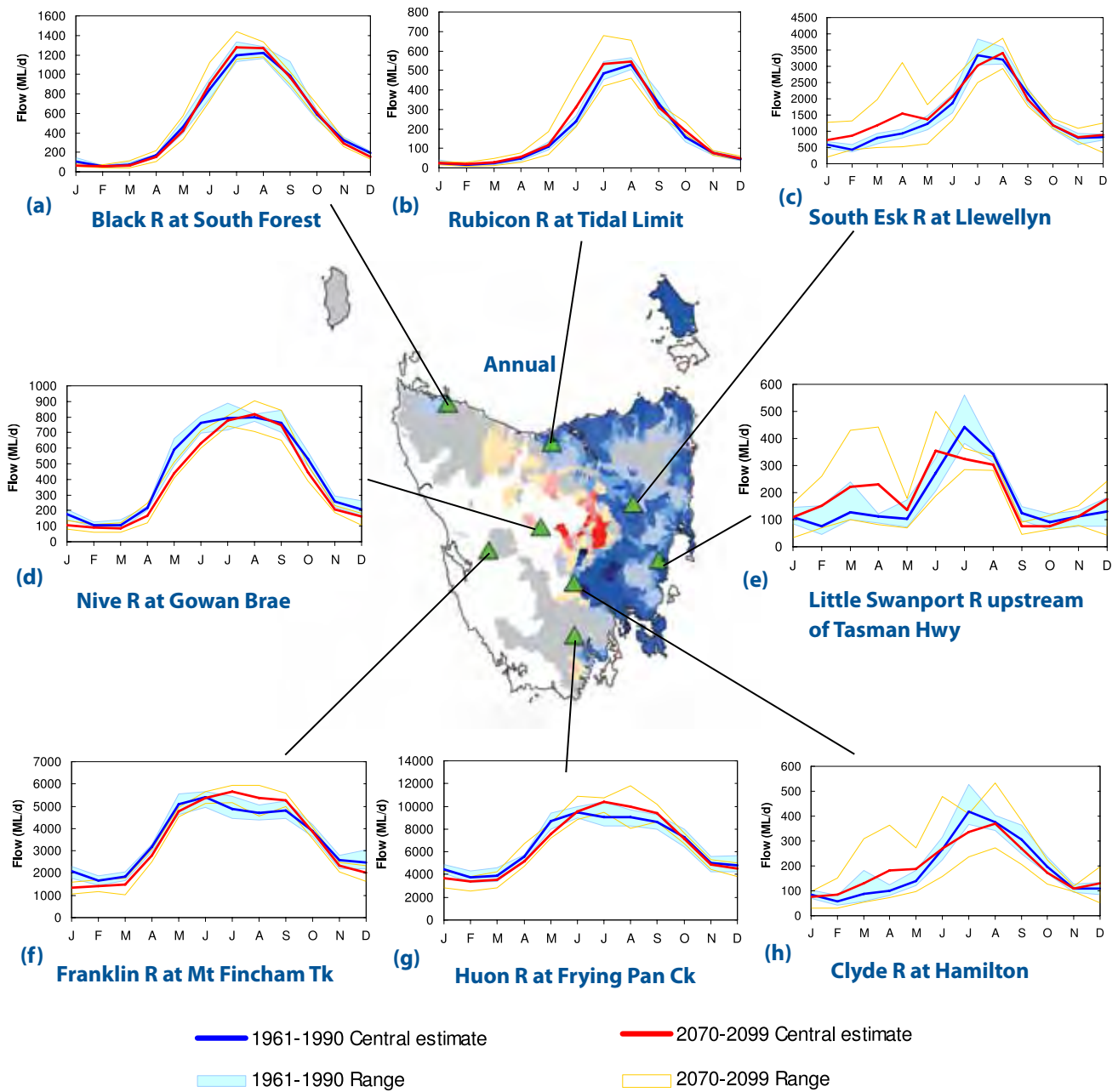


Figure 6.4 Percent change in annual (centre) and seasonal (bottom) river flow from reference period (1961-1990) to end-of-century (2070-2099) (central estimate): (a)-(h) give changes in seasonal flows for eight example gauges at existing flow gauges. White regions indicate areas of regulated flow for hydro-electric power generation (described by Figure 6.8) or regions for which catchment models were not developed.

6.1 Changes to irrigation storage inflows and reliabilities

Many catchments show changes at the subcatchment level in a future climate. These changes of river flow can affect water storage within a catchment depending on where subcatchment runoff changes occur. For example, the central estimate of flow at the Clyde River catchment outlet is projected to increase by 17% by end-of-century (Appendix E). However, these increases are caused by increased runoff in the lower part of the catchment while annual inflows to Lake Crescent/Sorell at the head of the Clyde catchment decrease by 20% by end-of-century (Figure 6.5c and Appendix F).

Large changes in lake inflows do not necessarily translate to large impacts on the reliability of storages. Reliability of supply has been calculated for each irrigation storage as the ratio of water volume supplied to water volume allocated, following the method of Ling et al (2009a, b, c, d, e) (Appendix G). Calculations of reliabilities of supply for Lake Crescent/Sorell (the two lakes form one water body) are shown in Figure 6.6. Four downscaled-GCMs show that Lake Crescent/Sorell will be able to meet water demand less regularly, with the extreme-case MIROC3.2(medres) showing a reduction in reliability of more than 60%. However, there is a wide range in the projections of reliability, with two downscaled-GCMs showing little or no change. Lake Crescent/Sorell is operated as the major irrigation storage for the Clyde River and offers an important buffer for farmers during drier years. Our projections suggest that it is likely to be less capable of fulfilling this function as reliably in the future.

Like the Clyde catchment, flows at the outlet of the Meander River decrease only slightly (-1.8%) by end-of-century (Appendix E), but inflows to Meander Dam (located at the head of the catchment) decrease by 12.6% (Figure 6.5a). This decrease in Meander Dam inflows has little effect on the reliability of supply calculated for this storage. This is because the operating rules for this storage were current at 31 December 2007, before the majority of water in the storage was allocated to irrigators (Meander Dam was commissioned in February 2008). In other words, projected reliabilities shown for Meander Dam are artificially high because demand (as defined by the operating rules) is artificially low. Recoding the Meander River model with more up-to-date operating rules was outside the scope of this project. Meander Dam highlights the difficulty of applying historical water use and land use rules to future projections. Applying the projections of runoff to scenarios of future land use and water use change was outside the scope of this project, but would be highly useful for adaptation research addressing management of irrigation storages under a changing climate.

Inflows to irrigation storages further to the east generally increase. For example, Lake Leake and Tooms Lake in the Macquarie River catchment and Craigbourne Dam in the Coal River catchment show marked increases in inflows (Figure 6.5d,e,f, and Appendix F), while Cascade Reservoir in the state's north-east shows a slight increase in inflows (Figure 6.5b and Appendix F). This improves the reliability of supply from eastern storages: Tooms Lake shows an increase in the central estimate of reliability by 2100, while Lake Leake maintains near 100% reliability for most projections. Tables of changes in inflows to all storages and to changes in reliabilities of supply from storages are presented in Appendix F and G, respectively.





Inflows to irrigation storages

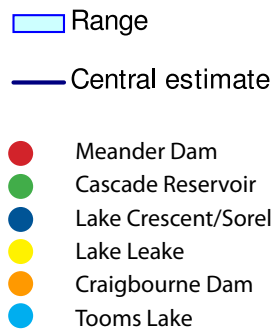
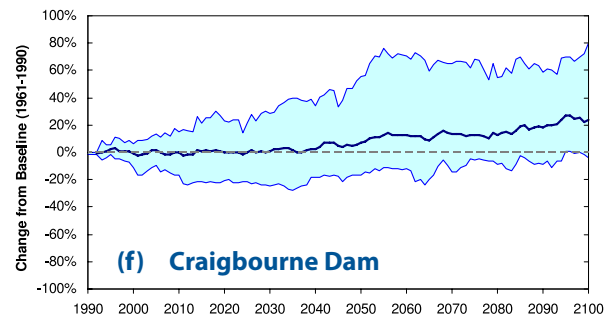
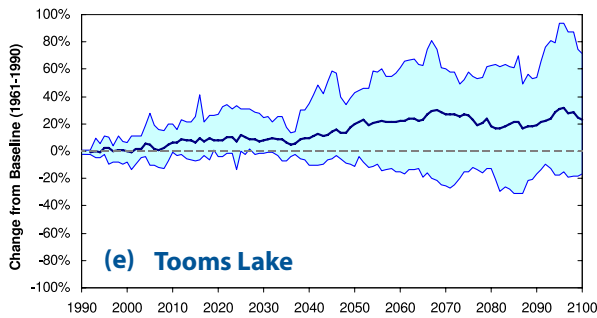
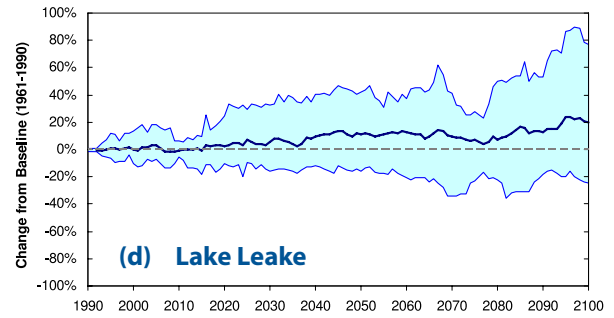
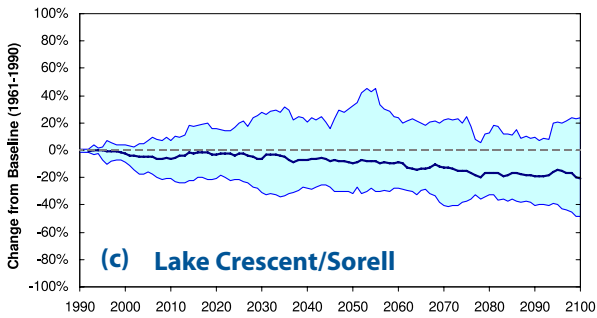
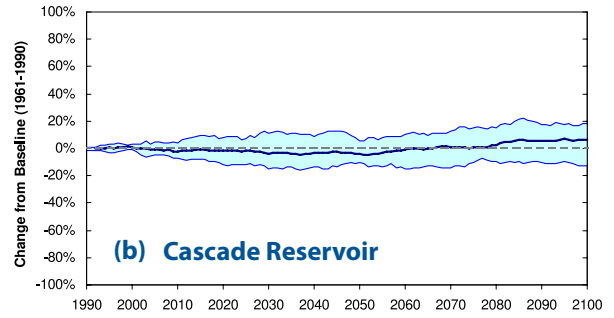
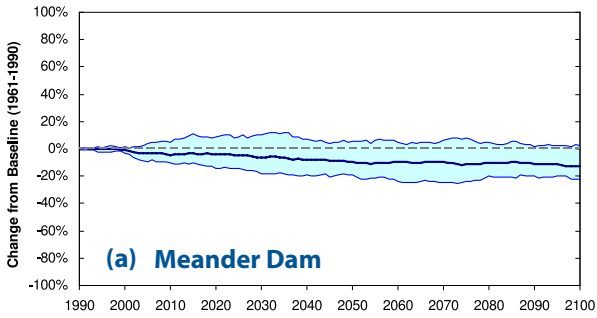


Figure 6.5 (a)-(f) Change in inflows to six important irrigation storages. Changes plotted are percent change of 30-year trailing moving average from average flow during the reference period (1961-1990).



Reliabilities of irrigation storages

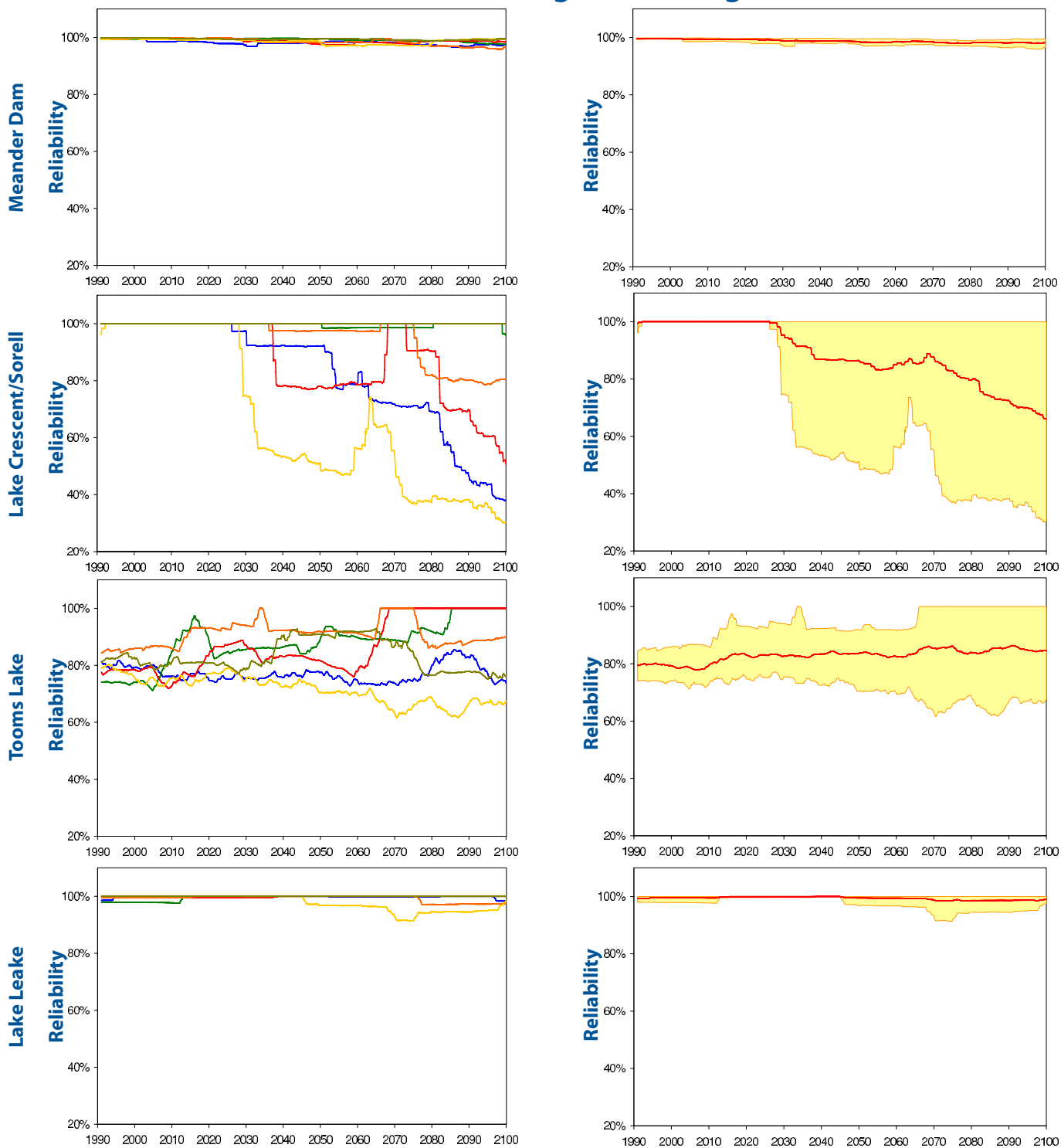


Figure 6.6 Reliabilities of supply for four example large-irrigation storages. Reliability is defined as the ratio of water supplied to water demanded for a moving 30-year period. Plots on left give change for each downscaled-GCM, plots on right show changes to central estimates and the range of the downscaled-GCMs. Locations of storages are shown in Figure 6.5.

6.2 Changes to inflows to the hydro-electric system

Changes to inflows to catchments feeding Tasmania's hydro-electric power generation system are shown in Figure 6.7. Observed inflows have declined through the 20th century. Projections indicate that inflows will continue to decline through the 21st century. The spatial distribution of end-of-century changes is shown in Figure 6.8. By end-of-century, eastern catchments show increased annual inflows, central plateau catchments show declines and western catchments show little change. Seasonal changes to inflows are particularly important to the operations of run-of-river hydro-electric power schemes (see Box 3, page 31). Inflows to the western catchments decline during summer and autumn by end-of-century, while inflows to the eastern catchments in the hydro-electric system increase during summer and autumn. Spring and winter inflows show little change in the western catchments. The increases in winter runoff on the west coast described in Section 5 occur mostly at lower elevations than are covered by the hydro-electric catchments, meaning that the hydro-electric system does not receive these increases. In winter, inflows declined moderately for the eastern catchments. Inflows to central plateau catchments declined markedly in all seasons and for all future periods.

Changes to inflows to the main catchments supplying hydro-electric power stations could lead to an overall reduction in power generation capacity compared to the reference period. The projected declines to central estimate inflows are likely to reduce generating capacity, while the lower range of the climate projections would reduce hydro-electric generation capacity markedly. Power generation capacity could be reduced not only because of the likely reduction in system inflows, but also because of the spatial distribution of changes to inflows. The eastern catchment where inflows increase feeds only the relatively small, run-of-river Trevallyn Power Station. Declines to inflows in the central plateau catchments will have a serious impact on power generation, because these catchments feed Poatina Power Station - a high-capacity (300 MW), large hydrostatic-head (900 m) power station. Because of the large hydrostatic head, this power station produces a very large amount of power per unit volume of water, meaning that small declines in water volumes lead to large declines in power generation. More strongly seasonally delineated inflows in the western catchments are likely to result in lost power generation in the run-of-river hydro-electric schemes in this region during summer and autumn. Hydro Tasmania is in the process of more complete analysis of the impacts of changes to inflows on power generation capacity and storage levels. These analyses are likely to be commercially sensitive and are beyond the scope of this report.

Box 9

Summary of changes to river flows

- By end-of-century, river flows in 40% of the catchments modelled are projected to change by more than 10%.
- More of the catchments modelled are likely to receive increased inflows than decreased inflows by end-of-century.
- Storages that rely on inflows from the central highlands are likely to receive reduced inflows in all seasons by end-of-century.
- Storages in the east of the state are likely to receive increased inflows by end-of-century.
- Changes to the seasonal and spatial distribution of inflows to hydro-electric power generation catchments are likely to reduce power generation capacity by end-of-century.

Inflows to the hydro-electric system

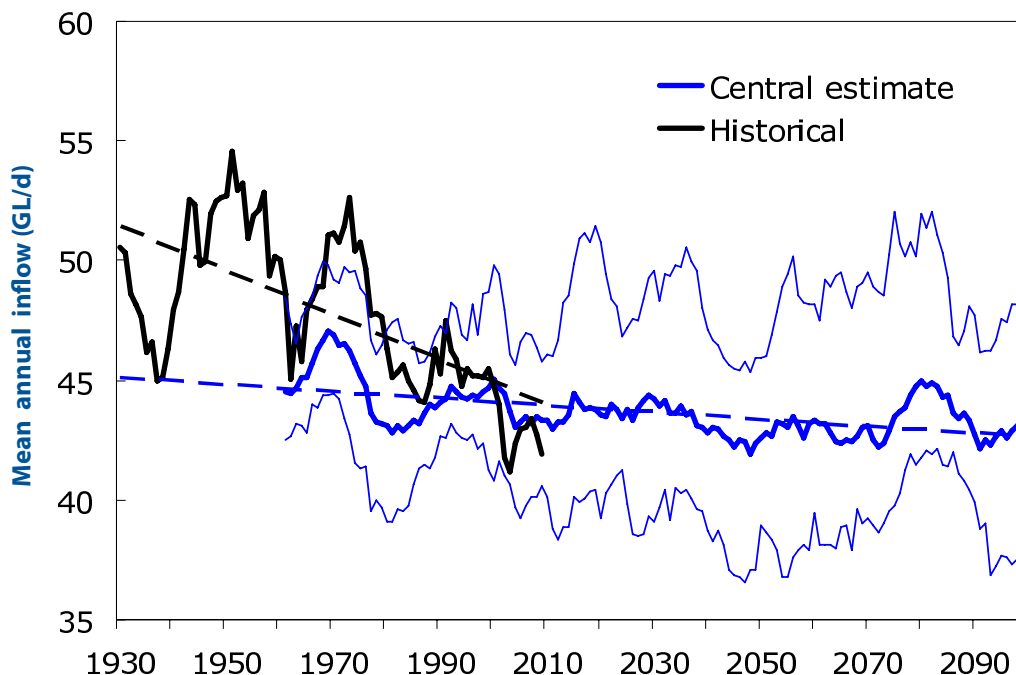


Figure 6.7 Observed and projected annual inflows to Hydro Tasmania catchments from 1930-2100. Curves are smoothed with an 11-year centred moving average. Black line shows synthesised inflow record provided by Hydro Tasmania, calculated from lake levels, power stations outflows and from regression relationships with stream flow and rainfall records. Lighter blue lines show range of downscaled-GCM projections, dark blue line shows central estimate. Dashed lines show linear trends of observed and simulated inflows.

Spatial changes to inflows to the hydro-electric system

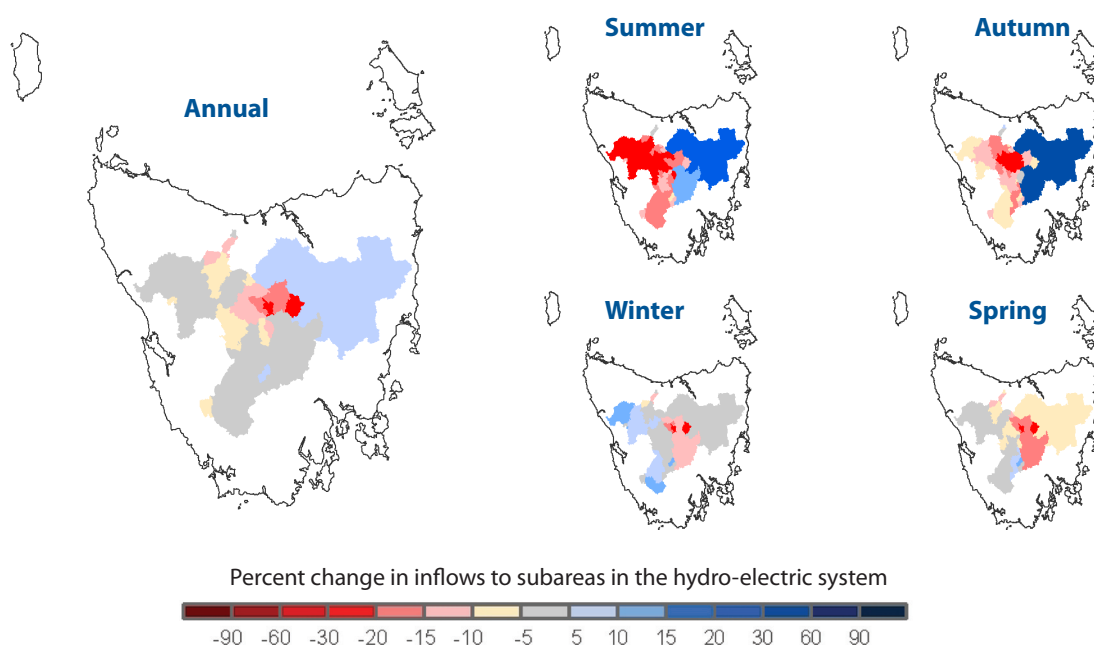


Figure 6.8 Percent change from reference period (1961-1990) to end-of-century (2070-2099) of mean annual and seasonal inflows to each sub-area in the hydro-electric power generation system (central estimate).

7 Future Work

The analyses presented in this report give an overview of hydrological changes over Tasmania projected by fine-resolution climate modelling. One of the great strengths of fine-resolution modelling is making detailed analyses of individual catchments to inform decisions about adapting to climate change. To this end, gridded runoff projections produced by our project are freely available through the Tasmanian Partnership for Advanced Computing TPAC www.tpac.org.au. The climate modelling output parameters are summarised in Appendix I.

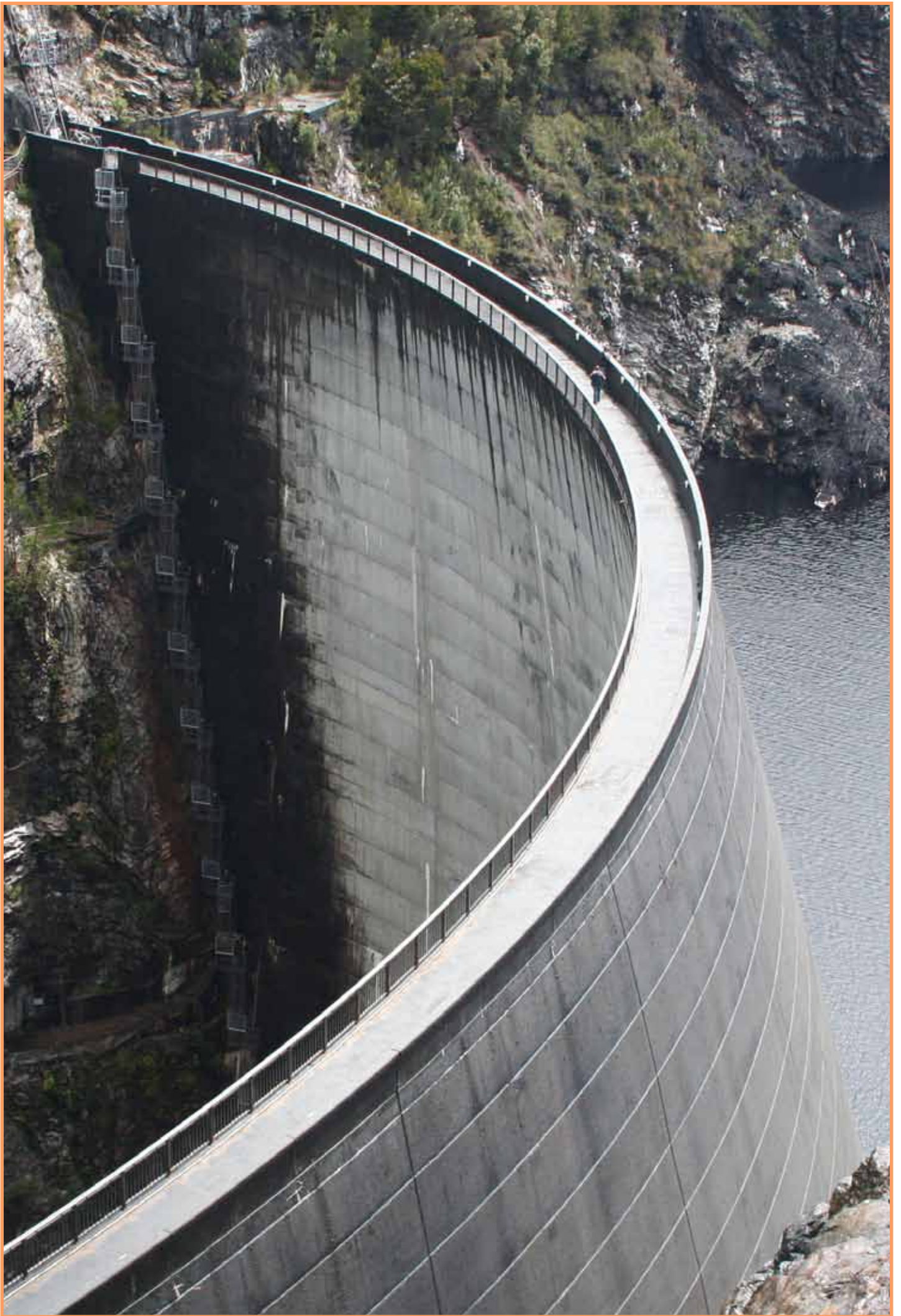
The tendency of the runoff models to produce lower river flows than observed (Section 3.1) should be investigated further. This will allow a more complete understanding of the effects of the bias-adjustment method with the aim of increasing the accuracy of the runoff models across a broader range of temporal and spatial scales.

Most of the quantitative assessments contained in this report describe statewide, or at best regional, impacts of changes to rainfall and runoff. The Tasmania Sustainable Yields project (TasSY) (CSIRO 2009) had a much greater focus on catchment scale change, however its assessments were carried out to 2030. Projections from our project could be used to assess the long-term impacts of anthropogenic climate change at the catchment scale on issues such as water availability and environmental response, such as changes to water quality and geomorphology.

Large changes in flows do not necessarily translate to large impacts on the reliability of water allocations. Estimating the reliability of allocations was outside the scope of this project, however time series of water allocated and water supplied have been generated as part of the river modelling. These estimates of reliabilities could be calculated for each class of water allocations in each catchment using these time series. In addition, river models could be updated with projected changes to water use and operating rules of storages or catchments to give better understanding of water availability in the future. These updated river models could then be re-run with the runoff projections generated for this project to give a better understanding of the combined effects of changing water use and a changing climate on river systems.

Graham et al (2009) quantified the environmental implications of changed stream flows for the TasSY project. Outputs from our modelling are directly compatible with the software Graham et al (2009) used to quantify environmental impacts and this work could be extended using modelling outputs from our study.

The hydrological simulations could also be combined with the results of the other components in our study to give more comprehensive responses to adaptation to anthropogenic climate change. For example, assessments of changes to agricultural productivity carried out by Holz et al (2010) could be paired with more detailed analyses of water reliabilities to assess the viability of agricultural development in particular basins or regions.



References

- Allison I, Alley RB, Fricker HA, Thomas RH & Warner RC 2009a, 'Ice sheet mass balance and sea level', *Antarctic Science*, vol. 21, pp. 413-426.
- Allison I, Bindoff NL, Bindschadler RA, Cox PM, de Noblet N, England MH, Francis JE, Gruber N, Haywood AM, Karoly DJ, Kaser G, Le Quéré C, Lenton TM, Mann ME, McNeil BI, Pitman AJ, Rahmstorf S, Rignot E, Schellnhuber HJ, Schneider SH, Sherwood SC, Somerville RCJ, Steffen K, Steig EJ, Visbeck M & Weaver AJ 2009b, *The Copenhagen diagnosis, 2009: updating the world on the latest climate science*, The University of New South Wales Climate Change Research Centre (CCRC), Sydney, Australia.
- Bennett JC, Willis MI & Graham B 2009, 'AWBM in Tasmania: Varying the AWBM loss model'. *Proceedings, H2009: 32nd Hydrology and Water Resources Symposium*, Newcastle, Australia.
- Bindoff NL, Willebrand J, V. Artale AC, Gregory J, Gulev S, Hanawa K, Quéré CL, Levitus S, Nojiri Y, Shum CK, Talley LD & Unnikrishnan A 2007, 'Observations: Oceanic Climate Change and Sea Level.' *Climate Change 2007: The Physical Science Basis. Contribution of Working Group I to the Fourth Assessment Report of the Intergovernmental Panel on Climate Change* [Solomon S, Qin D, Manning M, Chen Z, Marquis M, Averyt KB, Tignor M & Miller HL (eds)], Cambridge University Press, Cambridge, United Kingdom and New York, NY, USA.
- Boughton WC 2004, 'The Australian water balance model', *Environmental Modelling & Software*, vol. 19, pp. 943-956.
- Brown K 2011, *Using High-Resolution Regional Climate Projections to Investigate the Impact of Climate Change on Flood Inundation: a case-study from Tasmania*, Technical Report, Entura Consulting, Hobart.
- Bureau of Meteorology 2010, *Australian climate variability & change - Trend maps*. Viewed 6 Aug 2010, <<http://www.bom.gov.au/cgi-bin/climate/change/trendmaps.cgi?map=rain&area=aus&season=0112&period=1970>>.
- Burnash RJC, Ferral RL & McGuire RA 1973, *A generalized streamflow simulation system-conceptual modeling for digital computers*, Technical Report, Joint Federal and State River Forecast Center, Sacramento.
- Cechet RP, Sanabria A, Divi CB, Thomas C, Yang T, Arthur C, Dunford M, Nadimpalli K, Power L, White CJ, Bennett JC, Corney SP, Holz GK, Grose MR, Gaynor SM & Bindoff NL in prep, *Climate Futures for Tasmania: severe wind hazard and risk technical report*, Antarctic Climate and Ecosystems Cooperative Research Centre, Hobart, Tasmania.
- Chiew FHS, Peel MC & Western AW 2002, 'Application and testing of the simple rainfall-runoff model SIMHYD', *Mathematical models of small watershed hydrology and applications*, [Singh VP & Frevert DK (eds)], Water Resources Publications, Littleton, USA, pp. 335-367.
- Christensen JH, Hewitson B, Busuioc A, Chen A, Gao X, Held I, Jones R, Kolli RK, Kwon W-T, Laprise R, Magaña Rueda V, Mearns L, Menéndez CG, Räisänen J, Rinke A, Sarr A & Whetton P 2007, 'Regional Climate Projections', *Climate Change 2007: The Physical Science Basis*, [Solomon S, Qin D, Manning M, Chen Z, Marquis M, Averyt KB, Tignor M & Miller HL (eds)], Cambridge University Press, Cambridge, United Kingdom and New York, NY, USA.
- Corney SP, Katzfey JJ, McGregor JL, Grose MR, Bennett JC, White CJ, Holz GK, Gaynor SM & Bindoff NL 2010, *Climate Futures for Tasmania: climate modelling technical report*, Antarctic Climate and Ecosystems Cooperative Research Centre, Hobart, Tasmania.
- Croke BFW, Andrews F, Jakeman AJ, Cuddy SM & Luddy A 2006, 'IHACRES Classic Plus: A redesign of the IHACRES rainfall-runoff model', *Environmental Modelling & Software*, vol. 21, pp. 426-427.
- CSIRO 2009, *Water availability for Tasmania, Report one of seven to the Australian Government from the CSIRO Tasmania Sustainable Yields Project*, CSIRO Water for a Healthy Country Flagship, Australia.
- CSIRO & Bureau of Meteorology 2007, *Climate change in Australia*. Technical Report. <<http://www.climatechangeinaustralia.gov.au>>
- Della-Marta P, Collins DA & Braganza K 2004, 'Updating Australia's high-quality annual temperature dataset', *Australian Meteorological Magazine*, vol. 53, pp. 75-93.
- Domingues CM, Church JA, White NJ, Gleckler PJ, Wijffels SE, Barker PM & Dunn JR 2008, 'Improved estimates of upper-oceanwarming and multi-decadal sea-level rise', *Nature*, vol. 453, pp. 1090-1093.
- Donohue RJ, McVicar TR & Roderick ML 2010, 'Assessing the ability of potential evaporation formulations to capture the dynamics in evaporative demand within a changing climate', *Journal of Hydrology*, doi: 10.1016/j.

jhydrol.2010.03.020.

Fowler HJ, Blenkinsop S & Tebaldi C 2007, 'Linking climate change modelling to impacts studies: recent advances in downscaling techniques for hydrological modelling', *International Journal of Climatology*, Oct, vol. 27, pp. 1547-1578.

Fowler HJ & Kilsby CG 2007, 'Using regional climate model data to simulate historical and future river flows in northwest England', *Climatic Change*, Feb, vol. 80, pp. 337-367.

Gordon HB, O'Farrell S, Collier M, Dix M, Rotstayn L, Kowalczyk E, Hirst T & Watterson I 2010, *The CSIRO Mk3.5 Climate Model, CAWCR Technical Report*, The Centre for Australian Weather and Climate Research. <<http://www.cawcr.gov.au>>

Goswami M, O'Connor KM & Shamseldin AY 2002, 'Structures and performances of five rainfall-runoff models for continuous river-flow simulation'. *Proceedings, 1st Biennial Meeting of International Environmental Modeling and Software Society*, Lugano, Switzerland.

Graham B, Hardie S, Gooderham J, Gurung S, Hardie D, Marvanek S, Bobbi C, Krasnicki T & Post DA 2009, *Ecological impacts of water availability for Tasmania, A report to the Australian Government from the CSIRO Tasmania Sustainable Yields Project*, CSIRO Water for a Healthy Country Flagship, Australia. <<http://www.csiro.au/partnerships/TasSY.html>>

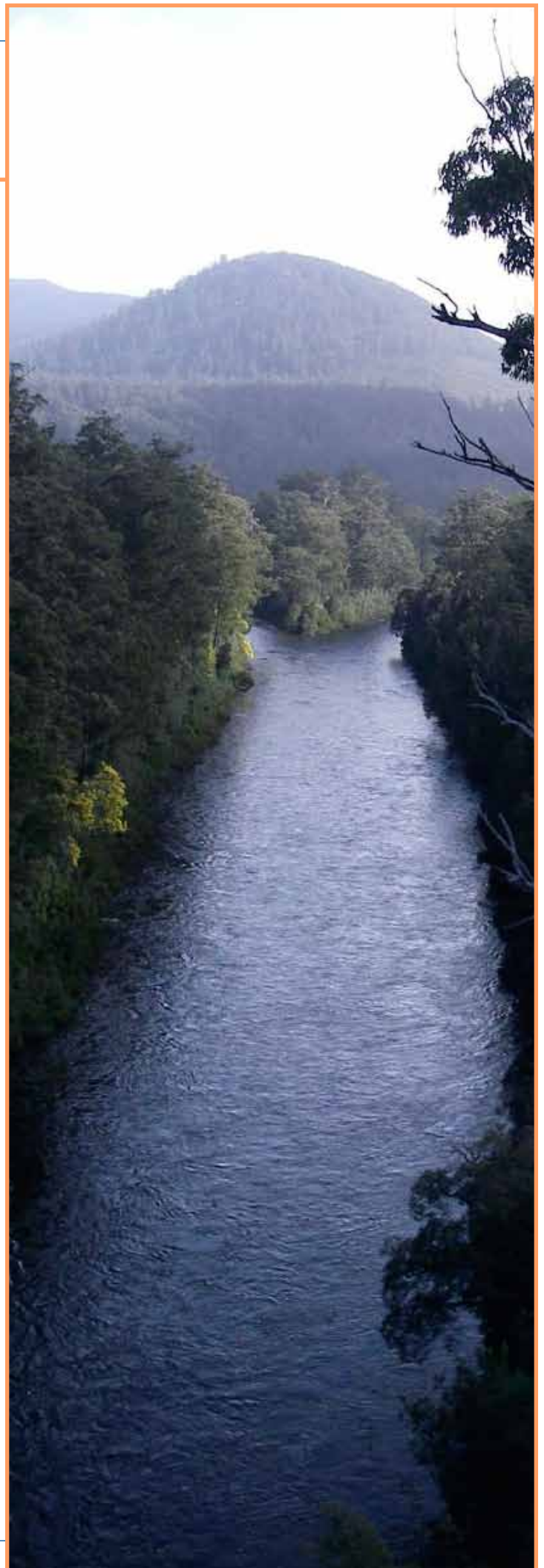
Grose MR, Barnes-Keoghan I, Corney SP, White CJ, Holz GK, Bennett JC, Gaynor SM & Bindoff NL 2010, *Climate Futures for Tasmania: general climate impacts technical report*, Antarctic Climate and Ecosystems Cooperative Research Centre, Hobart, Tasmania.

Hock R, de Woul M, Radić V & Dyurgerov M 2009, 'Mountain glaciers and ice caps around Antarctica make a large sealevel rise contribution', *Geophysical Research Letters*, vol. 36.

Holz GK, Grose MR, Bennett JC, Corney SP, White CJ, Phelan D, Potter K, Kriticos D, Rawnsley R, Parsons D, Lisson S, Gaynor SM & Bindoff NL 2010, *Climate Futures for Tasmania: impacts on agriculture technical report*, Antarctic Climate and Ecosystems Cooperative Research Centre, Hobart, Tasmania.

Ines AVM & Hansen JW 2006, 'Bias correction of daily GCM rainfall for crop simulation studies', *Agricultural and Forest Meteorology*, vol. 138, pp. 44-53.

IPCC 2007, *Climate change 2007: The Physical*



- Science Basis. Contribution of Working Group I to the Fourth Assessment Report of the Intergovernmental Panel on Climate Change*, [Solomon S, Qin D, Manning M, Chen Z, Marquis M, Avery KB, Tignor M & Miller HL (eds)], Cambridge University Press, Cambridge, United Kingdom and New York, NY, USA.
- Jeffrey SJ, Carter JO, Moodie KM & Beswick AR 2001, 'Using spatial interpolation to construct a comprehensive archive of Australian climate data', *Environmental Modelling and Software*, vol. 16, pp. 22.
- Jones DA, Wang W & Fawcett R 2009, 'High-quality spatial climate data-sets for Australia', *Australian Meteorological and Oceanographic Journal*, vol. 58, pp. 233-248.
- Ling FLN, Gupta V, Willis M, Bennett JC, Robinson KA, Paudel K, Post DA & Marvanek S 2009a, *River modelling for Tasmania. Volume 1: the Arthur-Inglis-Cam region, A report to the Australian Government from the CSIRO Tasmania Sustainable Yields Project*, CSIRO Water for a Healthy Country Flagship, Australia. <<http://www.csiro.au/partnerships/TasSY.html>>
- 2009b, *River modelling for Tasmania. Volume 2: the Mersey-Forth region, A report to the Australian Government from the CSIRO Tasmania Sustainable Yields Project*, CSIRO Water for a Healthy Country Flagship, Australia. <<http://www.csiro.au/partnerships/TasSY.html>>
- 2009c, *River modelling for Tasmania. Volume 3: the Pipers-Ringarooma region, A report to the Australian Government from the CSIRO Tasmania Sustainable Yields Project*, CSIRO Water for a Healthy Country Flagship, Australia. <<http://www.csiro.au/partnerships/TasSY.html>>
- 2009d, *River modelling for Tasmania. Volume 4: the South Esk region, A report to the Australian Government from the CSIRO Tasmania Sustainable Yields Project*, CSIRO Water for a Healthy Country Flagship, Australia. <<http://www.csiro.au/partnerships/TasSY.html>>
- 2009e, *River modelling for Tasmania. Volume 5: the Derwent-South East region, A report to the Australian Government from the CSIRO Tasmania Sustainable Yields Project*, CSIRO Water for a Healthy Country Flagship, Australia. <<http://www.csiro.au/partnerships/TasSY.html>>
- Lüthi D, Le Floch M, Bereiter B, Blunier T, Barnol J-M, Siegenthaler U, Raynaud D, Jouzel J, Fischer H, Kawamura K & Stocker TF 2008, 'High-resolution carbon dioxide concentration record 650,000–800,000 years before present', *Nature*, vol. 453, pp. 379-382.
- Mann ME, Zhang Z, Hughes MK, Bradley RS, Miller SK, Rutherford S & Ni F 2008, 'Proxy-Based Reconstructions of Hemispheric and Global Surface Temperature Variations over the Past Two Millennia.' *Proceedings of the National Academy of Sciences of the United States of America*, vol. 105.
- Maraun D, Wetterhall F, Ireson A, Chandler R, Kendon E, Widmann M, Brienne S, Rust H, Sauter T, Themeßl M, Venema V, Chun K, Goodess C, Jones R, Onof C, Vrac M & Theile-Eich I 2010, 'Precipitation downscaling under climate change: recent developments to bridge the gap between dynamical models and the end user', *Reviews of Geophysics*, 48, doi: 10.1029/2009RG000314.
- McGregor JL & Dix MR 2008, 'An updated description of the conformal-cubic atmospheric model', *High Resolution Simulation of the Atmosphere and Ocean*, [Hamilton K & Ohfuchi W (eds)], Springer, pp. 51-76.
- McInnes KL, O'Grady JG, Hemer M, Macadam I, Abbs DJ White CJ, Bennett JC, Corney SP, Holz GK, Grose MR, Gaynor SM & Bindoff NL in prep, *Climate Futures for Tasmania: extreme tide and sea level events technical report*, Antarctic Climate and Ecosystems Cooperative Research Centre, Hobart, Tasmania.
- McIntosh PC, Pook MJ & McGregor J 2005, *Study of future and current climate: a scenario for the Tasmanian region (stages 2 & 3) (CSIRO) - A report for Hydro Tasmania*, CSIRO Marine and Atmospheric Research, Hobart, Tasmania.
- Meehl GA, Stocker TF, Collins WD, Friedlingstein P, Gaye AT, Gregory JM, Kitoh A, Knutti R, Murphy JM, Noda A, Raper SCB, Watterson IG, Weaver AJ & Zhao Z-C 2007, *Global Climate Projections. In: Climate Change 2007: The Physical Science Basis. Contribution of Working Group I to the Fourth Assessment Report of the Intergovernmental Panel on Climate Change*, [Solomon S, Qin D, Manning M, Chen Z, Marquis M, Avery KB, Tignor M & Miller HL (eds)], Cambridge University Press, Cambridge, United Kingdom and New York, NY, USA.
- Morton FI 1983, 'Operational estimates of areal evapotranspiration and their significance to the science and practice of hydrology', *Journal of Hydrology*, vol. 66, pp. 1-76.
- Murray FW 1967, 'On the computation of vapor pressure', *Journal of Applied Meteorology*, vol. 6, pp. 203-204.
- Nakićenović N & Swart R (eds) 2000, *Special Report on Emissions Scenarios*, A Special Report of Working Group III of the Intergovernmental Panel on Climate Change, Cambridge University Press, Cambridge, United Kingdom and New York, NY, USA.
- Nash JE & Sutcliffe JV 1970, 'River flow forecasting through conceptual models part I - A discussion of principles', *Journal of Hydrology*, vol. 10, pp. 282-290.
- Piani C, Haerter J & Coppola E 2010, 'Statistical bias

- correction for daily precipitation in regional climate models over Europe', *Theoretical and Applied Climatology*, vol. 99, pp. 187-192.
- Post DA, Chiew FHS, Teng J, Vaze J, Yang A, Mpelasoka F, Smith I, Katzfey J, Marston F, Marvanek S, Kirono D, Nguyen K, Kent D, Donohue R, Li L & McVicar T 2009, *Production of climate scenarios for Tasmania, A report to the Australian Government from the CSIRO Tasmania Sustainable Yields Project*, CSIRO Water for a Healthy Country Flagship, Australia. <<http://www.csiro.au/partnerships/TasSY.html>>
- Rahmstorf S, Cazenave A, Church JA, Hansen JE, Keeling RF, Parker DE & Somerville RCJ 2007, 'Recent climate observations compared to projections', *Science*, vol. 316, pp. 709.
- Smith I & Chandler E 2009, 'Refining rainfall projections for the Murray Darling Basin of south-east Australia-the effect of sampling model results based on performance', *Climatic Change*, published online 11-Nov-2009, doi: 10.1007/s10584-009-9757-1.
- Smith I & Chiew FHS 2009, *Document and assess methods for generating inputs to hydrological models and extend delivery of projections across Victoria, Final report for Project 2.2.5P*, SEACI. <<http://www.seaci.org/docs/reports/Project2.2.5P.pdf>>
- Tan KS, Chiew FHS, Grayson RB, Scanlon PJ & Siriwardena L 2005, 'Calibration of a daily rainfall-runoff model to estimate high daily flows.' *Proceedings, Congress on Modelling and Simulation (MODSIM 2005)*, Melbourne, Australia.
- Thompson DWJ, Kennedy JJ, Wallace JM & Jones PD 2008, 'A large discontinuity in the mid-twentieth century in observed global-mean surface temperature', *Nature*, vol. 453, pp. 646-649.
- Trenberth KE, Jones PD, Ambenje P, Bojariu R, Easterling D, Tank AK, Parker D, Rahimzadeh F, Renwick JA, Rusticucci M, Soden B & Zhai P 2007, 'Observations: Surface and Atmospheric Climate Change', *Climate Change 2007: The physical science basis. Contribution of Working Group I to the Fourth Assessment Report of the Intergovernmental Panel on Climate Change*, [Solomon S, Qin D, Manning M, Chen Z, Marquis M, Averyt KB, Tignor M & Miller HL (eds)], Cambridge University Press, Cambridge, United Kingdom and New York, NY, USA.
- van Pelt S, Kabat P, ter Maat H, van den Hurk B & Weerts A 2009, 'Discharge simulations performed with a hydrological model using bias corrected regional climate model input', *Hydrology and Earth System Sciences*, vol. 12, pp. 2387-2397.
- Vaze J, Post DA, Chiew FHS, Perraud J-M, Viney N & Teng J 2010, 'Climate nonstationarity – Validity of calibrated rainfall-runoff models for use in climate change studies', *Journal of Hydrology*, doi: 10.1016/j.jhydrol.2010.09.018.
- Viney NR, Perraud J, Vaze J, Chiew FHS, Post DA & Yang A 2009a, 'The usefulness of bias constraints in model calibration for regionalisation to ungauged catchments.' *Proceedings, 18th World IMACS / MODSIM Congress*, Cairns, Australia, 13-17 July 2009.
- Viney NR, Post DA, Yang A, Willis M, Robinson KA, Bennett JC, Ling FLN & Marvanek S 2009b, *Rainfall-runoff modelling for Tasmania, A report to the Australian Government from the CSIRO Tasmania Sustainable Yields Project*, CSIRO Water for a Healthy Country Flagship, Australia. <<http://www.csiro.au/partnerships/TasSY.html>>
- Viney NR, Vaze J, Chiew FHS, Perraud J, Post DA & Teng J 2009c, 'Comparison of multi-model and multi-donor ensembles for regionalisation of runoff generation using five lumped rainfall-runoff models.' *Proceedings, 18th World IMACS / MODSIM Congress*, Cairns, Australia, 13-17 July 2009.
- Watterson IG 2008, 'Calculation of probability density functions for temperature and precipitation change under global warming', *Journal of Geophysical Research*, 113, D12106, doi: 10.1029/2007JD009254.
- White CJ, Sanabria LA, Grose MR, Corney SP, Bennett JC, Holz GK, McInnes KL, Cechet RP, Gaynor SM & Bindoff NL 2010, *Climate Futures for Tasmania: extreme events technical report*, Antarctic Climate and Ecosystems Cooperative Research Centre, Hobart, Tasmania.
- Wood A, Leung LR, Sridhar V & Lettenmaier DP 2004, 'Hydrologic implications of dynamical and statistical approaches to downscaling climate outputs', *Climate Change*, vol. 62, pp. 28.
- Yang A 2009, *Integrated Catchment Yield Modelling Environment*, CSIRO.

Appendices

Appendix A Bias-adjustment tests

Comparison of changes in rainfall calculated from bias-adjusted and unadjusted modelled projections

A central premise of bias-adjustment is that the signals transmitted by the downscaled-GCMs are preserved in the bias-adjusted projections. Proportional changes to bias-adjusted rainfall do indeed mirror unadjusted modelling output in both spatial distribution and quantity (Figure A.1), although bias-adjusted projected changes are as much as 8% higher than projected changes to the unadjusted downscaled-GCM simulations in the east of the state by the end of the century (Figure A.2).

Changes in variance in rainfall projected by downscaled-GCM simulations are also present in the bias-adjusted projections, though the bias-adjusted projections generally show a slightly increased future variance compared to the unadjusted CCAM projections (Figure A.3).

Split sample cross-validation

To test the temporal persistence of the bias-adjustment, we repeated the bias-adjustment calculation (Section 2.3.6) using SILO rainfalls from different periods. As we only had 47 years of overlap between downscaled-GCM simulations and SILO interpolated observations (1961-2007), this effectively meant shortening the period used to define the present climate (against which projections were adjusted). There is a fundamental trade-off in these tests: the shorter periods were necessary to perform the tests, but because they are shorter, these periods are less likely to represent natural climatic variation as satisfactorily.

We performed simple split-sample cross validation by bias-adjusting to observations from 1962-1984 (Case 1) and then to observations from 1985-2007 (Case 2). There has been a sharp decline in annual Tasmanian rainfall since the mid-1970s that is not present in the downscaled-GCM simulations (Grose et al 2010). The split samples used in Case 1 and Case 2 essentially represent two different rainfall regimes in the observed data. Case 1 represents a wetter regime and Case 2 a drier regime. This is reflected in the validation, where Case 1 over-predicts observed rainfall for 1985-2007 by up to 20%, and Case 2 under-predicts observed rainfall for 1962-1984 by up to 20% (Figure A.4a, b). In order to compare independent adjustments that sample from both wet and dry regimes, we performed the bias-adjustment

to observed climate data spliced together from odd years (1961,1963,..., 2003, 2005) (Case 3) and even years (1962,1964,...,2004, 2006) (Case 4). For all cases, the bias-adjusted projections were validated against observations for the period not used for the bias-adjustment. Case 3 and Case 4 are less biased in most regions than Cases 1 and 2 (Figure A.4a). Most cells for Cases 3 and 4 exhibit absolute biases of less than 10% (Figure A.4b). However, some cells in the south-west in Case 3 and on the west coast in Case 4 have absolute biases of greater than 10 % (greater than 14% in a few cells in Case 4). This indicates that the observed data exhibits more year-to-year variation than the downscaled-GCMs. There are few rain gauges in these regions and it is not clear whether this result is caused by the inability of the downscaled-GCMs to capture observed variability or whether the interpolated observations are overstating natural year-to-year variability.

Cases 1 and 2 may represent the types (and magnitudes) of bias that are likely to occur when the adjustment is trained on data from a drier climatic period and applied in a wetter period (and vice versa). If this were the case, this could cause biases in projections of a non-stationary climate. Grose et al (2010) demonstrated, however, that trends in bias-adjusted rainfall projections were almost indistinguishable from trends in unadjusted rainfall projections, indicating that this problem is unlikely to be significant for our study. In addition, we show (below) that choice of bias-adjustment period does not materially affect projected changes.

The higher biases of the cross-validation bias-adjustments in Cases 1 and 2 are likely the result of using periods too short to adequately cover longer term natural variability in rainfall. Using climate simulations that span a greater period results in a substantial reduction in biases. This can be seen in Cases 3 and 4 (even though the same number of training days was used). Cases 3 and 4 are more likely to capture longer-term cyclical fluctuations in rainfall and thus we speculate that the biases determined in Cases 3 and 4 are a truer reflection of errors in the bias-adjustment, as Cases 3 and 4 are more likely to capture longer-term cyclical fluctuations in rainfall. The very close matches of bias-adjusted downscaled-GCM simulations to AWAP observations reported by Corney et al (2010) are likely to overestimate the skill of the bias-adjustment.

Bias-adjusted and unadjusted rainfall

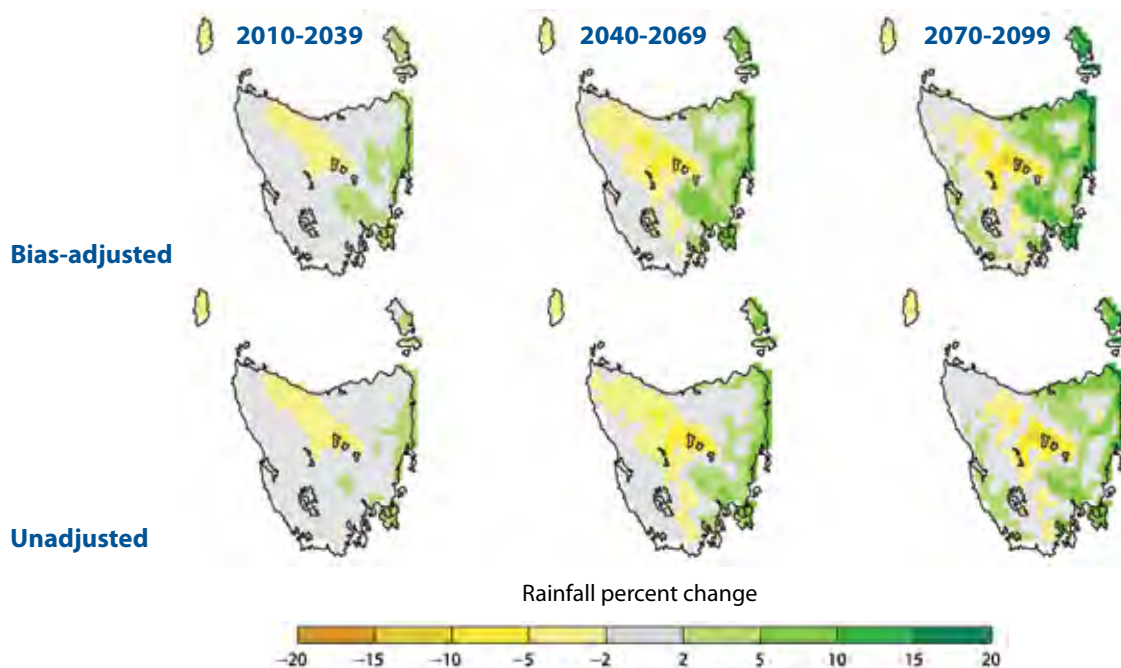


Figure A.1 Changes to rainfall from reference period (1961-1990) for three future periods measured using bias-adjusted and unadjusted modelled projections calculated from central estimates.

Bias-adjusted and unadjusted rainfall

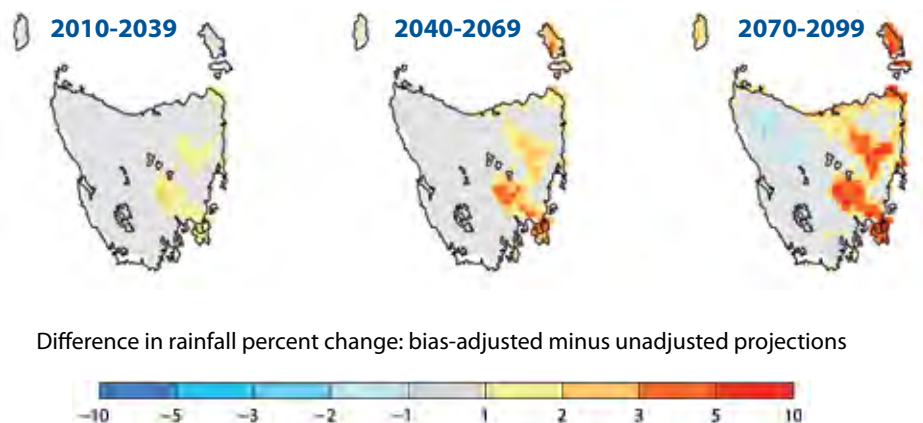


Figure A.2 Differences in projected change to rainfall between bias-adjusted and unadjusted modelled projections calculated from central estimates.

Coefficient of variation

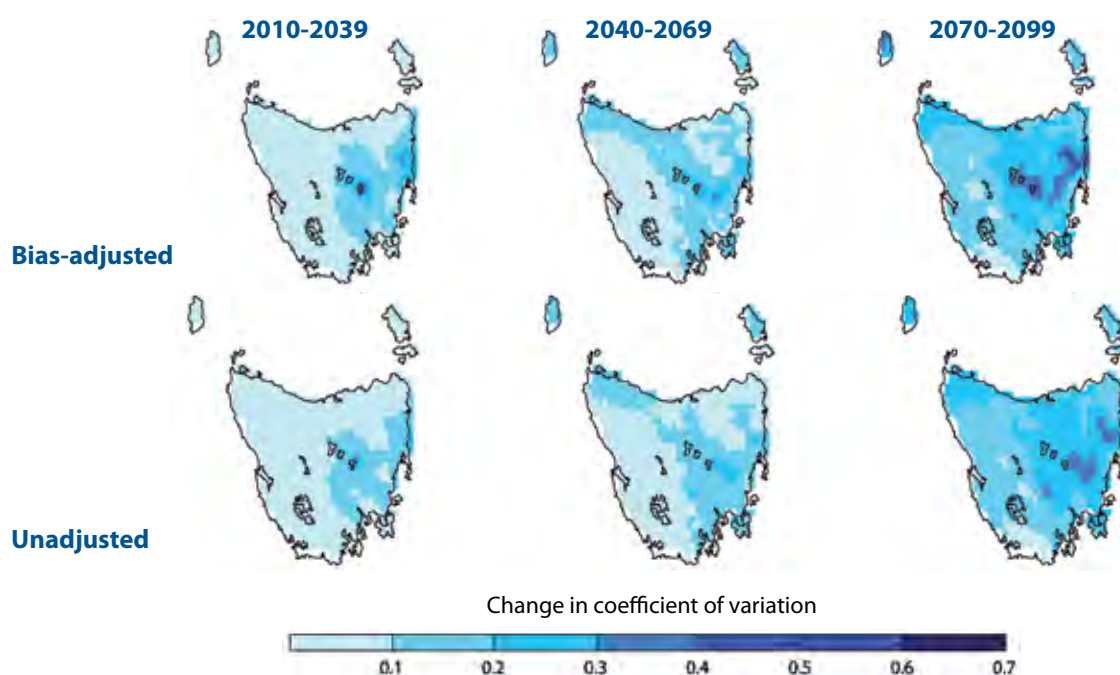


Figure A.3 Changes from reference period (1961-1990) to coefficient of variation of daily rainfall for three future periods measured using bias-adjusted and unadjusted modelled projections calculated from central estimates.

The choice of a training period for calculating bias-adjustments is necessarily arbitrary and often determined by the availability of observations. We suggest in general, however, that periods long enough to adequately encompass natural variability of 'current' climate should be used for bias-adjustments to be temporally consistent. In our case, we were limited by the duration of the period for which simulations and observed data were available (1961-2007). Conversely, the period chosen should not be too long: if, for example, Tasmania's recent rainfall decline is predominantly caused by anthropogenic climate change, the bias-adjustment could flatten future changes caused by warming projected by climate modelling. In our case this has not occurred: rainfall changes calculated from bias-adjusted projections show slightly greater change (Figure A.1) and greater variability (Figure A.2) than changes calculated from the unadjusted downscaled-GCM simulations.

The period chosen for the bias-adjustment does not seem to greatly affect projected changes. Cases 1 and 2 show the greatest variation in adjustment factors and give the greatest variation in future rainfall changes (not shown). However, the variation in rainfall changes is very slight. We calculated change in rainfall from 1961-1990 to 2070-2099 using Case 1 and Case 2. Each case was compared to change calculated for the same period using projections bias-adjusted to the full 47 years of observed data – the same case used to present rainfall changes in Section 4 (which, for this example, we will term the

'47-year Case'). Changes projected by Case 1 and Case 2 were always within $\pm 2\%$ of the 47-year Case (Figure A-5a, b, respectively). The differences between Case 1 and Case 2, cases calculated from independent observations, are almost always within $\pm 2\%$ and never greater than 4%. This indicates that the bias-adjustment period chosen does not greatly influence projections of rainfall change for this method of quantile-quantile bias-adjustment.

It was not possible to carry out these tests on runoff because of time constraints. Because the bias-adjustment does not replicate observed rainfalls perfectly, and because the spatial distribution of rainfalls can be altered by the bias-adjustment, the bias-adjusted rainfall may interact unpredictably with runoff model parameters in future periods. We suggest that it is unlikely that these effects will have a strong bearing on projected changes to runoff. However, this issue warrants further investigation and will be the subject of future research.

Cross-validation

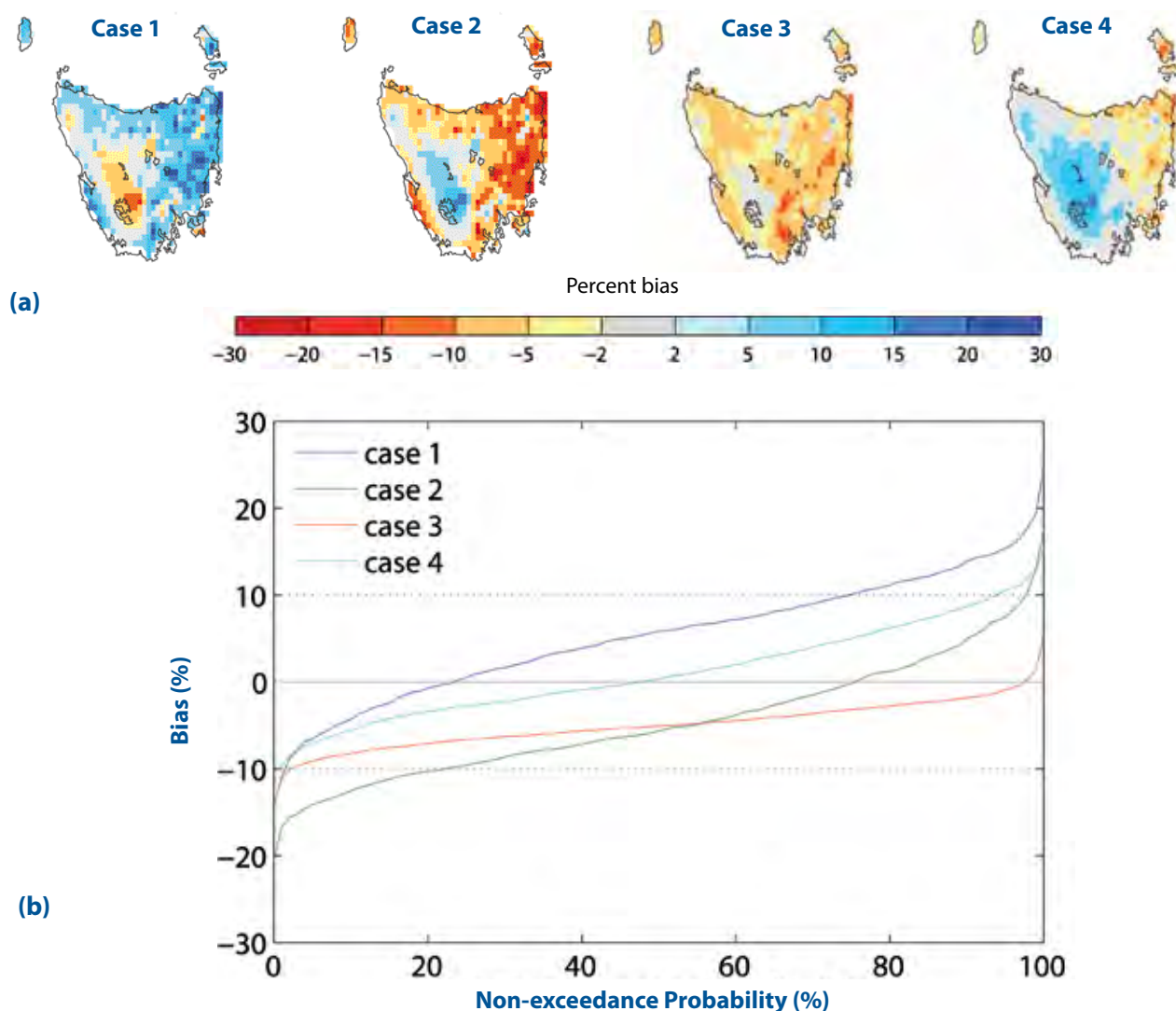


Figure A.4 Cross-validation biases of downscaled-GCM simulations calculated by comparing Case 1 to 1985-2007 observations; comparing Case 2 to 1962-1984 observations; comparing Case 3 to even-year observations (1962, 1964, ..., 2004, 2006); comparing Case 4 to odd-year observations (1961, 1963, ..., 2003, 2005). In each case, the observations from the comparison period were not used to calculate the bias-adjustment: (a) shows spatial distribution of biases and (b) gives exceedance probability of bias for each grid cell.

Cross-validation

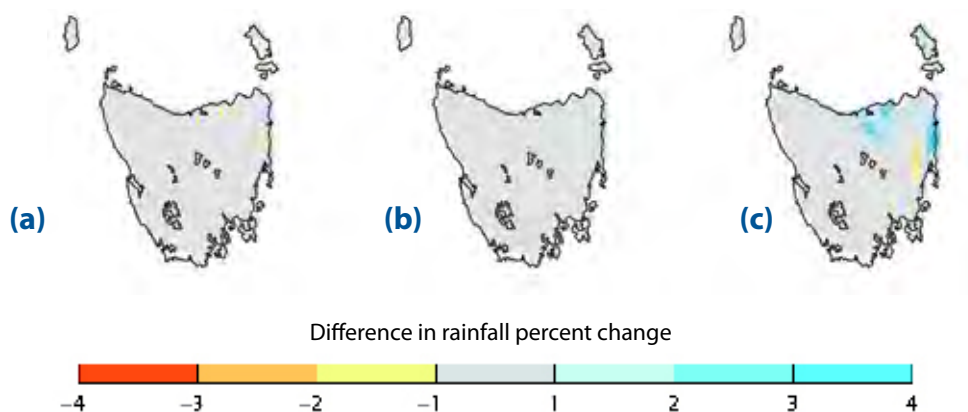


Figure A.5 Differences in percent change (1961-1990 vs 2070-2099) calculated using different cases of bias-adjustment: (a) Case 1 minus the 47-year Case, (b) Case 2 minus the 47-year Case and (c) Case 1 minus Case 2.

Appendix B

Adapting Tetsim to operate with downscaled-GCM simulations

Tetsim was designed to apply assumptions of future electricity prices and demand to historical inflows in order to predict system operation, storage levels and power yield for 20 years. Historical inflows used in Tetsim are calculated retrospectively with a series of models that employ a variety of methods, depending on available data. These methods include regression analyses with available data and water balances based on measured storage volumes and known outflows – for convenience we will collectively term these the ‘volume balance method’. The input data and models are reviewed annually, but the models have remained reasonably consistent since a major revision in 1992.

The volume balance method assumes that historical inflows will reflect future inflows. We sought to assess the impacts of changes to future inflows, so it was not enough to rely on historical inflows to the hydropower system. To calculate future inflows to the hydroelectric system we digitally delineated 47 catchments in the system, accounting for all diversions and other hydropower infrastructure. Projected runoff (Section 2.4.1) was then aggregated to generate inflows to each of these catchments – we will term this the ‘runoff aggregation method’.

The runoff aggregation method differs from the volume balance method in two important ways:

1. The two methods rely on different sets of input data.
2. The volume balance method uses measured changes in storage volumes, meaning evaporation from storages is calculated implicitly. This can result in negative inflows during the summer months at certain sites. The runoff aggregation method account for evaporation from a catchment, but not the elevated rates of evaporation that can be expected from a large water body. Inflows aggregated from runoff can never be negative.

Despite these differences, the two methods yield acceptably similar inflows. Daily inflows to the 47 catchments were generated for the period 1992-2008 with the runoff aggregation method using SILO interpolated observations as inputs to the Simhyd runoff models. These inflows were then compared to those calculated with the volume balance method. Annual volumes at each of the 47 sites agree reasonably well (Figure B.1a). The runoff aggregation method tends to slightly overpredict annual total system inflows (bias = +4%) and replicates seasonal patterns reasonably well (Figure B.1b), though there is considerable variation in seasonal matches from site to site (not shown). The runoff aggregation method tends to overpredict summer flows, indicating that evaporation from large water bodies is

underestimated. Nonetheless, the runoff aggregation method is reasonably efficient at replicating inflows calculated with the volume balance method, with about half the catchments giving daily Nash-Sutcliffe efficiencies (Nash & Sutcliffe 1970) of 0.6 or more (Figure B.1c). The runoff aggregation method also gives realistic power station outflows and power yield (not shown) when processed through Tetsim.

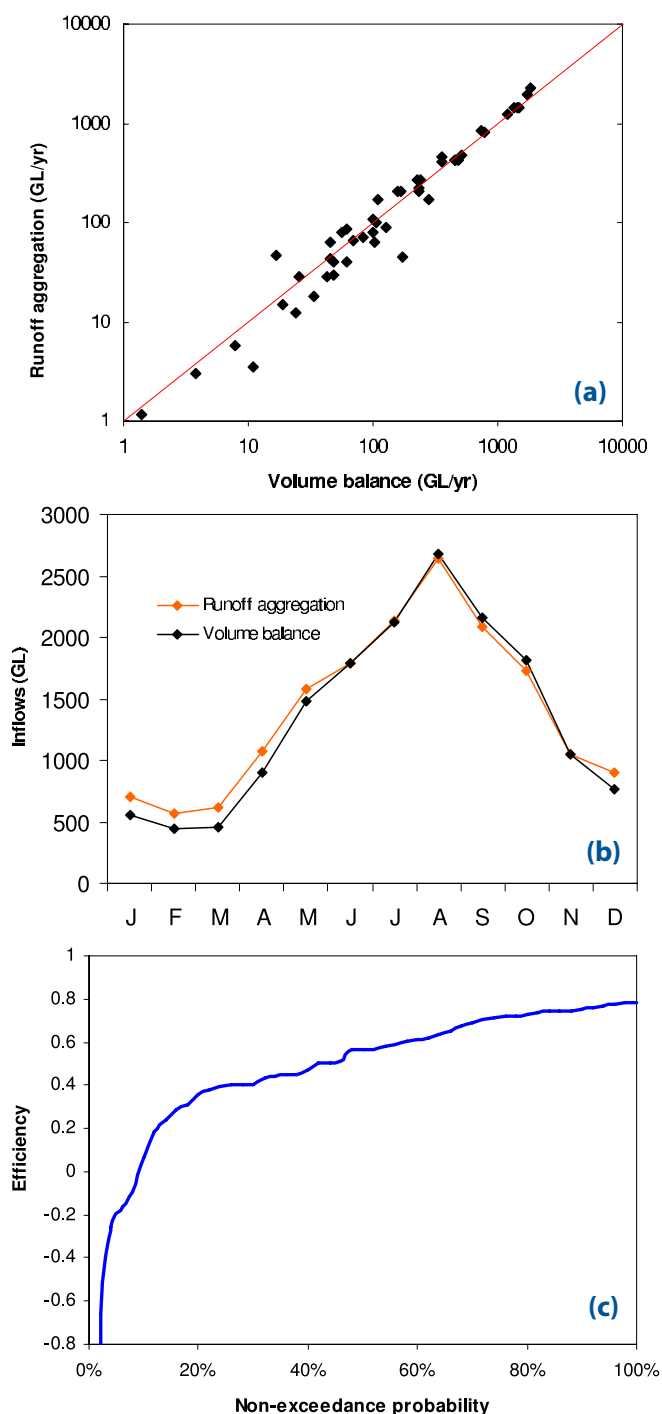


Figure B.1 Comparison of in inflows to the hydro-electric system 1992-2008 generated using the volume balance and runoff aggregation methods (Simhyd model): (a) annual inflows at 47 sites (b) monthly system inflows (c) efficiency of runoff aggregation method measured against volume balance method for 47 sites.

Appendix C

River catchments modelled

Table C.1 List of catchments modelled. Catchment areas relate only to portions of catchments not subject to hydro-electric power generation. Map label column gives key to map in Figure C.2.

| Catchment | Map label | Catchment area modelled (km ²) |
|---|-----------|--|
| Ansons River | 1 | 337 |
| Arm River | 2 | 86 |
| ‡Arthur, Rapid and Hellyer Rivers | 3 | 2493 |
| Blythe River | 4 | 365 |
| Boobyalla River | 5 | 259 |
| Brid River | 6 | 146 |
| *Brumbys Creek | 7 | 669 |
| ‡Cam River | 8 | 286 |
| Carlton Rivulet | 9 | 397 |
| Claytons Rivulet | 10 | 50 |
| ‡Clyde River | 11 | 1131 |
| ‡Coal River | 12 | 688 |
| Collingwood River | 13 | 267 |
| ‡Curries Rivulet | 14 | 113 |
| †Davey River | 15 | 689 |
| Derwent Estuary | 16 | 621 |
| *Derwent River | 17 | 1957 |
| Detention and Black Rivers | 18 | 578 |
| Don River | 19 | 139 |
| Duck River | 20 | 509 |
| ‡Emu River | 21 | 246 |
| Esperance River | 22 | 682 |
| †Fisher River | 23 | 36 |
| Flinders Island | 24 | 1316 |
| Florentine River | 25 | 440 |
| Flowerdale and Inglis Rivers | 26 | 537 |
| *Forth River | 27 | 179 |
| †Forth River above Lemonthyme Power Station | 28 | 311 |
| †Franklin River | 29 | 764 |
| Freycinet Peninsula | 30 | 142 |
| George River | 31 | 518 |
| †Gordon River | 32 | 461 |
| Great Forester River | 33 | 521 |
| †Henty River | 34 | 115 |
| Huon, Russell and Little Denison Rivers | 35 | 2273 |
| Hurst River | 36 | 105 |
| Huskisson River | 37 | 179 |
| Iris River | 38 | 35 |
| Jordan River | 39 | 1243 |

Table C.1 continued over page

Table C.1 continued

| Catchment | Map label | Catchment area modelled (km ²) |
|------------------------------------|-----------|--|
| Kermandie River | 40 | 207 |
| King Island | 41 | 1091 |
| ‡Lake River | 42 | 550 |
| ‡Leven and Gawler Rivers | 43 | 685 |
| Little Forester River | 44 | 350 |
| Little Swanport River | 45 | 875 |
| Lost Creek | 46 | 30 |
| ‡Macquarie River | 47 | 2726 |
| ‡Meander, Quamby and Liffey Rivers | 48 | 1563 |
| Meredith and Wye Rivers | 49 | 325 |
| *Mersey River | 50 | 1011 |
| Montagu River | 51 | 360 |
| Mountain River | 52 | 186 |
| Musselroe River | 53 | 583 |
| Nelson Bay River | 54 | 62 |
| Nicholls Rivulet | 55 | 308 |
| †Nive River | 56 | 175 |
| North Esk River | 57 | 1061 |
| North West Bay Rivulet | 58 | 118 |
| Orielton Rivulet | 59 | 119 |
| *Ouse River | 60 | 1109 |
| Panatana River | 61 | 69 |
| Pipers River | 62 | 602 |
| Prosser River | 63 | 1056 |
| Que River | 64 | 118 |
| ‡Ringarooma River | 65 | 955 |
| Rubicon River | 66 | 573 |
| Savage River | 67 | 294 |
| Scamander River | 68 | 660 |
| Sisters Creek | 69 | 34 |
| Snug Rivulet | 70 | 23 |
| South Esk River | 71 | 3352 |
| Stitt River | 72 | 32 |
| Swan and Apsley Rivers | 73 | 825 |
| Tamar Estuary | 74 | 1049 |
| Tasman Peninsula | 75 | 657 |
| Tomahawk River | 76 | 374 |
| Welcome River | 77 | 336 |
| †Whyte River | 78 | 320 |

†Whole catchment not modelled - partial (upper) catchment only.

*Catchment subject to inflows released from Hydro Tasmania hydro-electric power generation system.

‡Catchment contains large irrigation/water supply storages.

Catchments modelled

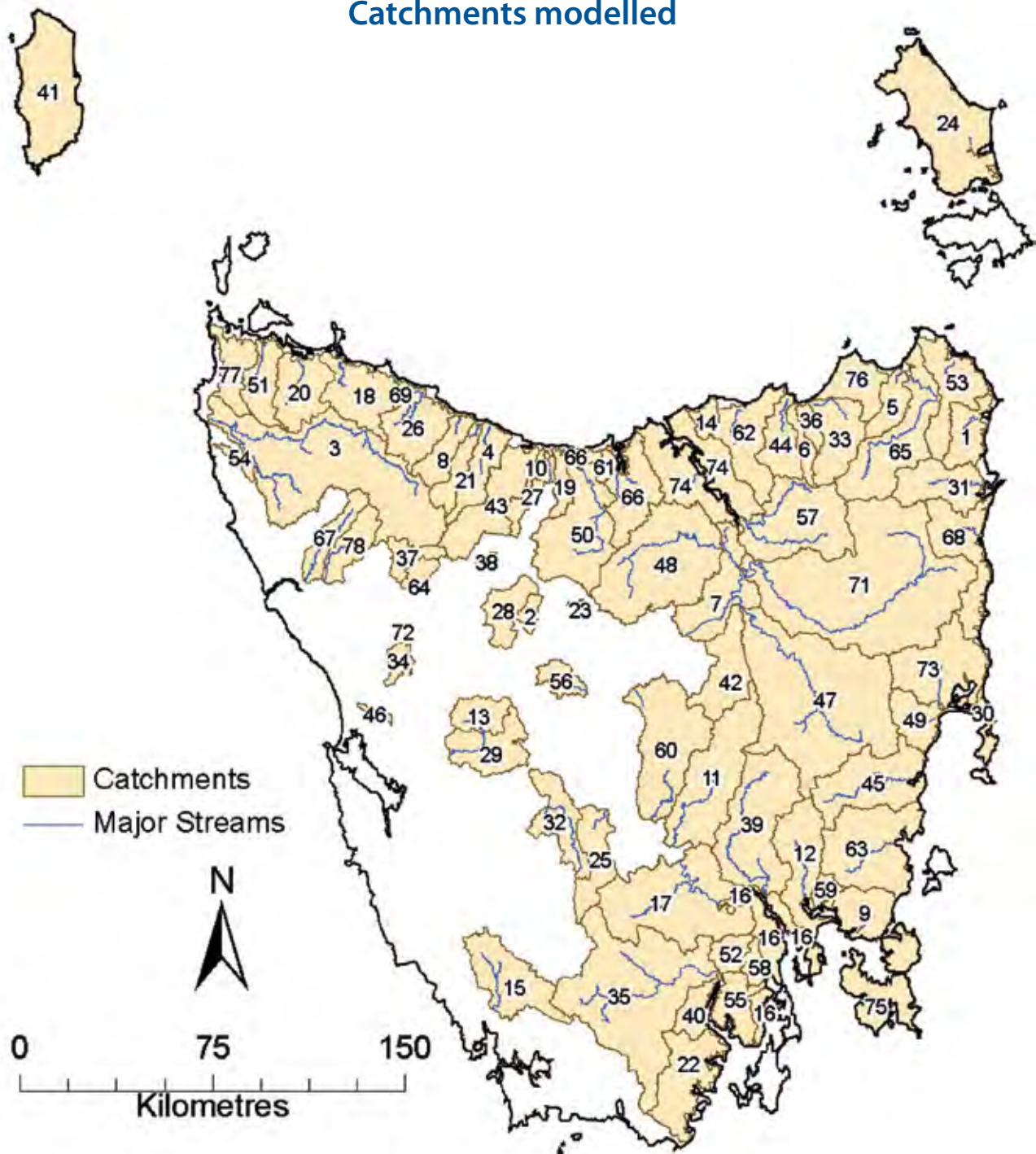


Figure C.2 Catchments modelled. Only portions of catchments not subject to hydro-electric power generation are shown. Key to labels is given in 'Map label' column in Table C.1.

Appendix D

Change in runoff in millimetres

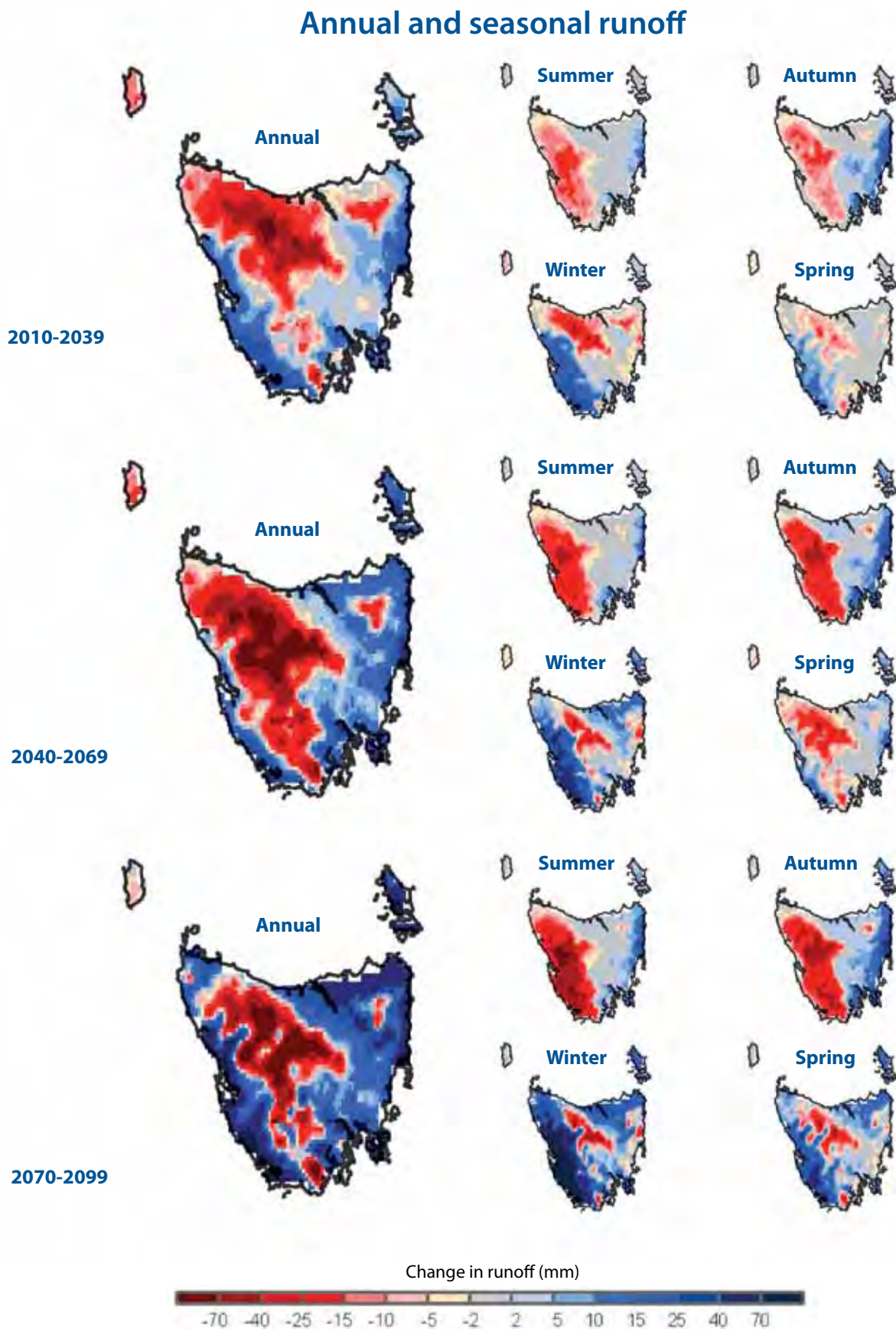


Figure D.1 Change in seasonal and annual runoff (mm) for three future periods compared to the reference period (1961-1990) from the Simhyd projections (central estimates).

Appendix E

Change in annual river flows by catchment

Table E.1 Reference period (1961-1990) discharge and change for three future periods for all catchments (central estimates). Locations of catchments are given by Figure C.2.

| Catchment | Reference (1961-1990) central estimate of annual flow (GL) | Change to central estimate by 2010-2039 (%) | Change to central estimate by 2040-2069 (%) | Change to central estimate by 2070-2099 (%) | Downscaled-GCM range of change by 2070-2099 (%) | No. downscaled-GCMs that agree with sign of change to central estimate by 2070-2099 |
|-----------------------------------|--|---|---|---|---|---|
| Ansons River | 69 | 2 | 11 | 21 | -12.6 to 51.5 | 5 |
| Arm River | 79 | -5 | -7 | -2 | -7.9 to 5.9 | 4 |
| *Arthur, Rapid and Hellyer Rivers | 2473 | -3 | -4 | -2 | -8 to 9.1 | 4 |
| Blythe River | 243 | -6 | -6 | -5 | -14.2 to 4.8 | 4 |
| Boobyalla River | 57 | -1 | 9 | 25 | -6.4 to 44.4 | 5 |
| Brid River | 48 | -2 | 4 | 14 | -7.3 to 31 | 5 |
| Brumbys Creek* | 2110 | -4 | -4 | 0 | -18 to 22.5 | 3 |
| ‡Cam River | 160 | -6 | -6 | -4 | -14.7 to 8.5 | 4 |
| Carlton Rivulet | 46 | 7 | 14 | 24 | 2.2 to 67.8 | 6 |
| Claytons Rivulet | 17 | -8 | -5 | 0 | -15.1 to 16 | 3 |
| ‡Clyde River | 45 | 5 | 6 | 17 | -21.4 to 110.3 | 3 |
| ‡Coal River | 37 | 5 | 17 | 34 | 3.8 to 108.9 | 6 |
| Collingwood River | 477 | -1 | -5 | -3 | -7.4 to 5.5 | 5 |
| *Curries Rivulet | 20 | -1 | 10 | 29 | -3 to 64.1 | 5 |
| †Davey River | 1354 | 1 | -1 | 2 | -2.4 to 12.2 | 4 |
| Derwent Estuary | 164 | 3 | 8 | 10 | -5.1 to 35.7 | 5 |
| *Derwent River | 3266 | -2 | -6 | -5 | -16 to 14.4 | 5 |
| Detention and Black Rivers | 311 | -5 | -4 | 1 | -10.2 to 16.5 | 2 |
| Don River | 48 | -8 | -4 | 1 | -15.9 to 17.9 | 3 |
| Duck River | 214 | -3 | -1 | 7 | -6 to 26.3 | 4 |
| *Emu River | 171 | -7 | -7 | -7 | -15.5 to 4.2 | 5 |
| Esperance River | 550 | -1 | -2 | -3 | -14.8 to 19.3 | 5 |
| †Fisher River | 49 | -4 | -7 | -8 | -12.4 to 3.5 | 5 |
| Flinders Island | 154 | 6 | 24 | 46 | 7.6 to 75.2 | 6 |
| Florentine River | 311 | -1 | -4 | -2 | -13.9 to 15.2 | 4 |
| Flowerdale and Inglis Rivers | 313 | -5 | -4 | -1 | -12.1 to 12.3 | 4 |
| *Forth River | 1929 | -5 | -8 | -8 | -12.6 to 1.1 | 5 |

Table E.1 continued over page

Table E.1 continued

| Catchment | Reference (1961-1990) central estimate of annual flow (GL) | Change to central estimate by 2010-2039 (%) | Change to central estimate by 2040-2069 (%) | Change to central estimate by 2070-2099 (%) | Downscaled- GCM range of change by 2070-2099 (%) | No. downscaled- GCMs that agree with sign of change to central estimate by 2070-2099 |
|--|--|---|---|---|--|---|
| Forth River above Lemonthyme Power Station | 422 | -4 | -8 | -6 | -9.5 to 1.7 | 5 |
| †Franklin River | 1300 | -1 | -4 | -2 | -6.7 to 6.3 | 4 |
| Freycinet Peninsula | 24 | 15 | 26 | 42 | -3 to 90.3 | 5 |
| George River | 203 | 0 | 3 | 6 | -14.5 to 26.5 | 4 |
| †Gordon River | 732 | -1 | -4 | -3 | -8.4 to 5.5 | 5 |
| Great Forester River | 154 | -1 | 5 | 17 | -5.1 to 32.6 | 5 |
| †Henty River | 280 | 0 | -3 | 0 | -3 to 7.3 | 4 |
| Huon, Russell and Little Denison Rivers | 2703 | 0 | -2 | 0 | -8.5 to 14.6 | 5 |
| Hurst River | 18 | 0 | 10 | 27 | -2.9 to 50.7 | 5 |
| Huskisson River | 388 | -2 | -4 | -2 | -6.2 to 6.4 | 5 |
| Iris River | 60 | -5 | -8 | -9 | -12.8 to -2.2 | 6 |
| Jordan River | 27 | 9 | 29 | 53 | 8.5 to 152.1 | 6 |
| Kermandie River | 85 | 1 | 5 | 8 | -5.9 to 36.4 | 5 |
| King Island | 211 | -7 | -7 | -2 | -11.2 to 13.3 | 4 |
| ‡Lake River | 54 | -11 | -18 | -22 | -43.2 to 20.1 | 5 |
| ‡Leven and Gawler Rivers | 533 | -6 | -8 | -7 | -15 to 2.5 | 5 |
| Little Forester River | 105 | -1 | 5 | 17 | -6.4 to 35.4 | 5 |
| Little Swanport River | 95 | 3 | 13 | 15 | -7.4 to 45.8 | 4 |
| Lost Creek | 43 | 1 | 1 | 4 | -0.8 to 17.7 | 5 |
| *Macquarie River | 196 | 4 | 9 | 17 | -8.4 to 60 | 4 |
| *Meander, Quamby and Liffey Rivers | 563 | -7 | -5 | -2 | -15.2 to 14.8 | 3 |
| Meredith and Wye Rivers | 61 | 9 | 12 | 14 | -10.8 to 42.6 | 4 |
| *Mersey River | 645 | -5 | -5 | -1 | -13 to 6.8 | 4 |
| Montagu River | 133 | -3 | -2 | 5 | -8.4 to 30.1 | 3 |
| Mountain River | 100 | 2 | 4 | 4 | -9.5 to 24.8 | 4 |
| Musselroe River | 102 | 2 | 14 | 30 | -5.5 to 60.1 | 5 |
| Nelson Bay River | 46 | -1 | -2 | 3 | -4.3 to 20.8 | 3 |
| Nicholls Rivulet | 85 | 0 | 6 | 8 | -12.1 to 48.9 | 4 |

Table E.1 continued over page

Table E.1 continued

| Catchment | Reference (1961-1990) central estimate of annual flow (GL) | Change to central estimate by 2010-2039 (%) | Change to central estimate by 2040-2069 (%) | Change to central estimate by 2070-2099 (%) | Downscaled-GCM range of change by 2070-2099 (%) | No. downscaled-GCMs that agree with sign of change to central estimate by 2070-2099 |
|------------------------|--|---|---|---|---|---|
| †Nive River | 163 | -5 | -10 | -12 | -19.6 to 0.8 | 5 |
| North Esk River | 455 | -2 | 1 | 7 | -9.2 to 21.6 | 5 |
| North West Bay Rivulet | 46 | 1 | 3 | 1 | -13.1 to 27.9 | 2 |
| Orielton Rivulet | 7 | 9 | 19 | 40 | 11.3 to 109.7 | 6 |
| *Ouse River | 79 | -2 | -6 | -4 | -27.8 to 50.7 | 4 |
| Panatana River | 9 | -5 | 5 | 24 | -7.6 to 61.1 | 5 |
| Pipers River | 146 | -1 | 6 | 21 | -4.8 to 43.5 | 5 |
| Prosser River | 110 | 3 | 7 | 12 | -12.5 to 55.3 | 3 |
| Que River | 149 | -1 | -3 | 0 | -3.6 to 8.6 | 2 |
| ‡Ringarooma River | 390 | -2 | 2 | 9 | -11.4 to 21.4 | 5 |
| Rubicon River | 126 | -6 | 2 | 12 | -9.2 to 36.8 | 4 |
| Savage River | 376 | -1 | -3 | 0 | -4.9 to 10.6 | 1 |
| Scamander River | 154 | 7 | 10 | 18 | -12.3 to 73.3 | 4 |
| Sisters Creek | 18 | -5 | -4 | -1 | -12.8 to 15.7 | 4 |
| Snug Rivulet | 7 | -1 | 3 | 1 | -17.2 to 39.6 | 2 |
| South Esk River | 682 | 2 | 3 | 12 | -12 to 38.1 | 5 |
| Stitt River | 72 | 0 | -2 | 1 | -1.8 to 8.9 | 2 |
| Swan and Apsley Rivers | 186 | 9 | 13 | 19 | -15.1 to 55.2 | 4 |
| Tamar Estuary | 233 | -2 | 5 | 18 | -6.6 to 41.1 | 5 |
| Tasman Peninsula | 176 | 6 | 16 | 28 | 6.7 to 58.9 | 6 |
| Tomahawk River | 55 | 1 | 14 | 35 | -1.4 to 63.5 | 5 |
| Welcome River | 74 | -4 | -5 | 2 | -15.6 to 42 | 3 |
| †Whyte River | 459 | -1 | -3 | 0 | -4.6 to 8.7 | 2 |

† Whole catchment not modelled - partial (upper) catchment only.

* Upper catchment subject to releases from Hydro Tasmania hydro-electric power generation system.

‡ Catchment contains large irrigation/water supply storages.

Appendix F

Changes to storage inflows

Table F.1 Reference period (1961-1990) inflows to irrigation storages and percent change for three future periods (central estimates).

| Storage | Reference period central estimate of average annual inflow 1961-1990 (GL) | Change in central estimate by 2010-2039 (%) | Change in central estimate by 2040-2069 (%) | Change in central estimate by 2070-2099 (%) | Downscaled-GCM range of change by 2070-2099 (%) | No. downscaled-GCMs that agree with sign of change in central estimate by 2070-2099 |
|----------------------|---|---|---|---|---|---|
| Cascade Dam | 17 | -3.2 | 1.1 | 6.7 | -12.3 to 17.9 | 4 |
| Companion Reservoir | 26 | -3.9 | -5.2 | -5.5 | -8.1 to 1 | 5 |
| Craigbourne Dam | 17 | 2.8 | 11.9 | 24.3 | -3 to 82.5 | 5 |
| Curries Reservoir | 3 | -0.5 | 9.0 | 27.3 | -2.3 to 58.4 | 5 |
| Frome Dam | 17 | -1.4 | 1.3 | 3.8 | -10.8 to 11.6 | 4 |
| Guide Reservoir | 11 | -6.9 | -7.6 | -7.3 | -16.4 to 2.9 | 5 |
| Lake Crescent/Sorell | 19 | -7.3 | -13.5 | -20.2 | -47.8 to 24.9 | 5 |
| Lake Isandula | 18 | -6.8 | -6.1 | -4.8 | -16.6 to 6.2 | 4 |
| Lake Leake | 5 | 9.2 | 7.8 | 22.6 | -22.8 to 78.9 | 4 |
| Lake Mikany | 15 | -3.7 | -1.7 | 6.3 | -7.9 to 25.8 | 3 |
| Meander Dam | 116 | -7.9 | -9.9 | -12.6 | -21.4 to 1.9 | 5 |
| Pet Reservoir | 12 | -5.6 | -5.5 | -4.8 | -13.9 to 4.4 | 4 |
| Talbots Lagoon | 20 | -3.8 | -5.9 | -5.3 | -9.7 to 1.5 | 5 |
| Tooms Lake | 3 | 10.9 | 26.1 | 25.6 | -14.2 to 76.5 | 4 |

Appendix G

Changes to reliability of water supplied by irrigation storages

Table G.1 Reference period (1961-1990) inflows to irrigation storages and percent change for three future periods (central estimates).

| Catchment | Reference period (1961-1990) reliability | End-of-century (2070-2099) reliability | Change from reference period to end-of-century |
|----------------------|---|---|--|
| Cascade Dam | 96% (94 to 98) | 95% (93 to 97) | 0% (-4 to 3) |
| Companion Dam | 97% (95 to 98) | 92% (89 to 96) | -5% (-7 to -1) |
| Craigbourne Dam* | 100% (100 to 100) | 100% (100 to 100) | 0% (0 to 0) |
| Curries Dam | 100% (100 to 100) | 100% (100 to 100) | 0% (0 to 0) |
| Frome Dam | 57% (50 to 61) | 63% (42 to 71) | 6% (-17 to 19) |
| Guide Reservoir | 100% (100 to 100) | 100% (100 to 100) | 0% (0 to 0) |
| Lake Crescent/Sorell | 100% (99 to 100) | 90% (78 to 100) | -10% (-22 to 0) |
| Lake Isandula | 91% (89 to 94) | 90% (89 to 92) | -1% (-4 to 2) |
| Lake Leake | 99% (96 to 100) | 98% (96 to 100) | 0% (-4 to 4) |
| Lake Mikany | 100% (100 to 100) | 100% (100 to 100) | 0% (0 to 0) |
| Meander Dam | 97% (96 to 98) | 94% (91 to 98) | -3% (-7 to 1) |
| Pet Reservoir | 100% (100 to 100) | 100% (100 to 100) | 0% (0 to 0) |
| Talbots Lagoon | 96% (94 to 100) | 92% (89 to 100) | -4% (-6 to 0) |
| Tooms Lake | 78% (71 to 86) | 81% (52 to 100) | 3% (-19 to 28) |

*Reliability of Craigbourne Dam is likely to be overstated in all periods because demand is a function of available water, as dictated by current operating rules. That is, demand for water from Craigbourne Dam is forced to match supply in the Coal River model, meaning reliability (supply:demand) will always be 100%.

Appendix H

Reference period flows and changes to river flows for all downscaled-GCMs by end-of-century

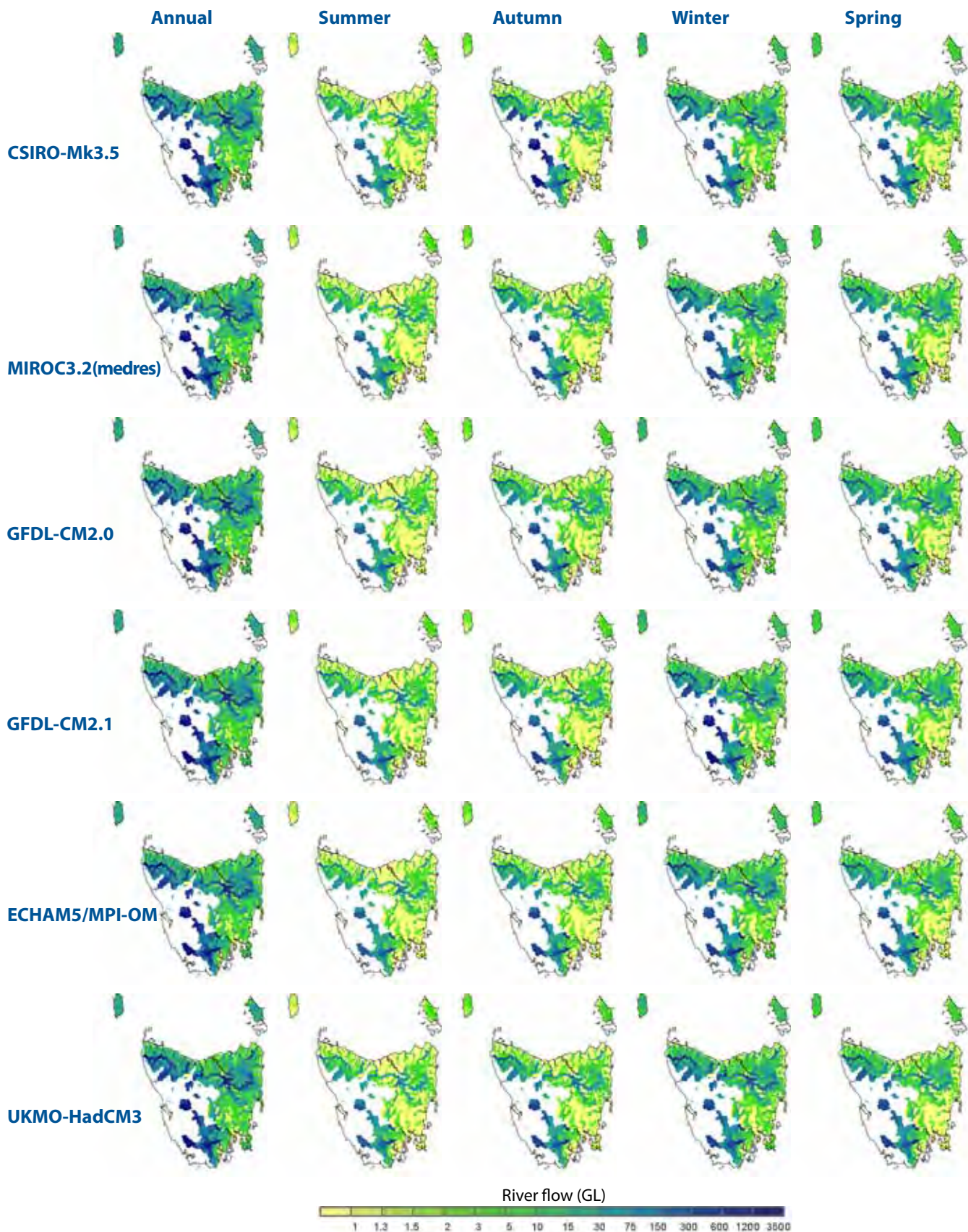


Figure H.1 Reference (1961-1990) average cumulative discharge by subcatchment for rivers modelled for each downscaled-GCM. Discharge is a function of runoff, subcatchment area and water extractions (where these apply). Subcatchment areas are not uniform. White regions indicate areas of regulated flow for hydro-electric power generation (described by Figure 6.7) or regions for which catchment models were not developed.

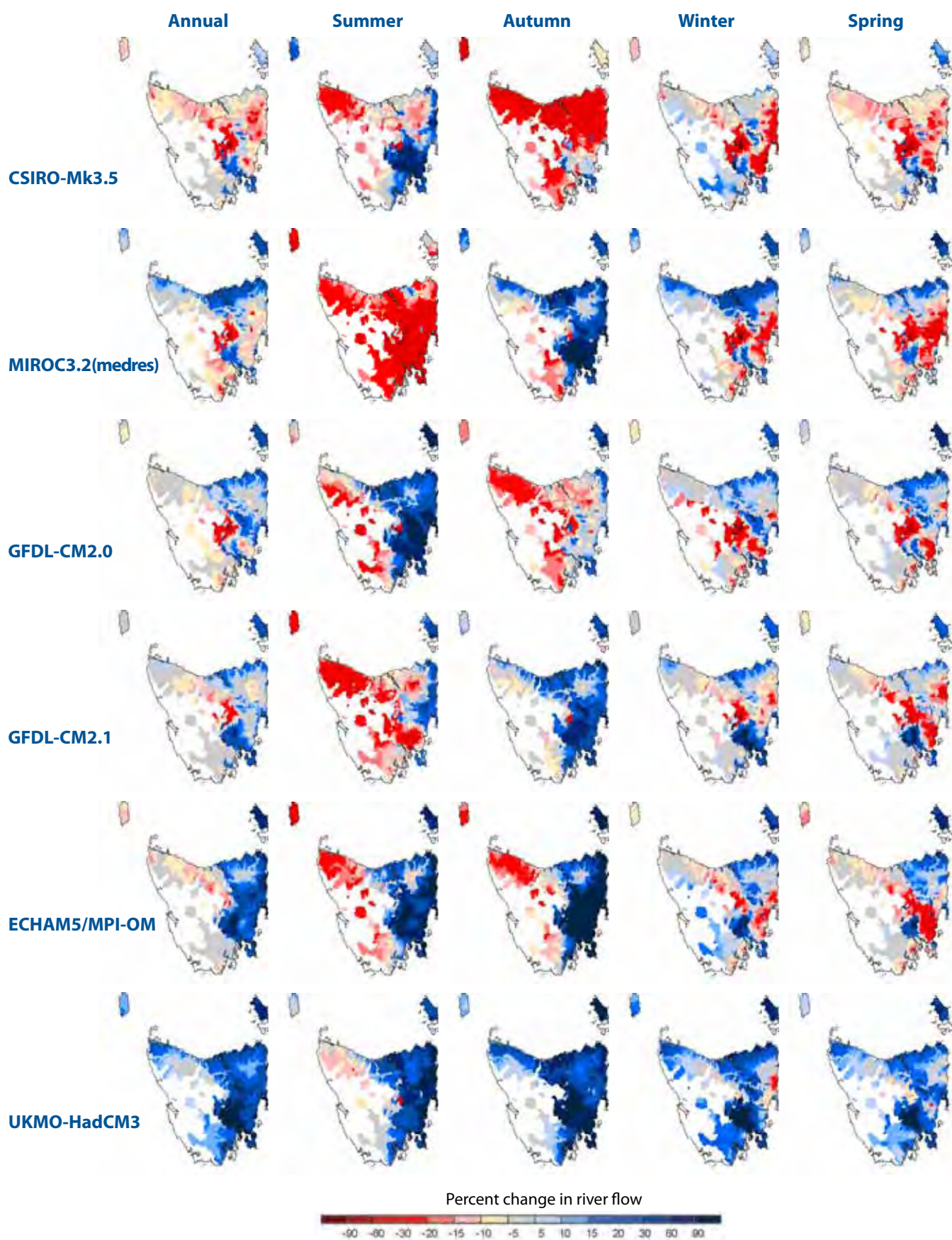


Figure H.2 Percent change in annual and seasonal river flow from reference period (1961-1990) to end-of-century (2070-2099) for each downscaled-GCM. White regions indicate areas of regulated flow for hydro-electric power generation (described by Figure 6.8) or regions for which catchment models were not developed.

Appendix I

Modelling outputs to be made available to researchers

The variables produced by the runoff modelling that will be made available by the Tasmanian Partnership for Advanced Computing (TPAC) are listed in Table I.1. In addition, many river catchment variables have been calculated, and these are listed for interested researchers in Table I.2. These additional variables will not be freely available for download from the TPAC internet portal but can be obtained by contacting TPAC. For more information visit www.tpac.org.au.

Table I.1 List of variables related to runoff modelling that are available from the Tasmanian Partnership for Advanced Computing (TPAC) at www.tpac.org.au.

| Gridded Variable | Resolution | Units | Time step | No. of runoff models | No. of downscaled-GCMs | Emissions scenario |
|---------------------------------|------------|-------|-----------|----------------------|------------------------|--------------------|
| Runoff | 0.05° | mm | Daily | 5 | 6 | A2 |
| Bias-adjusted rainfall | 0.05° | mm | Daily | 5 | 6 | A2 |
| Bias-adjusted Morton's wet APET | 0.05° | mm | Daily | 5 | 6 | A2 |

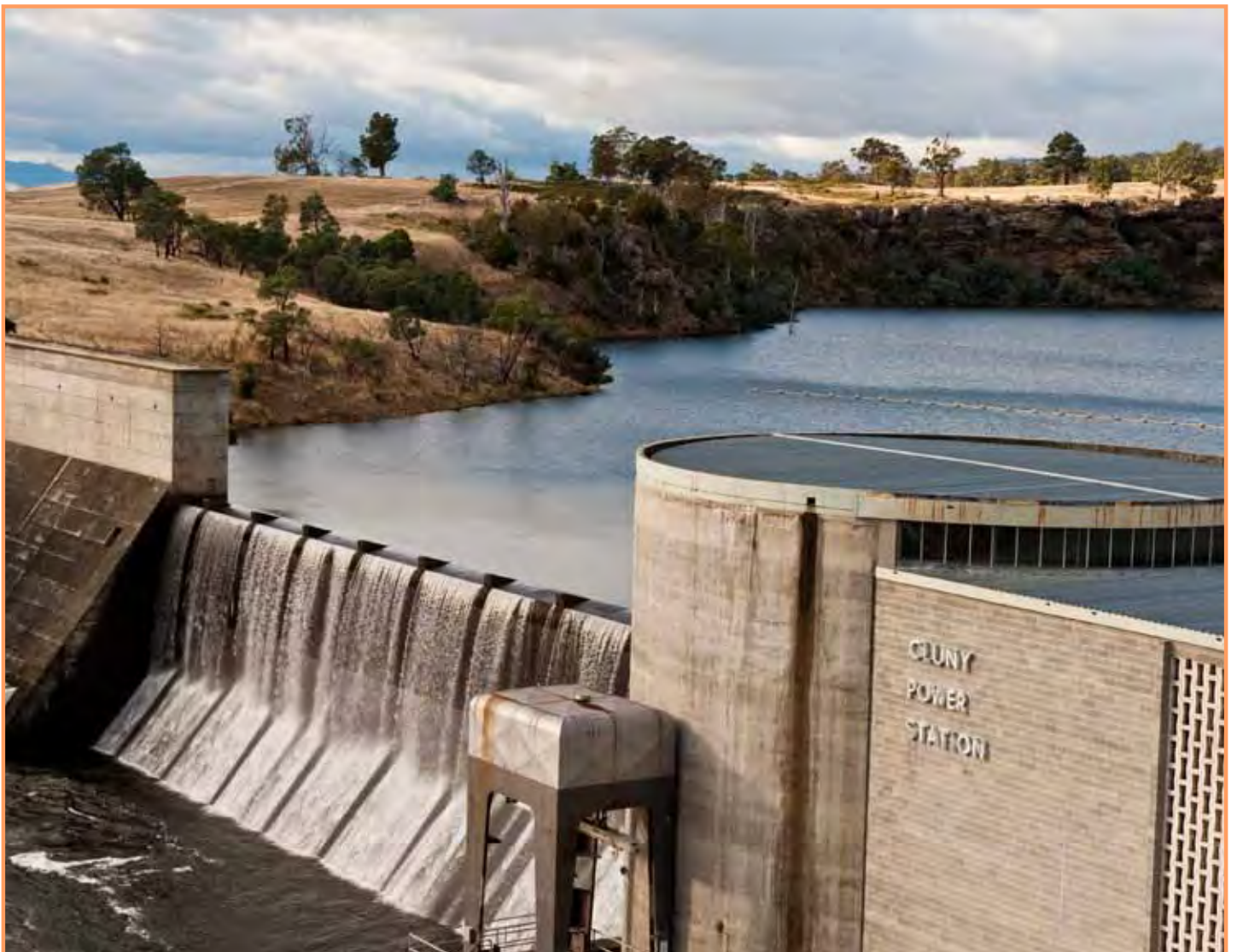
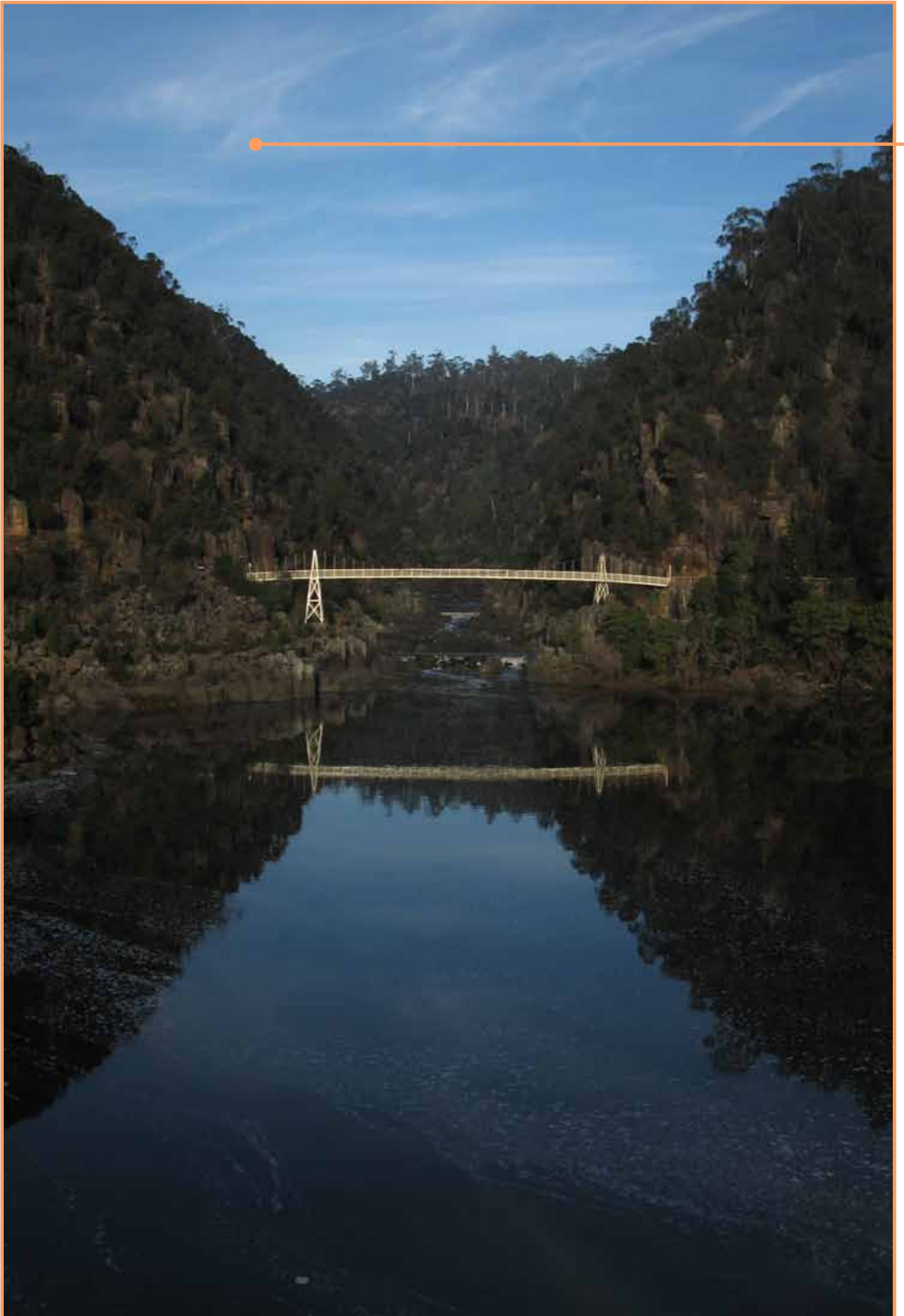


Table 1.2 List of river catchment variables calculated for this project. These are not available from an internet site but can be obtained by contacting the Tasmanian Partnership for Advanced Computing (TPAC) at www.tpac.org.au.

| Catchment variable | Resolution | Units | Time step | Runoff model | No. of downscaled-GCMs | Emissions scenario |
|--|------------|--------|-----------|--------------|------------------------|--------------------|
| River flow (with extractions accounted for) | Catchment | ML/day | Daily | Simhyd | 6 | A2 |
| River flow (with number extractions accounted for – ie ‘natural’ flow) | Catchment | ML/day | Daily | Simhyd | 6 | A2 |
| Surety 1 water extracted | Catchment | ML/day | Daily | Simhyd | 6 | A2 |
| Surety 2 water extracted | Catchment | ML/day | Daily | Simhyd | 6 | A2 |
| Surety 3 water extracted | Catchment | ML/day | Daily | Simhyd | 6 | A2 |
| Surety 4 water extracted | Catchment | ML/day | Daily | Simhyd | 6 | A2 |
| Surety 5 water extracted | Catchment | ML/day | Daily | Simhyd | 6 | A2 |
| Surety 6 water extracted | Catchment | ML/day | Daily | Simhyd | 6 | A2 |
| Surety 7 water extracted | Catchment | ML/day | Daily | Simhyd | 6 | A2 |
| Surety 8 water extracted | Catchment | ML/day | Daily | Simhyd | 6 | A2 |
| Unlicensed water extracted | Catchment | ML/day | Daily | Simhyd | 6 | A2 |
| Surety 1 allocation | Catchment | ML/day | Daily | Simhyd | 6 | A2 |
| Surety 2 allocation | Catchment | ML/day | Daily | Simhyd | 6 | A2 |
| Surety 3 allocation | Catchment | ML/day | Daily | Simhyd | 6 | A2 |
| Surety 4 allocation | Catchment | ML/day | Daily | Simhyd | 6 | A2 |
| Surety 5 allocation | Catchment | ML/day | Daily | Simhyd | 6 | A2 |
| Surety 6 allocation | Catchment | ML/day | Daily | Simhyd | 6 | A2 |
| Surety 7 allocation | Catchment | ML/day | Daily | Simhyd | 6 | A2 |
| Surety 8 allocation | Catchment | ML/day | Daily | Simhyd | 6 | A2 |
| Unlicensed demand | Catchment | ML/day | Daily | Simhyd | 6 | A2 |
| Net storage evaporation | Storage | ML/day | Daily | Simhyd | 6 | A2 |
| Spillway discharge | Storage | ML/day | Daily | Simhyd | 6 | A2 |
| Storage volume | Storage | ML | Daily | Simhyd | 6 | A2 |
| Storage inflow | Storage | ML/day | Daily | Simhyd | 6 | A2 |
| Demand for water to be released downstream | Storage | ML/day | Daily | Simhyd | 6 | A2 |
| Water released downstream | Storage | ML/day | Daily | Simhyd | 6 | A2 |
| Demand for water to be pumped from storage | Storage | ML/day | Daily | Simhyd | 6 | A2 |
| Water to be pumped from storage | Storage | ML/day | Daily | Simhyd | 6 | A2 |



Authors' Acknowledgements

Thanks to Stuart Allie, Katherine Brown, Bill Budd, Jack Katzfey, David Marshall, Roger Parkyn, Kim Robinson, Crispin Smythe, Ian Tye, Jai Vaze, Mark Willis and Simon Wotherspoon for advice, proof-reading and analyses. Thanks to Jin Teng for supplying evapotranspiration algorithms used in the Tasmania Sustainable Yields Project.

Project Acknowledgements

The Climate Futures for Tasmania project was funded primarily by the State Government of Tasmania, the Australian Government's Commonwealth Environment Research Facilities Program and Natural Disaster Mitigation Program. The project also received additional funding support from Hydro Tasmania.

Scientific leadership and contributions were made from a consortium of organisations including: Antarctic Climate & Ecosystems Cooperative Research Centre, Tasmania Department of Primary Industries, Parks, Water and Environment, Tasmanian State Emergency Service, Entura (formerly Hydro Tasmania Consulting), Geoscience Australia, Bureau of Meteorology, CSIRO, Tasmanian Partnership for Advanced Computing, Tasmanian Institute of Agricultural Research and the University of Tasmania.

The generation of the Climate Futures for Tasmania climate simulations was commissioned by the Antarctic Climate & Ecosystems Cooperative Research Centre (ACE), as part of its Climate Futures for Tasmania project. The climate simulations are freely available through the Tasmanian Partnership for Advanced Computing (TPAC) digital library at www.tpac.org.au.

The intellectual property rights in the climate simulations belong to the Antarctic Climate & Ecosystems Cooperative Research Centre. The Antarctic Climate & Ecosystems Cooperative Research Centre grants to every person a permanent, irrevocable, free, Australia wide, non-exclusive licence (including a right of sub-licence) to use, reproduce, adapt and exploit the Intellectual Property Rights of the simulations for any purpose, including a commercial purpose.

Climate Futures for Tasmania is possible with support through funding and research of a consortium of state and national partners.



Climate Futures for Tasmania is possible with support through funding and research of a consortium of state and national partners.



ANTARCTIC CLIMATE
& ECOSYSTEMS CRC



Australian Government

Department of Sustainability, Environment,
Water, Population and Communities



Tasmania
Explore the possibilities



Australian Government

Attorney-General's Department



Australian Government

Bureau of Meteorology

 Hydro
Tasmania
The power of natural thinking



Australian Government

Geoscience Australia



CSIRO



TPAC

